STATUS OF THESIS

Title of thesis	SYNTHESIS OF CALCIUM OXIDE FROM WASTE COCKLE SHELL FOR CO_2 ADSORPTION

I MUSTAKIMAH MOHAMED

hereby allow my thesis to be placed at the Information Resource Center (IRC) of Universiti Teknologi PETRONAS (UTP) with the following conditions:

1. The thesis becomes the property of UTP
2. The IRC of UTP may make copies of the thesis for academic purposes only.
3. This thesis is classified as

	Confidential
√	Non-confidential

If this thesis is confidential, please state the reason:

_____

_____

_____

The contents of the thesis will remain confidential for _____ years.

Remarks on disclosure:

_____

_____

_____

Endorsed by

_____ _____

Signature of Author

Signature of Supervisor

Permanent address:

Name of Supervisor

Lot 237 Kampung Chempaka,
Jalan Panji,
16100 Kota Bharu,
Kelantan.

Assoc. Prof. Dr. Suzana Yusup

Date: _____

Date: _____

UNIVERSITI TEKNOLOGI PETRONAS

SYNTHESIS OF CALCIUM OXIDE FROM WASTE COCKLE SHELL FOR CO_2 ADSORPTION

by

MUSTAKIMAH BT MOHAMED

The undersigned certify that they have read, and recommend to the Postgraduate Studies Programme for acceptance this thesis for the fulfilment of the requirements for the degree stated.

Signature: _____
ASSOC. PROF. DR. SUZANA YUSUP

Main Supervisor: _____

Signature: _____
ASSOC. PROF. DR. SHUHAIMI MAHADZIR

Head of Department: _____

Date: _____

SYNTHESIS OF CALCIUM OXIDE FROM WASTE COCKLE SHELL FOR CO_2 ADSORPTION

By

MUSTAKIMAH BT MOHAMED

A Thesis
Submitted to the Postgraduate Studies Programme
as a Requirement for the Degree of

MASTER OF SCIENCE

CHEMICAL ENGINEERING DEPARTMENT

UNIVERSITI TEKNOLOGI PETRONAS

BANDAR SRI ISKANDAR

PERAK

AUGUST 2011

DECLARATION OF THESIS

Title of thesis	SYNTHESIS OF CALCIUM OXIDE FROM WASTE COCKLE SHELL FOR CO_2 ADSORPTION

I_____MUSTAKIMAH MOHAMED_____

hereby declare that the thesis is based on my original work except for quotations and citations which have been duly acknowledged. I also declare that it has not been previously or concurrently submitted for any other degree at UTP or other institutions.

Witnessed by

_____ _____

Signature of Author

Permanent address:

Lot 237 Kampung Chempaka,
Jalan Panji,
16100 Kota Bharu,
Kelantan.

Signature of Supervisor

Name of Supervisor

Assoc. Prof. Dr Suzana Yusup

Date: _____

Date: _____

ACKNOWLEDGEMENTS

Alhamdulillah praises to The Almighty Allah for blessing me with the strength and health towards completing this project. It is a pleasure to thank the many people who made this thesis possible.

First and foremost, I would like to say a million of thankfulness to my supervisor, Assoc. Prof. Dr. Suzana Yusup who has been very supportive from the beginning to the end of the project. Her guidance, attention and advice are very much appreciated. My heartfelt gratitude also goes out to the lecturers of Chemical Engineering Department especially Assoc. Prof. Dr Azmi Bustam and Assoc. Prof. Dr Ye Lwin for the advices and knowledge sharing. Their suggestions, enthusiastic support, knowledge and constructive criticisms helped me greatly in understanding the project.

I also wanted to acknowledge UTP Bio-Hydrogen Research Group, Universiti Teknologi PETRONAS (UTP) and the postgraduate office staffs for providing the facilities and guidelines to ensure successful of each project. Not forgotten the technicians in Chemical and Mechanical Engineering Department who provide helps towards experimental work of this research.

My utmost appreciation goes to my family and friends who inspired, encouraged with never ending prayers and fully supported me for every trial that come in my way. Their advices will always be remembered and become the motivation in continuing the journey of my life. The love, support and precious time together has made this journey more meaningful.

DEDICATION

To Tuan Haji Mohamed Yusoff & Puan Hajjah Che Aminah Che Sof

To my family

To my supervisor

To my friends

ABSTRACT

Calcium oxide (CaO) is recognized as an effective carbon dioxide (CO_2) adsorbent. It can be synthesized via calcination of calcium carbonate ($CaCO_3$) sources including seashell. Malaysia is abundantly available with cockle shell and exploiting this resource as the potential alternative CO_2 adsorbent is an advantage. Main objective of this research is to synthesis CaO by calcining waste cockle shells and demonstrate its capability to capture CO_2 via carbonation reaction. The performance of calcination and carbonation reaction under various conditions such as particle sizes of sample, heating rate, calcination duration and temperature, are examined. Characterization analysis are conducted using x-ray fluorescence spectrometry (XRF), x-ray diffraction (XRD), energy dispersive x-ray spectrometry (EDX), scanning electron microscope (SEM) and physisorption analyzer while thermal stability, reactivity and kinetic analysis for calcination and carbonation of cockle shell are illustrated using thermal gravimetric analyzer (TGA). Material characterization indicates cockle shell is made up of aragonite and CaO can be synthesized at calcination temperature higher than 700°C and held for more than 20 minutes. Carbonation is maximized when CaO is synthesized at calcination temperature of 850°C for 40 minutes and heating rate is 20°C/min and using particle size of < 0.125 mm. At carbonation temperature of 600-650°C, 0.72kg of CO_2 can be captured by 1kg of synthesized CaO. During palm kernel shell (PKS) steam gasification, CO_2 released is 16% lesser once synthesized CaO is applied. Kinetics analysis shows that activation energy (E_a) to synthesis CaO from cockle shell is estimated to be 297.39kJ/mol and fit to zero order reaction where regression coefficient value is 0.999. Carbonation that been tested at 500-850°C shows that activation energy (E_a) at product layer diffusion control region is 102.5kJ/mol and chemical reaction control region is 72.7 kJ/mol. This study concludes that cockle shell is a good source to generate CaO adsorbent to capture CO_2. At selected condition, synthesized CaO able to adsorb more CO_2 and acquire lower activation energy compared to commercial CaO.

ABSTRAK

Kalsium oksida (CaO) dikenalpasti sebagai penjerap karbon dioksida (CO_2) yang efektif. Ia boleh dihasilkan melalui proses *calcination* menggunakan sumber kalsium karbonat ($CaCO_3$) seperti batu kapur dan cengkerang. Malaysia sangat kaya dengan kulit kerang dan mengeksploitasi sumber ini sebagai penjerab CO_2 alternatif yang berpotensi adalah satu keuntungan. Tujuan utama kertas kajian ini ialah untuk mengsintesis CaO dari buangan kulit kerang melalui *calcination* dan mendemonstrasi kebolehannnya dalam menjerap CO_2 melalui proses *carbonation.* Untuk mengsintesis CaO yang mempunyai keupayaan penjerapan yang baik, prestasi proses *calcination* dan *carbonation* diukur ketika pelbagai kondisi proses diadakan. Saiz partikel sampel, kadar pemanasan, tempoh *calcination* dan suhu adalah kondisi yang dimanipulasi. Analisis perwatakan dibuat menggunakan XRF, XRD, EDX, SEM dan penganalisa penjerab-fizikal manakala kestabilan therma, reaktiviti dan analisis kinetik untuk *calcination* dan *carbonation* oleh kulit kerang diilustratsi menggunakan TGA. Analisis perwatakan menunjukkan kulit kerang dibuat dari *Aragonite* dan melalui *calcination,* CaO dapat dihasilkan apabila suhu *calcination* ialah lebih dari 700°C and dikekalkan selama lebih 20 minit. *Carbonation* dimaksimumkan apabila CaO dihasilkan pada suhu 850°C untuk 40 minit dan kadar pemanasan ialah 20°C/min dengan menggunakan partikel saiz <0.125mm. Pada suhu tindakbalas ialah 600-650C, 0.72kg CO_2 dapat dijerap oleh 1kg CaO yang dihasilkan. Ketika proses gasifikasi stim untuk PKS, CO_2 terbebas ialah kurang 16% apabila menggunakan CaO yang dihasilkan. Analisis kinetik menunjukkan tenaga pengaktifan untuk menghasilkan CaO daripada kulit kerang ialah 297.39 kJ/mol dan sesuai dengan tindakbalas *zero-order* apabila analisa *regression coefficient* menunjukkan nilai 0.999. *Carbonation* yang dilakukan pada suhu 500-850°C menunjukkan tenaga pengaktifan dalam rejim kawalan difusi lapisan produk ialah 102.5kJ/mol dan rejim kawalan tindakbalas kimia is 72.7kJ/mol.

In compliance with the terms of the Copyright Act 1987 and the IP Policy of the university, the copyright of this thesis has been reassigned by the author to the legal entity of the university,

Institute of Technology PETRONAS Sdn Bhd.

Due acknowledgement shall always be made of the use of any material contained in, or derived from, this thesis.

© Mustakimah bt Mohamed, 2011

Institute of Technology PETRONAS Sdn Bhd

All rights reserved.

TABLE OF CONTENT

Status of thesis i

Cover page ii

Declaration of thesis iv

Acknowledgement v

Dedication vi

Abstract vii

Abstrak viii

Copyright page ix

Table of content x

Greek letters xxii

Chapter

1. INTRODUCTION 1
   1.1 Background 1
   1.2 Problem Statement 6
   1.3 Research Objective 7
   1.4 Scope of Work 8
   1.5 Thesis Organization 9

2. LITERATURE REVIEW 11
   2.1 Chapter overview 11
   2.2 Background on cockle availability and production in Malaysia 11
   2.3 Calcination of calcium carbonate material 15
   2.4 Carbon dioxide capturing 18
      2.4.1 Carbonation of CO_2 by calcium oxide based adsorbent 23
      2.4.2 Carbonation using biomass and natural material as CaO based adsorbent 28
   2.5 TG utilization for calcination and carbonation study 31
   2.6 Influence of experimental condition on calcination and carbonation 34
   2.7 Kinetic study 41
      2.7.1 Kinetics for calcination 43
      2.7.2 Kinetics for carbonation 54
   2.8 Summary 58

3. METHODOLOGY 60
   3.1 Chapter Overview 60

3.2 Overall Research Procedures 60
3.3 Raw material 61
3.3.1 Material Preparation 61
3.4 Material Characterization 62
3.4.1 Thermal Gravimetric Analyzer (TGA) 63
3.4.2 X-ray Diffraction (XRD) 63
3.4.3 X-ray Fluorescence (XRF) 64
3.4.4 Scanning Electron Microscopy (SEM) 64
3.4.5 Physisorption Analyzer 64
3.4.6 Energy Dispersive X-ray (EDX) 65
3.5 Effect of calcination conditions on carbonation 66
3.6 Comparison study on the performance of synthesized CaO with commercial adsorbent 67
3.7 Chapter Summary 69

4. RESULTS AND DISCUSSION 70
4.1 Chapter Overview 70
4.2 Material Characterization 71
4.2.1 X-Ray Fluorescence Analysis (XRF) 71
4.2.2 X-Ray Diffraction Analysis (XRD) 72
4.2.3 Scanning Electron Microscopy Analysis (SEM) 76
4.2.4 Energy Dispersive X-ray Analysis 80
4.2.5 Physisorption Analysis 83
4.3 Thermal Gravimetric Study on Behavior of Calcination and Carbonation Reaction of Cockle Shell 86
4.4 Effect of Calcination Conditions towards Carbonation of Cockle Shell 89
4.4.1 Particle sizes 89
4.4.2 Calcination temperature 94
4.4.3 Heating rate 98
4.4.4 Calcined duration 102
4.5 Performance of Synthesized CaO 107
4.5.1 Carbonation temperature 107
4.5.2 Comparison of carbonation capacity between synthesized CaO and commercial adsorbent 111
4.5.3 Application of synthesized CaO in pyrolysis and steam gasification of palm kernel shell (PKS) 114
4.6 Kinetic Analysis 116
4.6.1 Calcination using different particle sizes of the sample 116
4.6.2 Calcination at different calcination temperature 118
4.6.3 Calcination at different holding time 120
4.6.4 Calcination at different heating rate 122
4.6.5 Calcination using different carbonate sources 124
4.6.6 Carbonation at different reaction temperature 126
4.7 Chapter Summary 131

5. CONCLUSIONS AND RECOMMENDATIONS 133

5.1 Conclusion 133
5.2 Recommendations 136

REFERENCES 137

Appendix A..... 143

Appendix B..... 145

Appendix C..... 147

Appendix D..... 149

LIST OF TABLES

Table 1-1: Pollution emissions to the atmosphere for Malaysia [2]..... 2
Table 1-2: Chemical analysis (wt%) for different type of shells and limestone [10] ... 4

Table 2-1: Calcination temperaturas of certain metal carbonate [27] 16
Table 2-2: Technologies of CO_2 capturing techniques [31] 22
Table 2-3: Comparison of each CO_2 separation and capturing technology [33] 23
Table 2-4: Application of calcium oxide as CO_2 adsorbent [35] 25
Table 2-5: Summary on previous research applying natural material/ biomass as CO_2 adsorbent 33
Table 2-6: Particle sizes of marketed calcium carbonate [9] 35
Table 2-7: Summary on previous research on the effect of calcination conditions on carbonation performance of the adsorbents. 41
Table 2-8: Mathematical equation for each type of reaction order 45
Table 2-9: Classification of mathematical expressions of reaction mechanism [47].. 48
Table 2-10: Characterization of kinetic mechanisms based on the shape of TG plots [47] 49
Table 2-11: Classification of mathematical model for reaction mechanism [7]..... 53
Table 2-12: Summary of previous research on kinetic analysis of calcination process 54
Table 2-13: Summary on kinetic analysis by previous research for carbonation 58

Table 3-1: Summary on the characterization approach that adopted and the sample involved. 65
Table 3-2: Experimental condition to study the effect of calcination conditions on carbonation..... 67
Table 3-3: Experimental condition for carbonation of synthesized CaO 68
Table 3-4: Experimental conditions for PKS gasification 69
Table 3-5: Experimental condition using different carbonate sources 69

Table 4-1: Elemental analysis of raw cockle shell using XRF 72
Table 4-2: EDX analysis of synthesized CaO at different calcination duration 82

Table 4-3: Summary of physisorption analysis using sample with particle size less than 0.125mm 84
Table 4-4: Calcination and carbonation condition to study the effect of particle sizes 89
Table 4-5: Physisorption analysis for sample with different particle sizes 92
Table 4-6: Calcination and carbonation condition to study the effect of calcination temperature on carbonation 95
Table 4-7: Condition for calcination and carbonation of cockle shell to study the effect of different heating rate 99
Table 4-8: Conditions of other parameters during calcination and carbonation reaction to study the effect of calcined period 103
Table 4-9: Conditions of calcination and carbonation reaction to test the performance of cockle shell at different carbonation temperature 107
Table 4-10: Calcination and carbonation condition to compare the performance of each adsorbent 111
Table 4-11: Comparison of CO_2 amount in outlet gas during pyrolysis and steam gasification of PKS using synthesized CaO and commercial CaO as the adsorbent 115
Table 4-12: Kinetic analysis using each order of reaction for samples at different particle sizes 118
Table 4-13: Kinetic analysis using each order of reaction for different calcination temperature 120
Table 4-14: Kinetic analysis using each order of reaction for samples at different calcination time 121
Table 4-15: Kinetic analysis using each order of reaction for samples at different heating rate 123
Table 4-16: Findings on kinetic analysis done by Samtani et al. (2002) [7] 124
Table 4-17: Kinetic analysis using each order of reaction for samples with different carbonate source 126
Table 4-18: Kinetics analysis for calcination and carbonation reaction using cockle shell 130
Table 4-19: Kinetics analysis obtained by Lee (2004) [48] for CaO carbonation 130

LIST OF FIGURES

Figure 1-1: Average concentration of CO_2 in global atmosphere [1]..... 2

Figure 2-1: Location of Malaysia in South East Asia region [26] 12

Figure 2-2: Cockle of *Anadara Granosa* type found in Kapar, Selangor [23] 12

Figure 2-3: Percentage distribution of value of gross output by industry in 2008 [21] 13

Figure 2-4: Cockles production in Malaysia for the year of 1990 to 2006 [21] 14

Figure 2-5: Mineral content in cockle shell of West Coast Malaysia [24]..... 15

Figure 2-6: Different behaviors of solid particle during calcination [11] 17

Figure 2-7: Constant concentration of solid reaction based on (a) Shrinking Core Model (SCM); (b) Progressive Conversion Model (PCM) [11] 19

Figure 2-8: Carbonation reaction occurred between CaO with CO_2 that produced product layer of $CaCO_3$. 26

Figure 2-9: Carrying capacity of each adsorbent against number of calcination /carbonation cycles [37]..... 29

Figure 2-10: Adsorbents performance during 100 cycles of calcination/ carbonation (S: Crustacean shell; D: Dolomite; A: Aragonite; M: Marble; B: La Blanca limestone; H: Havelock commercial limestone; C: Cadomin commercial limestone; P: Planadera limestone; K: Piasek limestone) [20] 31

Figure 2-11: Carbonation conversion along with radius of the sample particle [43].. 35

Figure 2-12: Influence of temperature towards equilibrium CO_2 partial pressure (a) Sakadjian et al. [34]; (b) Senthoorselvan et al. [44]..... 37

Figure 2-13: Amount of CO_2 captured for different types of CO_2 adsorbent (ES: Eggshell; LC: Linwood carbonate; PCC: Precipitate $CaCO_3$) [38] 38

Figure 2-14: Carbonation conversion for the sample that been calcined at different temperature [44] 39

Figure 2-15: Carbonation conversion at different (a) calcination temperature and (b) calcination time [18]..... 40

Figure 2-16: Behavior of reacting particle at different limiting factor (a) chemical reaction; (b) gas film (c) diffusion through ash layer [11] 42

Figure 2-17: (a) Typical TGA plot showing Ti diffuse and Tf sharp and (b) typical dTG plot showing the half plot [47] 49
Figure 2-18: Flow chart showing the procedures in recognizing the kinetic mechanisms [47] 50
Figure 2-19: Plot of *1/X* against *1/t* using conversion data of (a) Bhatia and Perlmutter; (b) Gupta and Fan [48] 56
Figure 2-20: "Slope extraction with the aid of the grain model during early stages of carbonation for 38–45 µm Strassburg limestone particles at 700 °C with 15% CO_2 and 85% He" [49] 57

Figure 3-1: Flowchart of overall process involved in the study (PKS: Palm kernel shell) 60
Figure 3-2: Preparation of cockle shell powder to be used in this study 62

Figure 4-1: XRD spectra of the raw cockle shell (▲= $CaCO_3$) 73
Figure 4-2: XRD spectra of synthesized CaO (■= CaO; ●= impurity) 74
Figure 4-3: XRD spectra of commercial calcium carbonate (▲= $CaCO_3$; ■ = CaO; ● = Impurity) 75
Figure 4-4: SEM image of aragonite in cockle shell obtained for the study 77
Figure 4-5: SEM image of aragonite obtained from limestone by Hu et al. [56] 77
Figure 4-6: SEM image of synthesized CaO under inert condition at 850°C obtained in the study 78
Figure 4-7: SEM images of calcined limestone under inert condition at 850°C, found by Sun et al [49] 78
Figure 4-8: SEM image of synthesized CaO in inert condition at 850°C for 30 minutes which is mixed with Aldrich calcium oxide 79
Figure 4-9: SEM image of synthesized CaO after carbonation at 650°C in 100% CO_2 80
Figure 4-10: SEM image of carbonated calcium oxide as studied by Abanades and Alvarez [17] 80
Figure 4-11: EDX spectrum of raw cockle shell 81
Figure 4-12: Elemental content in raw cockle shell through EDX analysis 81

Figure 4-13: Isotherm log plot of (a) Aldrich calcium oxide, (b) raw cockle shell and (c) synthesized CaO 85
Figure 4-14: TG and dTG curves obtained for calcination and carbonation in TGA by using MUSE software (Calcination T; 750°C; Carbonation T: 650°C; Heating rate: 20°C /min; Particle size: < 0.125mm, Calcined duration: 60 min) 86
Figure 4-15: (a) TG curves and (b) dTG curves for calcination and carbonation reaction using samples with different particle sizes. 91
Figure 4-16: Conversion plot for calcination and carbonation reaction using samples with different particle sizes 93
Figure 4-17: Amount of CO_2 captured by shell with different particle size during carbonation 94
Figure 4-18: (a) TG curves (b) dTG curve during calcination and carbonation of cockle shell at different calcination temperatures 96
Figure 4-19: Conversion plot for calcination and carbonation at different calcination temperature 97
Figure 4-20: Amount of CO_2 captured per kilogram of synthesized CaO at different calcination temperature 98
Figure 4-21: (a) TG curves (b) dTG curves for calcination and carbonation for cockle shell at different heating rate 100
Figure 4-22: Conversion of cockle shell during calcination and carbonation at different heating rate 101
Figure 4-23: Total conversion and amount of CO_2 captured by synthesized CaO at different heating rate 101
Figure 4-24: (a) TG curves (b) dTG curves for calcination and carbonation of cockle shell at different calcination duration 104
Figure 4-25: Conversion plot of cockle shell during calcination and carbonation reaction 105
Figure 4-26: Carbonation conversion and amount of CO_2 captured at different calcination duration 106
Figure 4-27: (a) TG (b) dTG curves during calcination and carbonation of cockle shell at different carbonation temperature 108

Figure 4-28: Conversion plot for calcination and carbonation of cockle shell at different carbonation temperature 109
Figure 4-29: Carbonation conversion of (a) Bhatia and Perlmutter [19]and (b) Gupta and Fan [27] at different carbonation temperature [48] 110
Figure 4-30: Carbonation conversion and amount of CO_2 captured at different carbonation temperature 110
Figure 4-31: (a) TG curves (b) dTG curves during calcination and carbonation of each potential adsorbent material 112
Figure 4-32: Conversion during calcination and carbonation experienced by different carbonate sources 113
Figure 4-33: Amount of CO_2 captured and carbonation conversion experienced by each adsorbents 113
Figure 4-34: Concentration of CO_2 in the outlet gas during PKS gasification (a) pyrolysis (b) steam gasification 115
Figure 4-35: Plot of ln K against 1/T using reaction equation of zero order for different particle size during calcination 117
Figure 4-36: Plot of ln k against 1/T using reaction equation of zero order for different calcination temperature 119
Figure 4-37: Plot of ln K against 1/T using reaction equation of zero order for different calcination time 121
Figure 4-38: Plot of ln K against 1/T using reaction equation of zero order for different heating rate 123
Figure 4-39: Plot of ln K against 1/T using reaction equation of zero order for different carbonate source 125
Figure 4-40: Plot of carbonation conversion against time in order to proceed with kinetic analysis developed by Lee (2004) [48] 127
Figure 4-41: Plot of 1/X against 1/T in order to obtain regions of chemical reaction kinetic control and product layer diffusion control 128
Figure 4-42: Plot of 1/X against 1/t for (a) chemical reaction kinetic control and (b) product layer diffusion control 129
Figure 4-43: Plot of ln K against 1/T in order to obtain kinetics parameter in regions of chemical reaction control and product layer diffusion control regimes 129

LIST OF ABBREVIATIONS

CO_2	Carbon dioxide
CFC	Chlorofluorocarbon
CaO	Calcium oxide
$CaMg(CO_3)_2$	Dolomite
$CaCO_3$	Calcium carbonate
MV	Macta Veneriformis shell
MM	Maoming limestone
JN	Jining limestone
XRD	X-ray Diffraction
XRF	X-ray Fluorescence
TGA	Thermal Gravimetric Analyzer
EDX	Energy Dispersive X-ray
BET	Brunaeur Emmet Teller
MgO	Magnesium oxide
SiO_2	Silicon dioxide
Fe_2O_3	Iron oxide
SEM	Scanning Electron Microscope
GC	Gas chromatography

Na_2O	Sodium oxide
LOI	Loss of Ignition
SCM	Shrinking Core Model
CGSM	Changing Grain Size Model
NGM	Nucleation Grain Model
Ca	Calcium
Mg	Magnesium
K	Potassium
Na	Sodium
$PbCO_3$	Lead carbonate
$CuCO_3$	Copper carbonate
$MnCO_3$	Manganese carbonate
MEA	Mono ethanol amine
HPC	Hydroxy propyl cellulose
d	Diameter
L	Length
avrg	Average
N_2	Nitrogen
ES	Egg shell
PCC	Precipitate calcium carbonate

LC	Linwood carbonate
dTG	Differential thermal gravimetry
r	radius
CCR	Calcination carbonation cycle
A	Frequency factor of Arrhenius
T_i	Temperature initial
T_f	Temperature final
T_p	Temperature peak
L	Length
H	Height
ATGA	Atmospheric thermal gravimetric analyzer
PKS	Plam kernel shell
P	Phosphorus
$ZnCO_3$	Zinc carbonate

GREEK SYMBOLS

Symbol	Nomenclature	Unit
α	Fraction decomposed	-
E	Activation energy	kJ/ mol
X	Conversion	-
MW	Molecular weight	kg/kmol
Mt	Metric ton	1000kg
Ha	Hectare	$10000m^2$
T	Temperature	°C
P	Pressure	atm
t	time	min
m	mass	kg
Y	Mass CO2 captured	kg
K	Specific rate constant	1/min
R	Reaction gas constant	J/mol K
H	Reaction enthalpy	J/mol
w	Weight	kg
a,b	Heating rate	°C/min

CHAPTER 1

INTRODUCTION

1.1 Background

Carbon dioxide, CO_2 is a common gas that been released to the atmosphere due to many activities such as combustion or burning of the fossil fuel, usage of chlorofluorocarbon (CFC) in refrigeration system, fertilizer, and more. CO_2 is an acidic oxide which may cause toxic or harmful effects to human being such as dizziness at high concentration. Carbon dioxide is a major contributor for global warming or greenhouse effect. The issue of global warming that caused by the CO_2 might catch the attention of the whole world as many conferences, campaigns, and laws been regulated and conducted regarding the emission of CO_2 to the atmosphere.

Figure 1-1 indicates the increasing amount of CO_2 in the global atmosphere including various sources such as industries, mobile sources and domestic activities [1]. The highest amount recorded was 385ppm that been released in 2008. In Malaysia, the total amount of polluted gas which consist of CO_2 that been emitted to the atmosphere in 1998-2008 falls in the range of 1700-3700 000 tones. Table 1-1 described the scenario of pollution emissions in Malaysia where mobile source is a major contributor toward the pollution.

In addition, CO_2 removal step also is a concerned to many sectors in industries. For example, natural gas processing plant treat CO_2 as the impurity to its product gas stream, thus the removal steps is very crucial. Other than that, industries have to adhere to the environmental laws and regulation to reduce the emission rate of CO_2 to the surrounding. Therefore, a number of studies have been conducted to improve the existing unit operation in industry by introducing various types of adsorbent that are

compatible fit with the corresponding process condition so that CO_2 can be captured efficiently.

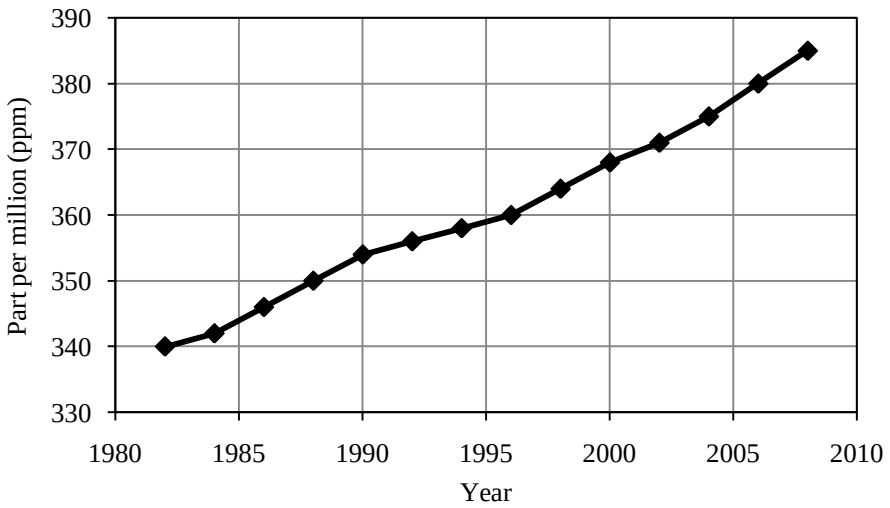

Figure 1-1: Average concentration of CO_2 in global atmosphere [1]

Table 1-1: Pollution emissions to the atmosphere for Malaysia [2]

000 tones					
Year	Stationary sources		Mobile sources	Others	Total
	Industrial	Power plant			
1998	706.5	-	2402.8	146.5	3255.8
1999	461.4	-	2563.1	114.2	3138.7
2000	566.7	-	2642.6	29.2	3238.5
2001	308	-	2561.7	8.6	2878.3
2002	702.1	-	2939.9	14.6	3656.6
2003	125.1	127.4	1649.1	163.2	2064.8
2004	372.4	359	1478.6	38.7	2248.7
2005	157.3	148.8	1538	23.1	1867.2
2006	158.7	150.7	1631	44.9	1985.7
2007	132.9	178.2	2172.8	49.4	2533.3
2008	148.7	221.4	1630	54.4	2055.3

Adsorbents that are made up of calcium oxide, CaO, is an effective substance to trap CO_2 [3]. The statement is also agreed by previous researchers in that calcium based adsorbents that rooted from biomass material is technically feasible, costly effective and advantageous to certain extent in capturing CO_2 [4]. Plants normally

apply CO_2 capturing technique using calcium based adsorbent like lime, CaO or dolomite, $CaMg(CO_3)_2$, in the final storage stage. Normally the adsorption and desorption process relies on the cycle of carbonation and calcination reaction [5]. Calcination- carbonation is a reversible reaction. Calcination is an endothermic reaction where at high temperature (>700°C), $CaCO_3$ is decomposed into CaO and CO_2 would be released, as denoted by Equation 1.1. Thus, to favor the forward reaction (calcination), suitable process conditions like temperature and pressure are crucial.

$$CaCO_3\ (s) \rightarrow CaO\ (s) + CO_2\ (g) \tag{1.1}$$

Carbonation is the reverse reaction of calcination where the adsorption of carbon dioxide (CO_2) occurs. As illustrated in the Equation 1.2, lime, CaO, will adsorb carbon dioxide (CO_2) and yield calcium carbonate, $CaCO_3$. The process normally occurs at lower temperature (<700°C) compared to calcination.

$$CaO\ (s) + CO_2\ (g) \rightarrow CaCO_3\ (s) \tag{1.2}$$

Thus, through calcination process, synthesis of calcium oxide is possible, while carbonation reaction is the CO_2 adsorption step for the adsorbent. These two processes are widely adopted by the industries and several systems for CO_2 capture using CaO as regenerable adsorbents are under development [6].

It is known that limestone, magnesite, and dolomite are the major sources of calcium carbonate ($CaCO_3$) [7]. To have a bulk quantity of $CaCO_3$ as the raw material for a process, the source is usually obtained from the mining or quarrying of limestone hills or caves. The activity is quite common in Malaysia as the country is rich with limestone hill. It is estimated that Peninsular Malaysia own 26000 ha of limestone forest where it represents the home for 14% of the region's plant species where about 130 species are known to grow only in limestone areas and nowhere else [8]. The method of mining or quarrying to explore the resources like $CaCO_3$ is unfavorable to the environment as it is destructive to the nature.

Rather than depending on these natural occurrence sources mentioned above, seashell is found to be an alternative potential biomass source for calcium carbonate.

It fits to be the best candidate as the alternative material for CO_2 adsorbent as seashell is made up of at least 95% of calcium carbonate [4] [9]**.** In addition, Li et al. [10] found that CaO composition in seashell is higher than the limestone used in their study. The comparison of chemical analysis found by Li et al. [10] is shown in Table 1-2.

Table 1-2: Chemical analysis (wt%) for different type of shells and limestone [10]

Sample	CaO	MgO	SiO_2	Fe_2O_3	Al_2O_3	Na_2O	Others	LOI
MV shell	52.41	0.22	0.11	0.07	0.17	0.37	0.33	46.32
Mussel shell	50.45	0.18	0.78	0.09	0.12	0.24	0.82	47.32
Scallop shell	54.35	0.27	0.00	0.04	0.16	0.49	0.47	42.41
MM limestone	48.83	4.8	2.76	0.28	0.54	0.02	0.36	42.41
JN limestone	50.28	2.54	4.21	0.51	0.95	0.01	0.32	41.18

LOI: Loss of ignition; MV: Macta veneriformis; MM: Maoming limestone; JN: Jining limestone

The mechanism of metal carbonate decomposition can be explained by a few types of model such as Shrinking Core Model (SCM), Changing Grain Size Model (CGSM) and Nucleation and Growth Model (NGM). Many researchers claimed that calcination of metal carbonate is best to be described by SCM [11]. Based on SCM, the reaction occurs first at the outer layer of the particle then move into the solid which finally leaving the completely converted material and inert solid that is known as ‘ash’ [11].

Compared to SCM, CGSM explains more on the solid structure that consists of a matrix of very small grains usually spherical in shape and also assumes that particle consist of a number of non porous spherical grains with uniform initial radius [12]. The mechanism describes by NGM is based on competition between the process of nucleation and growth of the new phases, in this case calcium oxide, CaO, which

nucleates at the surface of initial particles [13]. However, the best model to describe the mechanism of a process really depends on the condition of the reaction and also the understanding of the occurring reaction mechanism.

By understanding the reaction mechanism, it helps to better recognize the condition parameter that can influence calcination process. Cheng and Specht [14] describe that calcination consist of five sub processes which are heat transfer from ambient to solid surface, heat conduction from surface to reaction front, chemical reaction at the front, diffusion of CO_2 through porous oxide layer to the surface and finally mass transfer to the surrounding. The process can be influenced by certain factors such as temperature, particle sizes, heating rate, partial pressure of CO_2, gas flow rate, atmosphere of the process, sample mass and more. For example, Garcia-Labiano et al. [12] claimed that particle sizes and partial pressure of CO_2 may introduce resistance to the process in the means of mass transfer, heat transfer and gas diffusion. In addition, calcination temperature also can determine whether the process is experiencing sintering and attrition effect or not as it occurs at a very high calcination temperature [15]. In addition, the limiting step for overall reaction depends on experimental conditions, experimental setup and sample size [16].

The process conditions also control the performance of CO_2 capturing process. Based on the study that been done by Lu et al. [3] on CO_2 uptake by calcium based material, carbonation of CaO is based on two step reaction which are fast stage and slow stage. The fast stage is controlled by the chemical reaction while the second stage is controlled by diffusion of CO_2 within the product layer. These actions depend on certain factor like particle size or CO_2 presence during the reaction.

According to Abanades and Alvarez [17] carbonation occurs in two different regions which include microporosity of grains, grain boundaries and walls of large pores within the grain. Carbonation will stop when $CaCO_3$ has filled up the available microporosity while carbonation in the second region is limited by diffusion of CO_2 through the product layer [18]. Carbonation decreases as calcination carbonation cycle increases because porosity of the small pores that cause the formation of larger pores in the calcined grains is reduced [17].

Bhatia and Pulmutter [19] had carried an early study of the carbonation reaction using limestone under atmospheres containing 0-20% CO_2 and it was observed that as the concentration of CO_2 increased, the pore sizes became larger and the size distribution is becoming less spread. According to Stanmore and Gilot [15], the key parameter for carbonation conversion is the fraction of porosity associated with small macropores and mesopores. After a certain number of cycles, the $CaCO_3$ formed during carbonation will occupy all the spaces in the small pores, plus the small fraction of the large voids. However, thickness of the product layer build up on the free CaO surface will introduce the limitation to fill the large pores [20].

1.2 Problem Statement

Carbon dioxide, CO_2, can be the byproduct of a process or also an intermediate gas released or reactant in a process. The emission of CO_2 to the surrounding does not only bring negatives impact to the humans or living organisms but also to the environment. As the concern has arisen to abide to the laws, the involved sectors have taken the steps to control the emission of CO_2.

Many kind of CO_2 adsorbent have been produced which however are not suitable for a high temperature process other than dolomite, magnesite or limestone [17]. Chemical adsorbent on the other hand can be costly, uneffective to the process and may introduce unfavorable effect to the environment and the spent adsorbent need to have special treatment before been disposed or it can pollute the environment.

As CO_2 sequestration is very common in gas and petrochemical plant, quite a number of studies have been done to upgrade the process including research on improving the adsorbent. Currently, the existing technology to adsorb CO_2 utilize amine-based adsorbent, soluble carbonate, activated carbon, molecular sieve, ionic liquid that can only withstand low-temperature process (313K-433K) [3]. It is known that CaO based adsorbent is an effective method of capturing carbon dioxide (CO_2) [3]. This type of adsorbent can prevent the release of CO_2 to atmosphere other than able to resist the high-temperature process (823K-1223K) at the same time [3].

On the other hand, seashell is claimed to be a reliable potential source of biomass to be converted to CaO based adsorbent. Seashell major contains is calcium which is a major substance for CO_2 adsorbent [4] [9]. Li et al. [10] study the performances of limestones and seashells like mussel and scallop shells as CO_2 adsorbent through calcination and carbonation cycle. Based on this study, maximum adsorption of CO_2 occurs at 680-700°C. At calcination temperature of 780-980°C and carbonation temperature of 550-750°C in 15% CO_2 85% N_2, seashells achieve maximum carbonation conversion compared to limestone.

In Malaysia, the production of cockle is very high with three main cockle cultivation centers (Juru at Penang, Kuala Selangor at Selangor and Matang at Perak) while other places like in Jarum Mas at Perak, and Kapar at Selangor, also accelerate their effort to increase the production [21]. Cockles are quite common to be served in daily dishes of Malaysian's cuisine. However, the shells have no utilization and normally been dumped, left untreated at the dumping site. Thus waste cockle shells are abundantly available in Malaysia and its utilization as CO_2 adsorbent should be expanded. This research focused on synthesis of novel adsorbent to adsorb carbon dioxide by exploring the potential of waste cockle shell in Malaysia.

1.3 Research Objective

The main objective of this study is to produce calcium based adsorbent using biomass material to capture CO_2. It aims to create an added value to the waste shells by introducing it as the potential source for CO_2 adsorbent besides limestone or dolomite, in addition to reduce the amount of waste shells generated. Specific objectives of the research are given in the following paragraphs:

1. To characterize cockle shell which is the main raw material used in this study.

2. To determine the factors influencing calcination and carbonation reaction including particle sizes, heating rates, calcination temperature and time.

3. To perform kinetic analysis for calcination and carbonation process to understand the effect of different operating conditions in synthesizing CaO.

4. To examine the performance of cockle shell as the CO_2 adsorbent in order to verify the capability of synthesized adsorbent from cockle shell.

1.4 Scope of Work

The work involves synthesis of CaO based adsorbent using cockle shell as the raw material and testing its capability to capture CO_2. Factors influencing calcination and carbonation are studied. Kinetic analysis is also performed in this study to further elaborate the reactions occurred during synthesizing the adsorbent and CO_2 capturing process. Cockle shell from the species of *anadara granosa* is selected as the source of raw material. The factors that been studied are:

1. Particle sizes

Four ranges of particle sizes have been studied which are +0.125-0.25 mm, +0.25-0.5 mm, 1-2 mm and 2-4 mm. This factor is crucial since particle sizes of the sample may introduce the resistance in heat transport or gas diffusion which may cause an effect to the process.

2. Heating rates

Three heating rates were performed which are 10°C/min, 15°C/min and 20°C/min. A very high heating rate is unfavorable to the process as it might cause another problem like agglomeration or sintering effect [15]. Thus, optimum value of this parameter is important.

3. Calcination duration

At constant temperature, calcination duration can change structure properties of the sample such as sample conversion during synthesis process, sintering effects towards the adsorbent and energy involved in the process. Overall the right calcination duration play role to synthesis an effective adsorbent at economical process condition. Three calcination duration been tested which is 30, 40 and 60 minutes.

4. Temperature

Calcination and carbonation of carbonate also depends on temperature of the process. This factor may introduce the heat resistance to the process or may caused sintering effect to the sample. This study involves three temperatures which are 600°C, 750°C, and 950°C.

To understand the kinetics of the reaction of calcination and carbonation, the following assumptions have been adopted:

- Thermal decomposition of calcium carbonate, $CaCO_3$ suits the best to shrinking core model (SCM) [17] [22]. The model visualizes that the reaction occurs first at the outer layer of the particle then move into the solid which finally leaving the completely converted material and inert solid that is known as 'ash' [11].

- Chemical analysis indicates that the cockle shell under studied also contained other compound such as ferum, Fe, and strontium, Sr, in minor proportion. The effect of their presents on calcination and carbonation process is ignored.

1.5 Thesis Organization

This dissertation consists of five chapters as described below:

1. Chapter 1 is the introduction of the study or undertaking research. The chapter provides the reader with the basic idea of the study and background information of the study which includes the introduction of the research, objective, scope of research and thesis outline.
2. Chapter 2 is the literature review chapter. It gives the detail on certain findings, argument, theory or current issue that been found by previous researchers that related to the study. The chapter highlights background knowledge about the study.
3. Chapter 3 is on methodology of the research study. It includes the overall methodology of the study, experimental procedures, characterization sample and analytical approval adopted.

4. Chapter 4 is the results and discussion chapter. The chapter collects all the findings and analysis throughout the study and it also discussed the possible theory or reason behind the observation of the finding.
5. Chapter 5 is the final part of this report which summarizes the findings and recommendation for future work.

With anticipation of this study, it is hoped that the findings of the study may be used as a future references for the development of cockle shell as an efficient CaO based adsorbent for the purpose of CO_2 capturing system.

CHAPTER 2

LITERATURE REVIEW

2.1 Chapter overview

This chapter will cover the detail of cockle availability and production in Malaysia besides the property of cockle shell. The chapter also explains the process of synthesizing CaO from carbonate sources mainly through calcination and its mechanism to adsorp CO_2 via carbonation reaction. The studies by previous researchers on synthesizing CaO as CO_2 adsorbent is included either by using shells or limestone and the effect of certain parameters such as particle sizes, temperature and times are being discussed in this chapter. In addition, kinetics analysis on calcination of carbonate sources and carbonation of CaO are included at the end of this chapter.

2.2 Background on cockle availability and production in Malaysia

Malaysia is a country that is located in South East Asia, where it is closely neighbored to Thailand, Brunei and Indonesia as shown in Figure 2-1. Surrounded by South China Sea, has enabled this country to become very resourceful of shellfish such as mussel, oyster, cockle, clam and scallop as the shellfish grew well in muddy coastal area and in estuaries. Fishing cockles is an additional economical activity for some fisherman especially during April and November since it is the peak season of the natural cockle production in the river [23].

Cockle or ‘kerang’ as better known by Malaysian, is one type of shell fish that has high market demand in Malaysia. It is a cheap protein source and commonly been

prepared as local dishes. It is a type of bivalve that comes from the family of Cardiidae. There are many kinds of cockles species existed such as and the most common species in Malaysia is *anadara granosa* which belongs to *Arcidae* family as given in Figure 2-2 [24].

Figure 2-1: Location of Malaysia in South East Asia region [26]

Figure 2-2: Cockle of *Anadara Granosa* type found in Kapar, Selangor [23]

In order to reduce the reliance on the natural production at the coastal area and enhance the production of cockles that can ensure the continuous supply, Malaysia has taken the initiative to culture the cockles. Government promotes its citizens to

farm the cockles and continue the effort of supporting the farmers that involve in cultivating cockles. The government also helps the farmers by conducting the training and consultation, and organizing the promotion and marketing on behalf of the farmers to boost the demand and production. Besides, farmers also are able to request for capital or loan from the agencies in order to start the cockle farming or setting up cultivation center. By having cultivation center, around 1.5 to 2 tonnes of cockles per day can be produced and the size of cockle can reach to 55mm which used to been recorded in Kapar cultivation center, Kelang [23].

The cultivating activity has started since 1948 in Perak. The common culturing areas in Malaysia are mangrove-fringes coastal mudflats, Kuala Selangor, and mangrove-based in estuaries, Matang and Merbok [21] and Kapar, Klang [23]. The development of aquaculture industries like cockles is quite electrified since it becomes an important socio-economic activity to the involved farmers. As illustrated in Figure 2-3, 73% of gross output in Malaysia comes from aquaculture industry which includes the farming of cockles.

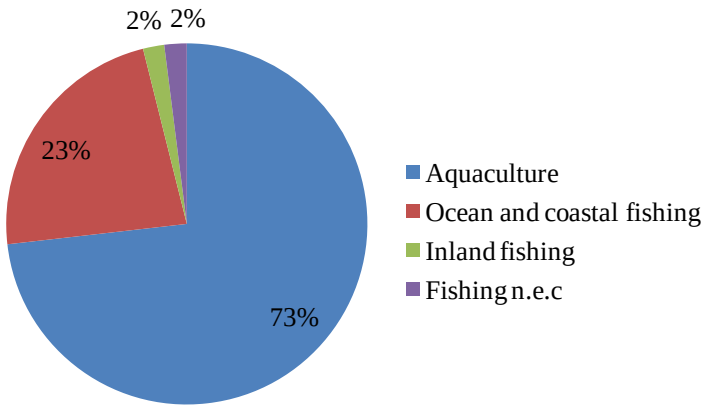

Figure 2-3: Percentage distribution of value of gross output by industry in 2008 [21]

Figure 2-4 indicates the production figures of cockle in Malaysia for the year of 1990 to 2006 [21]. However the production of cockles started to decline from the year of 2002 till 2006 which is believed due to limited suitable culture area for expansion in Peninsular Malaysia and not much significant spat fall area in Sabah and Sarawak.

Higher operational cost and reduction of mangrove area that helps to supply the cockle seed also contributed towards the decline production of cockle.

However, according to the Director of Malaysia Fisheries Department, the government is expecting to produce 13000mt of cockles during Ninth Malaysia Plan [25]. By state, Selangor is expecting to produce 10mt/ha/yr of cockles during 2010 and till 2007 Malaysia is having 1055 farmers working on cockles' cultivation which involving 6000ha of cultivation area [25]. Thus several steps has been recommended to realize the target, such as reserving and gazette the spat fall area, reducing the operational cost, and research on development of more spat fall area [21].

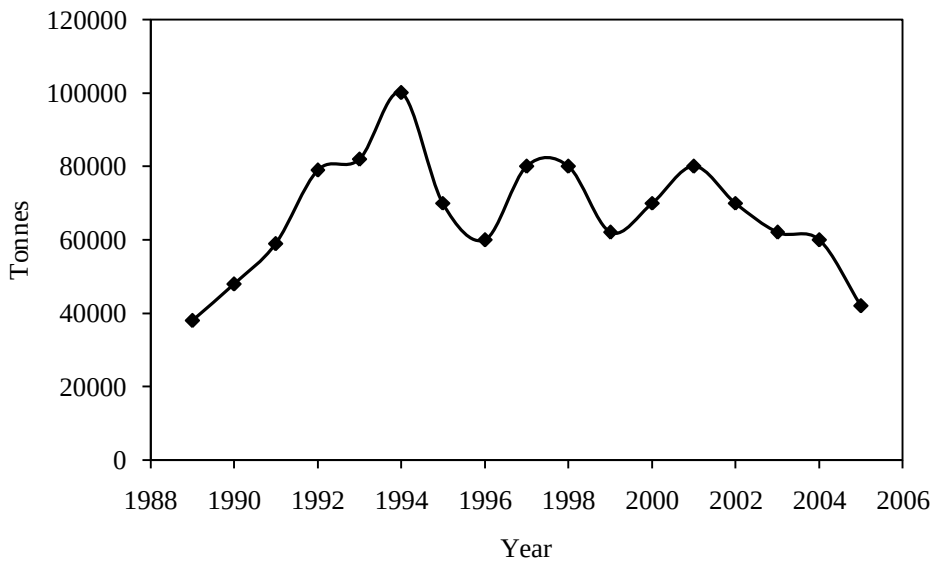

Figure 2-4: Cockles production in Malaysia for the year of 1990 to 2006 [21]

Seashell is known to contain high content of calcium carbonate $CaCO_3$ where based on literature, seashells contain 95%-99% by weight of $CaCO_3$ [4] [9]. Li et al. [10] also agree that the primary chemical component of shell is $CaCO_3$ where it can be an alternative biomass sources for calcium. Figure 2-5 shows the content of minerals in cockle shell at three main cultivation centers in Penang, Kuala Selangor and Malacca and cockle shell is found to contain around 98% of calcium and less than 1% for other minerals [24]. However, it is proved that the amount of other minerals in the cockles which is relatively very small won't affect calcination and carbonation process as its major contain is calcium carbonate [4] [9]. The results also indicate that amount of calcium carbonate is almost the same regardless the sources. In addition,

Gupta and Fan [27] also mentioned that CaO adsorbents obtained from natural occurrence precursors are usually micro-porous which can give better effect on adsorption.

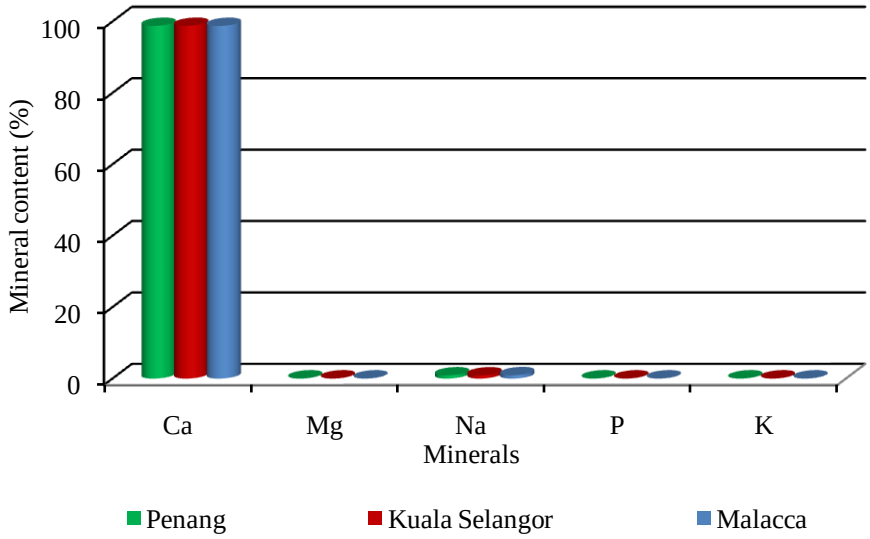

Figure 2-5: Mineral content in cockle shell of West Coast Malaysia [24]

2.3 Calcination of calcium carbonate material

Usually, calcium oxide is extracted via decomposition of calcium carbonate sources such as limestone, dolostone and magnesite. The process that is better known as calcination, is an endothermic reaction where heat is used to decompose the solid material and cause volatile removal or phase transition. Calcination is favored by high temperature (higher than 700°C) and normally takes place either in inert atmosphere or using fuel for a rapid combustion process which then released carbon dioxide, CO_2. Calcination can be carried out in lime kiln, furnace, incinerator tube furnace, thermal gravimetric analyzer (TGA), fluidized bed reactor and fixed bed reactor. Martavaltzi et al. [28] carried out calcination of the adsorbent material in an open box type furnace under air atmosphere.

Some studies concentrate on calcination with presence of air or fuels while some using inert gases such as nitrogen, argon and helium [29]. The main concern is to make sure the carrier gas will not contaminate the sample or takes place in the

reaction which might affect the results. Normally, calcination is done in cycle with carbonation as a regeneration step as it is a reversible reaction. Based on the above equation, the forward reaction is favored by higher temperature. However, according to Gupta and Fan [27], metal carbonates that decompose beyond 1000°C are not suitable for this purpose because the calcination would impose severe energy penalties. Table 2-1 indicates the calcination temperature of several metal carbonate, based on Gupta and Fan [27] research work.

Table 2-1: Calcination temperaturas of certain metal carbonate [27]

Metal carbonate	$CaCO_3$	$MgCO_3$	$ZnCO_3$	$PbCO_3$	$CuCO_3$	$MnCO_3$
Calcination temperature (°C)	750	385	340	350	225-290	440

According to Karagiannis et al. [29], the study on calcination has been conducted extensively since the last twenty years and many thermo-analytical techniques have been widely used in order to understand the mechanism of the process. However, there is not much consensus answer on the limiting steps on every experimental work that has been done due to different working condition which determines the limiting steps of a process.

Previous studies have listed many variables that can influence calcination process such as calcination temperature, particle size, heating rate, partial pressure of CO_2, the chemical and physical properties of the material and more [22]. According to Garcia-Labiano et al. [12], based on literature work by Bonquet et al. [18], calcination rate can be affected by temperature, CO_2 partial pressure, total pressure and particle diameter. Thus, it is crucial to know the pattern of these factors to ensure the efficiency of the process.

Figure 2-6 illustrates the different type of behaviors involved during calcination as it can act differently depending on the properties of the solid materials and the condition of the process [11]. By understanding these behaviors, it is much easier to estimate the limiting step that controls the process. By referring to Levienspiel [11], generally, calcination is governed by two types of reaction which are un-reacted

shrinking core and progressive conversion model. Based on Figure 2-6, some particle will shrink or might disappear according to time once the calcination being conducted but some material will remain in shape and having constant size once calcination is done.

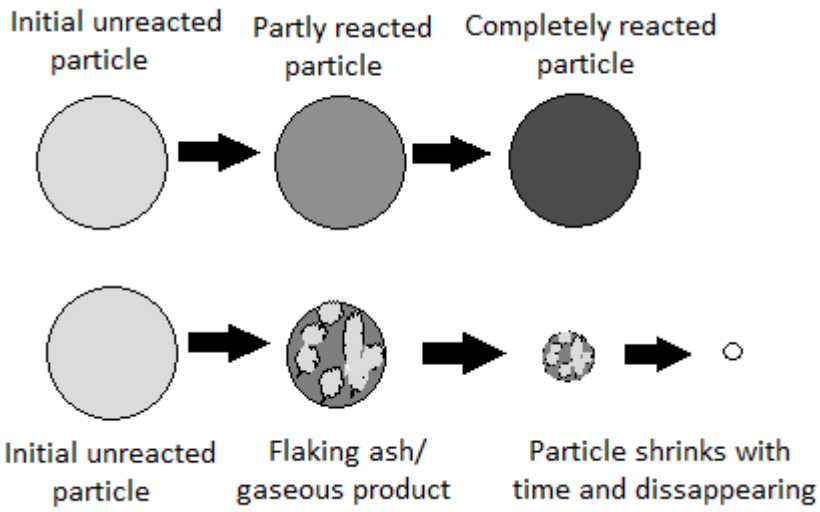

Figure 2-6: Different behaviors of solid particle during calcination [11]

The mechanism of the behaviors can be described by several models such as Shrinking Core Model (SCM), Progressive Conversion Model (PCM), and Nucleation Conversion Model (NCM). Many researchers claimed that calcination of metal carbonate is best to be described by SCM [11]. Based on SCM, the reaction occurs first at the outer layer of the particle then move into the solid which finally leaving the completely converted material and inert solid that is known as 'ash' [11].

Compared to SCM, changing grain size model (CGSM) explains more on the solid structure which consists of a matrix of very small grains usually spherical in shape and also assumes that particle consist a number of non porous spherical grain of uniform initial radius [12]. The mechanism describes by NCM is based on competition between the process of nucleation and growth of the new phases, in this case calcium oxide, CaO, which nucleates at the surface of initial particles [13].

However, many investigators claimed that the mechanisms and the rate expressions for the calcination reactions are recognized to follow the principle of shrinking core model (SCM). Ar and Dogu [22] mentioned that calcination of metal

carbonate involves quite complicated five-step mechanism which causes uncertainty in predicting its behavior. However, Cheng and Specht [14] described calcination consist of five sub-processes. It started with heat transfer from ambient to solid surface then heat conduction from surface to the reaction front followed by chemical reaction at the front and diffusion of CO_2 through the porous oxide layer to the surface and finally the mass transfer to the surroundings. On the other hand, Alvarez et al. [17] mentioned that calcination takes place on a receding interface according to a shrinking core model and the product layer consists of a network of CaO micrograin which is highly porous.

Levienspiel [11] also described the different pattern of solid reaction concentration based on reaction behavior. Concentration of solid reactant is constant throughout the process but the sample size is decreased once the reactant followed the shrinking core model. Inversely, the concentration of solid reactant is reduced yet the size of the grain is constant if the behavior is described based on progressive conversion model. Both of the model description is visualized in Figure 2-7 as referred from Levienspiel [11].

2.4 Carbon dioxide capturing

CO_2 separation was motivated by enhanced oil recovery process as the gas is considered impurities to the product. However, since the awareness of proper removal step of CO_2 is rising due to climate changes, there are a growing number of improvements on the adsorbent and process applied for the sorption to be conducted. Industries of natural gas sweetening, cement, iron and ammonia production, normally implement CO_2 capturing system efficiently. The proper approach of capturing CO_2 is crucial since it can be a major part of the plant operation cost.

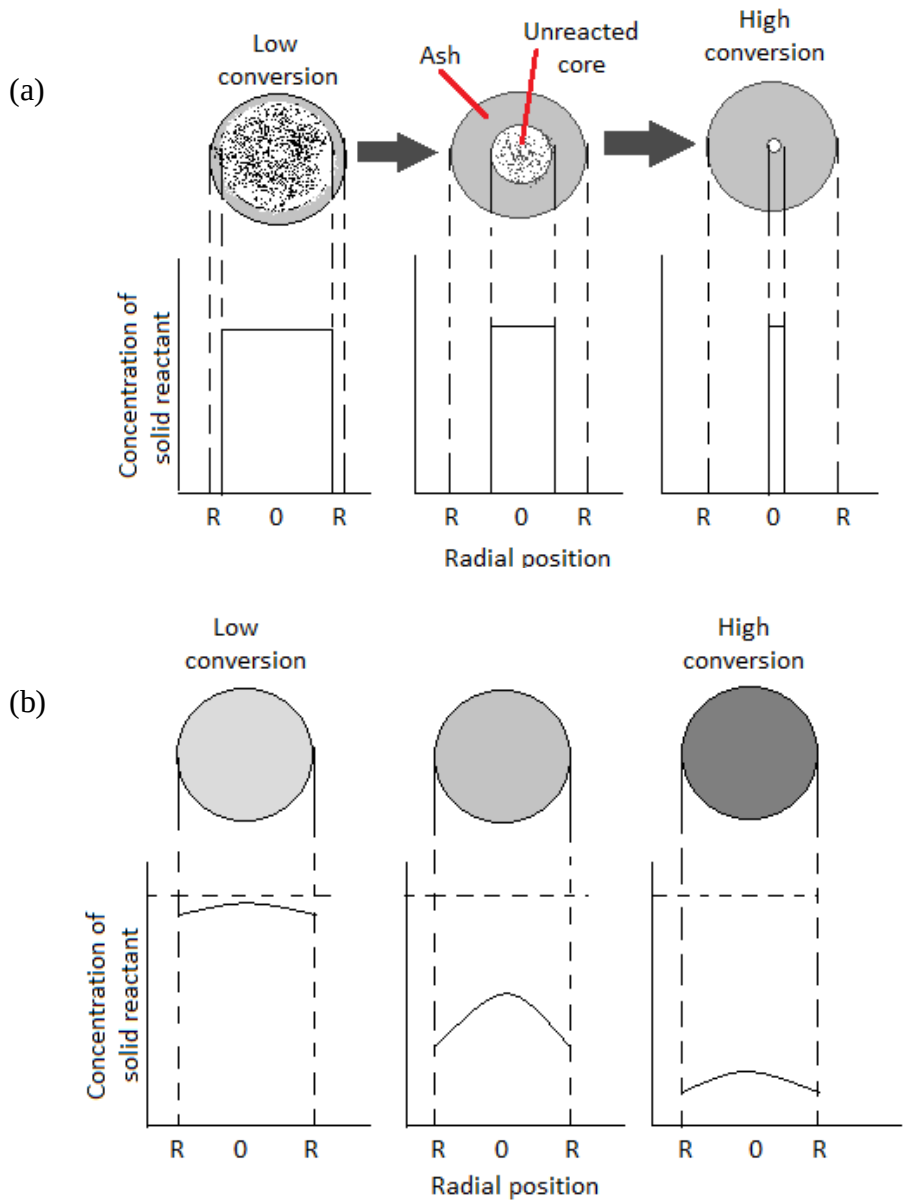

Figure 2-7: Constant concentration of solid reaction based on (a) Shrinking Core Model (SCM); (b) Progressive Conversion Model (PCM) [11]

Thambimuthu et al. [31] mentioned that there are four basic systems in capturing CO_2 as contained in the following paragraphs;

- Capture from industrial process streams: CO_2 been captured from the industrial process stream then been vented to atmosphere since there is no intention or requirement of keeping the gas.

- Post-combustion capture: CO_2 been captured from the flue gas rooted by combustion of fossil fuel and biomass in air then been passed through equipments that separates most of the CO_2 gas before the remaining flue gas been vented to atmosphere.

- Oxy-fuel combustion capture: The capturing system is the same with post-combustion capture system but flue gas containing mainly CO_2 and H_2O is produced once the nearly pure oxygen is used for combustion. Thus, it eased the capturing process.

- Pre-combustion capture: Synthetic gas composed of carbon monoxide and hydrogen is reacted with steam in shift converter to produce more hydrogen while CO_2 is then separated via absorption.

Thambimuthu et al. [31] also classified the sorption method of CO_2 as below:

- Separation with adsorbents/solvents: Liquid absorbent or solid adsorbent is in a close contact with the gas which contained CO_2. The adsorbent that already captured CO_2 will be transported to another vessel to be heat up under certain condition for regeneration (released CO_2) purpose and been cycled back into previous vessel to capture CO_2. The make-up flow of fresh adsorbent is required to compensate the decayed adsorbents.

- Separation with membranes: The separation occurs due to selective permeation of the membrane and pressure difference across the membrane.

- Distillation of liquefied gas stream and refrigerated separation: The gas is compressed, cooled and expanded to convert into liquid form so that the gas can be separated by distillation column.

Table 2-2 described the overview on current and emerging technologies of carbon dioxide capturing application [31].

Considering for the case of sorption method using liquid or solid adsorbent, solid adsorbent is more preferential due to some limitation in utilizing liquid adsorbent such

as liquid amines, a liquid adsorbent that been used for quite a number of time. Satypal et al. [32] listed the followings as the disadvantages of liquid amines:

- Require high temperature for regeneration (typically 100-120° C).
- High equipment costs and maintenance cost for pumping or spraying liquids since contaminant and acid gasses accelerate the corrosive effects of liquid amines and byproducts.
- Amine loss due to evaporation and latent energy penalty.
- Liquids are difficult to handle compared to solids.
- Amines must typically be maintained at 40% (occasionally up to 30%) concentration (to reduce corrosion), thereby compromising CO, removal capacity.
- Additives are required to prevent foaming.
- Oxygen typically has to be limited to prevent reaction with the solvent' (<8%).

Rubin and RaO [33] in their report on CO_2 capturing technology using amine based adsorbent described the following comparison (Table 2-3) on the options for CO_2 separation and capture. Based on this comparison, overall, the adsorption process is an efficient method of capturing and removing CO_2 although it requires lots of pressure which consumed lots of energy and costly. Yet as stated by Sakadjian et al. [34], the required pressure depends on the temperature of the reaction where high temperature reaction can favor carbonation reaction by lowering the equilibrium pressure and vice versa. Therefore, the balance between the parameters can help to optimize energy consumed and cost of operation.

Table 2-2: Technologies of CO_2 capturing techniques [31]

Separation medium	Process Streams		Post-combustion capture		Oxy-fuel combustion capture		Pre-combustion capture	
	Current	Emerging	Current	Emerging	Current	Emerging	Current	Emerging
Solvents (Absorption)	Physical solvents Chemical solvents	Improved solvents Novel contacting equipment Improved design of processes	Chemical solvents	Improved solvents Novel contacting equipment Improved design of processes	n.a	Biometic solvents e.g. hemoglobine-derivative	Physical solvents Chemical solvents	Improved solvents Novel contacting equipment Improved design of processes
Membranes	Polymeric	Ceramic Facilitated transport Carbon Contactors	Polymeric	Ceramic Facilitated transport Carbon Contactors	Polymeric	Ion transport membranes Facilitated transport	Polymeric	Ceramic Palladium Reactors Contactors
Solid adsorbents	Zeolites Activated carbon	n.a	Zeolites Activated carbon	Carbonates Carbon based adsorbents	Zeolites Activated carbon	Adsorbents for O_2/N_2 separation Perovskites Oxygen chemical looping	Zeolites Activated carbon Alumina	Carbonates Hydrotalcites Silicates
Cryogenic	Ryan-Holmes	n.a	Liquefaction	Hybrid process	Distillation	Improved distillation	Liquefaction	Hybrid process

Table 2-3: Comparison of each CO_2 separation and capturing technology [33]

Technology option	System Requirement	Advantages	Drawbacks
Absorption (Chemical)	Absorber and stripper sections Chemical solvent (e.g. MEA, HPC)	Suitable for dilute CO_2 streams (typical flue gas from power plants) Operates at normal T&P Commercially available, proven technology	Heat of solvent regeneration is very high. Significant solvent losses due to acidic impurities in the gas stream.
Absorption (Physical)	Absorber and stripper sections. Physical solvent (e.g Selexol)	Less energy required. Solvents are less susceptible to impurities in the gas stream.	Requires high operating pressure. Works better with gas stream having high CO_2 content.
Adsorption	Adsorber beds	Very high CO_2 possible removal	Require high operating pressure. Costly.
Membranes	Membrane filter	Upcoming promising technology. Space efficiency	Require high operating pressure. May need multiple units and recycling due to lower product purity. Very costly.

MEA: Mono ethanol amine; HPC: Hydroxy propyl cellulose

2.4.1 Carbonation of CO_2 by calcium oxide based adsorbent

According to the study done by Gupta and Fan [27], CaO has the advantage on its capture capacity compared to other adsorbent like MEA and silica gel. Under ideal condition, MEA able to capture 60 g of CO_2/kg MEA while silica gel adsorbs 13.2 g of CO_2/kg silica gel, and an activated carbon can adsorb 88 g of CO_2/kg activated carbon. In contrast, a CaO-based adsorbent managed to capture 393 g of CO_2/kg by

assuming a 50% conversion of CaO over repeated cycles. According to Gupta and Fan [27], reaction based adsorption like carbonation is able to utilize more parts of the adsorbent compared to other method that might heavily dependent and easily effected due to pressure and temperature difference.

Gupta and Fan [27] also described the selection on the types of adsorbent to be applied must be based on several characteristics as follows:

- High capacity of CO_2 capture
- Function in presence of moisture or steam
- Have a fast reaction and regeneration kinetics
- High durability
- Able to be regenerated at lower energy consumption
- Able to remove other pollutants

The above characteristics enable to categorize the effectiveness and capability of the adsorbent while performing CO_2 adsorption. Higher capacity of CO_2 denotes more CO_2 can be captured by the adsorbent and higher durability. Some reaction may introduce moisture or steam. Therefore, an effective adsorbent must be able to function in this condition. Besides, an effective adsorbent need to be economical towards the process when it comes to regeneration steps and should be quite versatile to remove other pollutant than CO_2. Table 2-4 described the application of calcium oxide (CaO) as the CO_2 adsorbent in the studies conducted by previous researchers, obtained by Florin and Harris [35].

Table 2-4: Application of calcium oxide as CO_2 adsorbent [35]

		Carbonation condition			Calcination condition				
adsorbent properties	Reactor	T (°C)	P_{CO2} (atm)	t (min)	T (°C)	P_{CO2} (atm)	t (min)	N cycles	Reference
CaO, sieved <45µm	TGA	600	0.15	20	700	0	20	50	Florin and Harris (2008)
CaO, d_p>1mm	Continuous fluidized system	816	1.28	-	1060	4	<10	70	Curran et al. (1996)
CaO pressed pellet, d_p=10mm	Quartz tube reactor w/electrobalance	750	0.2	60	100	0	180	10	Aihara et al. (2001)
CaO, avrg cube L=2.5µm	Highpressure-electrobalance reactor	750	0.15	60	750	0	60	5	Silaban and Harrison (1995)
CaO, d_p=20µm	TGA	577	1	1440	629	0	240	20	Baker (1973)

d_p : diameter of the particle; L: length

Carbonation is a reaction based method for CO_2 separation as the metal oxide will react with CO_2 through sorption process and producing metal carbonate. In this case, the reaction is between the synthesized CaO powder which is the source for calcium oxide based substance (CaO) and carbon dioxide (CO_2) from the product gas. The process is yielding calcium carbonate, $CaCO_3$ and it is the reverse reaction of calcination as illustrated in the Equation 1.2.

Carbonation is run at lower temperature compared to calcination and it can occur at flue gas temperatures. Based on the study that been done by Lu et al. [3] on CO_2 uptake by calcium based material, carbonation of CaO is based on two step reaction which are fast stage and slow stage. The first stage is very dominant due to chemical reaction. The weight gain experienced by the sample which occurred rapidly represents the CO_2 uptake by the adsorbent. The second stage is controlled by diffusion of CO_2 within the product layer.

The same behavior been described by Alvarez et al. [17] whereby carbonation occurred on the surface of the CaO micrograins and forming carbonate layer that moves toward the micrograins center. Once the carbonate layer reaches thickness of

50-100nm, the fast reaction started to react slowly as carbonation is started to be controlled by CO_2 diffusion, in case where CaO still exist. Gupta and Fan [27] also claimed the same behavior of carbonation where it experienced two rate-controlling regimes. The first regime involves a rapid, heterogeneous chemical reaction while the second regime involves the formation of impervious layer of $CaCO_3$ which cause the reaction to become slow. The reaction is described in Figure 2-8.

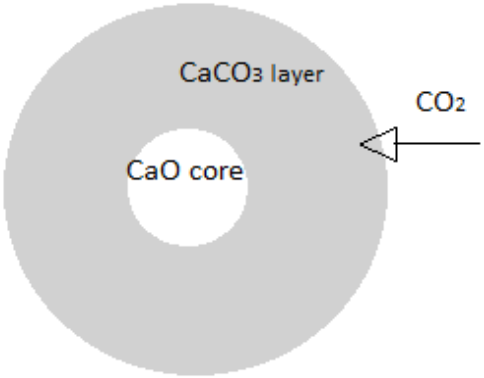

Figure 2-8: Carbonation reaction occurred between CaO with CO_2 that produced product layer of $CaCO_3$.

In addition, according to Grasa et al. [36], and Gupta and Fan [27], the product layer of $CaCO_3$ reduces the contact area of the un-reacted CaO in the particle with CO_2 for more carbonation reaction to occur. Thus, carbonation conversion will decrease and CO_2 capturing will stop once there are no pores or voids left in the particle or at the surface of the CaO. Carbonation also decreases as calcination carbonation cycle increases since $CaCO_3$ tends to fill up the pores and reduce the porosity of the pores in the grains [17].

Normally, carbonation study was conducted together with calcination and both processes were conducted in several numbers of cycles. To demonstrate the capability of the adsorbent in capturing CO_2; carbonation conversion, amount of CO_2 captured per kilogram of adsorbent and carbonation decay are the common values that need to be determined. Besides, the structural changes of the material also can be studied to further visualized and understand the performance of calcium oxide based adsorbent.

According to Sakadjian et al. [31], the conversion of carbonation, X, is based on the weight changes recorded by TGA, which is as follows:

$$X = \frac{(m_t - m_{CaO})/44}{m_{CaO}/56} \tag{2. 1}$$

44 = Molecular weight of carbon dioxide (kg/kmol)

56 = Molecular weight of calcium oxide (kg/kmol)

m_t = Current mass of the sample (kg)

m_{CaO} = Initial mass of the adsorbent at t = 0

Carbonation conversion (X) indicates the mol ratio of CaO been converted into $CaCO_3$ with respect to initial mol of synthesized CaO. The number of mol of CaO been converted into $CaCO_3$ is obtained by the weight increase of the synthesized CaO due to CO_2 capture. Therefore, carbonation conversion can be used as the based to estimate the amount (kg) of CO_2 that can be captured by 1 kg of synthesized CaO. The amount of CO_2 captured, Y, is calculated as follows:

$$Y = \frac{\left(\frac{kg\ CO_2}{44kg/kmol}\right)}{\left(\frac{kg\ CaO}{56\ kg/kmol}\right)} \tag{2. 2}$$

$$Y = 0.9 = \frac{\left(\frac{kg\ CO_2}{\frac{44kg}{kmol}}\right)}{\left(\frac{1\ kg\ CaO}{56\frac{kg}{kmol}}\right)}$$

$$\therefore Y\ kg\ CO_2 = 0.9 \times \left(\frac{1\ kg\ CaO}{56\frac{kg}{kmol}}\right) \times \left(\frac{44kg}{kmol}\right) = 0.72$$

Thus, the amount of CO_2 captured per kilogram of synthesized CaO used is 0.72 kg.

2.4.2 Carbonation using biomass and natural material as CaO based adsorbent

Recently biomass and waste utilization in certain processes has been a new attraction in the industries. For example, the production of methanol from waste sugar cane, hydrogen from empty fruit bunch, methane gas from cow dump, application of solar, wave and wind energy as the alternatives energy and fly ashes or coals as the catalyst. Waste shells are also one of the current interests in developing the resources for certain application.

Ives et al. [37] has conducted a study on removing CO_2 from combustion gas using natural adsorbent such as chicken eggshells, mussel shells and limestone. By utilizing the fact that these materials contained $CaCO_3$ and in calcining it will produce CaO, a well known CO_2 adsorbent, the performance of each material are compared. Since calcination and carbonation are reversible, the process of removing the gas and regenerate the adsorbent were conducted simultaneously in a number of cycles using fluidized bed reactor. Calcination and carbonation was conducted at 750°C in N_2 with 2g of sample with particle size of 600 µm. The carrying capacity of eggshell was declined marginally slowest, followed by the limestone then mussel shells as shown in Figure 2-9. The study found that neither eggshell nor mussel shell were significantly superior to Purbeck limestone in capturing CO_2. The initial pore size of eggshells and mussel shells were different to limestone but the abilities of capturing CO_2 and its behavior were similar. Plus, the performance of adsorbing the gas was linear to the amount of voidage in the samples [37].

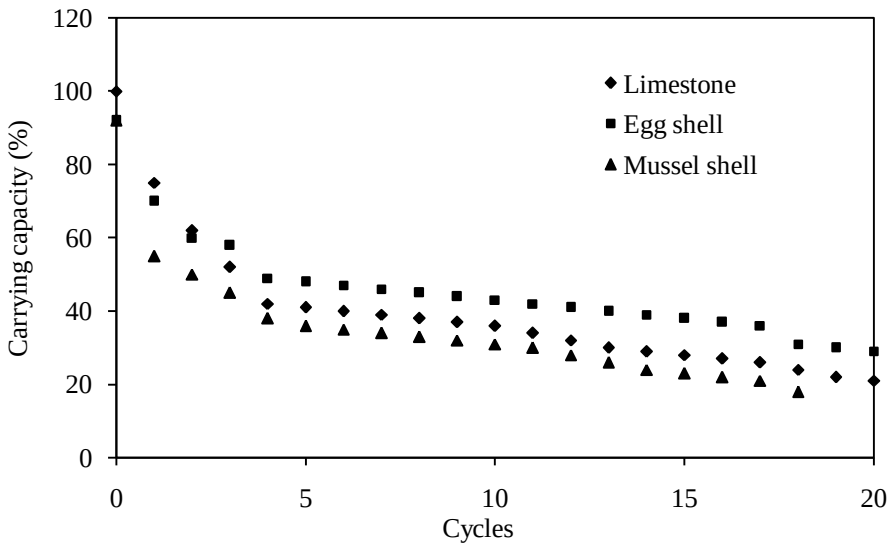

Figure 2-9: Carrying capacity of each adsorbent against number of calcination /carbonation cycles [37]

Li et al. [10] conducted calcination and carbonation study to demonstrate the performance of seashells and limestone. The sample was calcined in a reactor system at temperature 780-980°C in N_2 and carbonated at 550-750 C in 15 vol% CO_2, 85 vol% N_2. The process condition was at atmospheric pressure and the particle size of the adsorbent was less than 0.125 mm. Carbonation was found to occur in two stages which is rapid chemical reaction and diffusion of CO_2 through the product ($CaCO_3$) layer. In less than 20 minutes of carbonation, the carbonation conversion rate of limestone was higher than the shells. However, it is approaching zero after 20 minutes compared to shells that only can reach zero conversion after 60 minutes.

The difference behavior was probably due to microstructural characteristics of the materials. Carbonation was found to occur in kinetically chemical reaction control region and diffusion controlled region. Carbonation decrease rapidly once carbonation temperature increased (750 °C) since CaO shows low CO_2 capture capacity if it is close to thermodynamic equilibrium temperature. However, the effect of sintering behavior of shell is weaker than on limestone for calcination at 850°C. [10].

Bonquet et al. [18] studied on carbonation efficiency of CaO in a series of calcination/carbonation cycles using TGA (SETARAM) and fixed bed reactor system. 20mg of Mexican limestone was used as the adsorbent and been calcined for 30

minutes at 850°C using 20°C/min heating rate, in nitrogen gas, flow at 5 l/h. Carbonation was started once temperature has reached 650°C for the same heating rate and duration with 20 vol% CO_2 diluted in nitrogen was used. TG curves showed carbonation rate decreased after 30 minutes which was caused by sintering of CaO. Sintering effect due to CO_2 emission during the reaction is negligible since small mass of sample in TGA and flow of purge gas. In addition, CO_2 need to diffuse along grain radius through the carbonate (product layer) to reach the CaO core surfaces. Based on the developed asymptotic model, voids between micrograins of the adsorbent were filled by carbonate when it reached critical layer thickness of 43nm. Then the reaction was controlled by diffusion and carbonation conversion kept decreasing.

Iyes and Fan [38] demonstrates the novel use of refuse chicken eggshells as the adsorbent to remove CO_2 for large scale purposes in fossil fuel fired plant. Moreover, acetic acid treatment was introduced to the material in order to improve the adsorption properties of the egg shells. The shells were calcined in TGA at temperature 650-700°C in a flowing N_2 to yield the adsorbent. The calcined sample was injected in pure CO_2 stream in TGA with temperature ramp from 50-900°C for carbonation. Change in weight percent of CO_2 capacity was observed to be as high as 70 wt%. Eggshell (ES) also was prepared in pellet form and its capture capacity was determined to be similar as precipitate calcium carbonate (PCC) and Linwood carbonate (LC). The kinetics of ES was also better than PCC and LC which might be due to improved mass transfer characteristics. However, the capture capacity of the original ES dropped to 40% after 10 cycles compared to the acid treated ES that experienced 30.3% dropped in capacity after 15 cycles.

Alvarez et al. [20] conduct a study to compare the behavior and capability of different naturally occurrence adsorbent for CO_2 removal. The study involved five types of limestone, a dolomite, an ornamental marble, and mixture of crustaceans shell. The particle size of the sample is 0.4-0.6 mm and the cycles were carried out in small fixed bed reactor. Calcination was conducted for 10 minutes at 960°C in 100% CO_2 environment and 5 minutes for carbonation at 650°C in 100% CO_2 environment. Based on capability and thermal and mechanical shocking resistance, this study

concluded that limestone tend to behave better then aragonite, dolomite, highly crystalline carbonate or amorphous carbonates. In addition, dolomite was found to be a good resistance to thermal shock but weak at mechanical strength compared to limestone with particle size of <4µm. Figure 2-10 described the findings of the study [20].

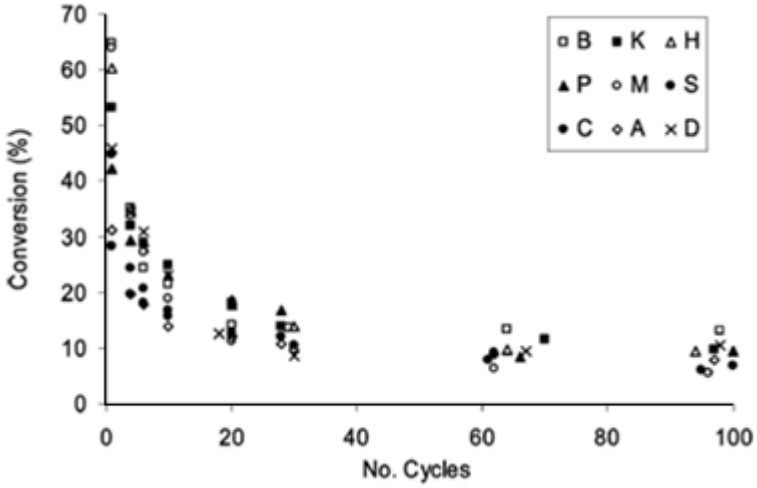

Figure 2-10: Adsorbents performance during 100 cycles of calcination/ carbonation (S: Crustacean shell; D: Dolomite; A: Aragonite; M: Marble; B: La Blanca limestone; H: Havelock commercial limestone; C: Cadomin commercial limestone; P: Planadera limestone; K: Piasek limestone) [20]

2.5 TG utilization for calcination and carbonation study

TGA is one of the equipment commonly used to study calcination and carbonation reaction. According to Gaur and Reed [39], thermal analysis (TA) is referring to analytical techniques where the dependence on physical property of a substance is related to the temperature changes. The techniques include thermogravimetry (TG) and differential thermogravimetry (DTG). Isothermal thermogravimetry records mass change of sample at constant temperature as a function of time. The plotted graph can be used to analyze the thermal stability of the sample, decomposition rate, and the kinetics of reactions occurred as studied in this research work [39].

One of the most common types of thermogravimetric analysis is dynamic thermogravimetry where continuous reading of sample weight change is recorded. During the process, the atmosphere gas can be kept flowing or static with respect to time or temperature. Through this technique, the derivative of weight of the sampler versus time or temperature can be figured out which indicates the reaction period and this method of TG data reporting is known as differential thermogravimetry (DTG) [39].

According to Gaur and Reed [39], thermogravimetric analysis is widely applied in the following fields: metallurgy, ceramics, inorganic and organic chemistry, polymers, biochemistry, geochemistry, and forensics. The analysis can be applied for the purpose of thermal decomposition of organic, inorganic, and polymeric substances in an inert atmosphere to help in determining the pyrolysis kinetics of decomposition or to determine the thermal stability of the sample; reaction chemistry of solid samples where one of the products is in gaseous state; distillation and evaporation of liquids; proximate analysis; vapor pressure determinations; and evaporation and sublimation.

"Since 1960s, the use of thermogravimetry has been extended to the determination of kinetic parameters for various gas-solid reactions. Several methods have since been developed to analyze TG data for quantitative estimate of kinetic parameters. Recent application of TG has been for the deconvolution of biomass components such as hemicelluloses, cellulose and lignin. This technique is still at the development stage." [39].

Table 2-5 indicates the summary on the finding of previous research that applies natural material or biomass as CO_2 adsorbent as been explained in the above paragraphs. The literatures show the vast approach and effort has been done to apply the potential ability of the natural material as CO_2 adsorbent. The patented work of Iyer and Fan [38] by implementing egg shells as CO_2 adsorbent can be a good motivation for this study to embark on the utilization of cockle shell as CO_2 adsorbent.

Table 2-5: Summary on previous research applying natural material/ biomass as CO_2 adsorbent

Author	Objective	Natural material	Outcome
Ives et al. [37]	Study the capability of natural adsorbents in removing CO_2 in a number of cycles.	Chicken eggshells, mussel shells, and limestone.	Capturing capacity (wt %) and pore size distribution (µm) rapidly reduced with increase the cycles.
Li et al. [10]	Comparing capability of shells with limestone during calcination carbonation cycles	*Mactra veneriformis (MV)* shell, mussel shells, scallop shells, Maoming limestone, Jining limestone	Carbonation of shells occurs highest at carbonation temperature of 680-700 °C. MV and mussel shells experienced 10% higher conversion compared to limestone. MV shell showed anti-sintering behavior at calcination temperature of 920 °C. More sodium ion contained in shells which were reported to improve the sorption ability.
Bonquet et al. [18]	Carbonation efficiency during calcination carbonation cycle of CaO	Mexican limestone	Carbonation level obtained in TGA was 5-8% higher than one obtained from fixed bed reactor. Yield of carbonation decreased along the cycles due to sintering of CaO micrograins. After 30 minutes, carbonation is proportional to specific surface area of non sintered micrograins available after calcination.
Iyer and Fan, [38]	Engineered eggshells to obtain high capacity CO_2 sorption	Chicken eggshells	Acetic acid enables eggshell to increase its sorption capacity and endurance during multiple cycles of calcination and carbonation. The performance of engineered adsorbent is better compared to commercial calcium carbonates.
Alvarez et al. [20]	Capability as CO_2 adsorbent in calcium looping system.	Limestone, dolomite, marble, aragonite, crustacean shells	Based on capability and thermal and mechanical shocking resistance, limestone tend to behave better then aragonite, dolomite, highly crystalline carbonate or amorphous carbonates. Dolomite is a good resistance to thermal shock but weak at mechanical strength.

2.6 Influence of experimental condition on calcination and carbonation

Calcination process can be influenced by various factors according to the operating condition and the physical or chemical properties of the solid reactant. Factors including pore diffusion inside the particle and chemical reaction will depend on temperature, CO_2 concentration, total pressure and particle size. In order to reduce or avoid the effect of these limiting steps, the operating conditions need to be correct. In addition to optimize the efficiency and operating cost of synthesizing the adsorbent and capturing CO_2 reaction, the best operating condition need to be determined.

Particle size plays main role in calcination and carbonation reaction since the factor may introduce mass and heat transfer limitation. Ye et al. [40] claimed that fine grinding below 5 µm towards the sample is unfavorable due to the cost of grinding and destruction of pore volume while a decrease below 1-2 µm is said to have limited effect on a conversion although pore diffusion limitations are entirely absent. Cheng et al. [41] claimed that decomposition of 14 µm particles at 1000 °C is controlled by chemical reaction. Borgwardt [42] on the other hand considered limestone particle less than 90 µm in diameter can be calcined uniformly.

Barros et al. [9]described three types of calcium carbonate products which depend on particle sizes of the material. The main characteristics are described in Table 2-6. In 2006, calcium carbonate in the form of flakes with diameter ranges of less than 2mm hits the highest types of calcium carbonate that been marketed. Calcium carbonate in powder form however was not favorable in the market since it showed the lowest amount marketed among the three types. Therefore, the produced adsorbent need to have an appropriate particle sizes in order to suit for certain application besides being efficient and economical.

Table 2-6: Particle sizes of marketed calcium carbonate [9]

Type of commercial $CaCO_3$	Annual quantity (ton/year 2006)	Particles	
		Mean size (diameter)	Shape
A	30.92	20µm	Powder
B	74.21	< 4mm	Flakes
C	1269.08	< 2mm	Flakes

Figure 2-11 shows the predicted profile on the extent of calcination with respect to radial position of a 63 µm limestone into nitrogen at 1473K based on model developed by Hu and Scaroni [43]. The radial position indicates the ratio of location radius, r, to particle radius, r_0, that indicates the middle point towards the surface or outer layer of the sample. The conversion ranged from 85% at the surface *(r/ r_o* = 1), to 29% at the center*(r/r_o* = 0.5). Using the model, increasing extent of calcination at the surface towards the center, will drop once the sample complete its calcination. The model demonstrated the extent of calcination is different at various locations which are due to the effect of internal temperature and CO_2 partial pressure gradient.

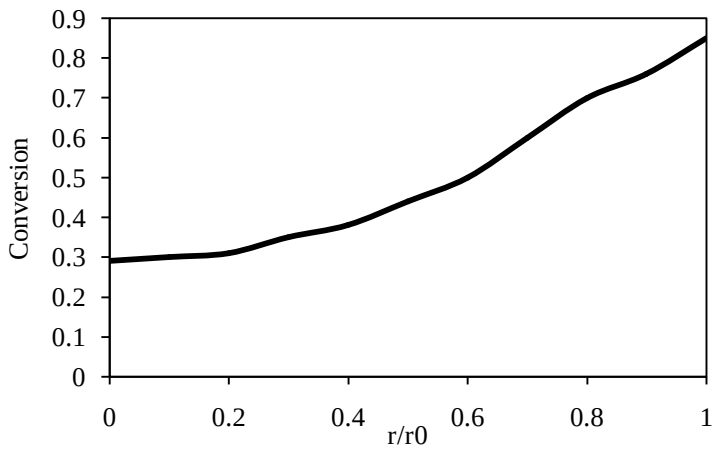

Figure 2-11: Carbonation conversion along with radius of the sample particle [43]

Temperature of calcination and carbonation can be a crucial point that determines the efficiency of the developed adsorbent material. A correct temperature range must be reached in order to ensure the conversion of the raw material into the desired new substance. Sintering effect will be presence if the temperature used to synthesize the material is too high which in turn reduce the capability of the adsorbent in capturing the gas. In addition, the developed adsorbent also needs to be examined so that it can

be applied at the right temperature. Certain adsorbent cannot function when the temperature is too low or too high.

Li et al. [10] also studied on the effect of reaction temperature towards carbonation behavior. It is found that all shells exhibits maximum carbonation at carbonation temperature of 680-700°C. Li et al [10] found that, carbonation conversion of scallop and mussel shells decreased once the calcination temperature was increased from 850°C to 920°C. The capture capacity of the shell also reduced once the synthesized temperature is increased. Higher portion of sodium ion in shells compared to limestone is believed to improve the cyclic calcination and carbonation performance [10].

The observed behavior can be due to thermodynamics relationship of the particle CO_2 with the reaction temperature. Figure 2-12(a) shows the thermodynamics relationship of partial CO_2 pressure with respect to calcination temperature that obtained using the analysis of HSC CHEMISTRY 5.0 software from Outokumpu Research Oy, Finland [34]. The plot shows that higher partial pressure of CO_2 compared to equilibrium pressure will favor carbonation reaction and vice versa. Hence calcination would be favored if the actual partial pressure of CO_2 were lower than 0.1 bar. Calcination at partial pressure of 0.1bar can be induced by increasing calcination temperature beyond 760°C (thermal swing) or at 760°C by reducing the partial pressure below 0.1 bar (pressure swing).

Senthoorselvan et al. [44] also conducted the study on calcination and carbonation. By referring to Figure 2-12(b), equilibrium between calcium carbonate and calcium oxide depends on temperature and CO_2 pressure. At 1 bar, the temperature needs to be around 900°C in order for $CaCO_3$ to be converted into CaO. However, at lower pressure such as 0.2bar, calcination temperature can only be at 800°C for possible calcination to occur. In this study, calcination temperature is varied to study the favorable condition in synthesizing the adsorbent for CO_2 capture.

Thus, to ensure calcination process to occur, the temperature of the process needs to be at least 800°C so that decomposition pressure is able to favor the forward reaction. Based on the CO_2 uptake study done by Lu et al. [45] calcium based material

will completely decompose at 700°C under helium atmosphere since CO_2 partial pressure is zero and the condition is below its equilibrium pressure of 0.03bar. As shown in Figure 2-12, by conducting the process at atmospheric pressure, the external mass transfer resistance can be avoided.

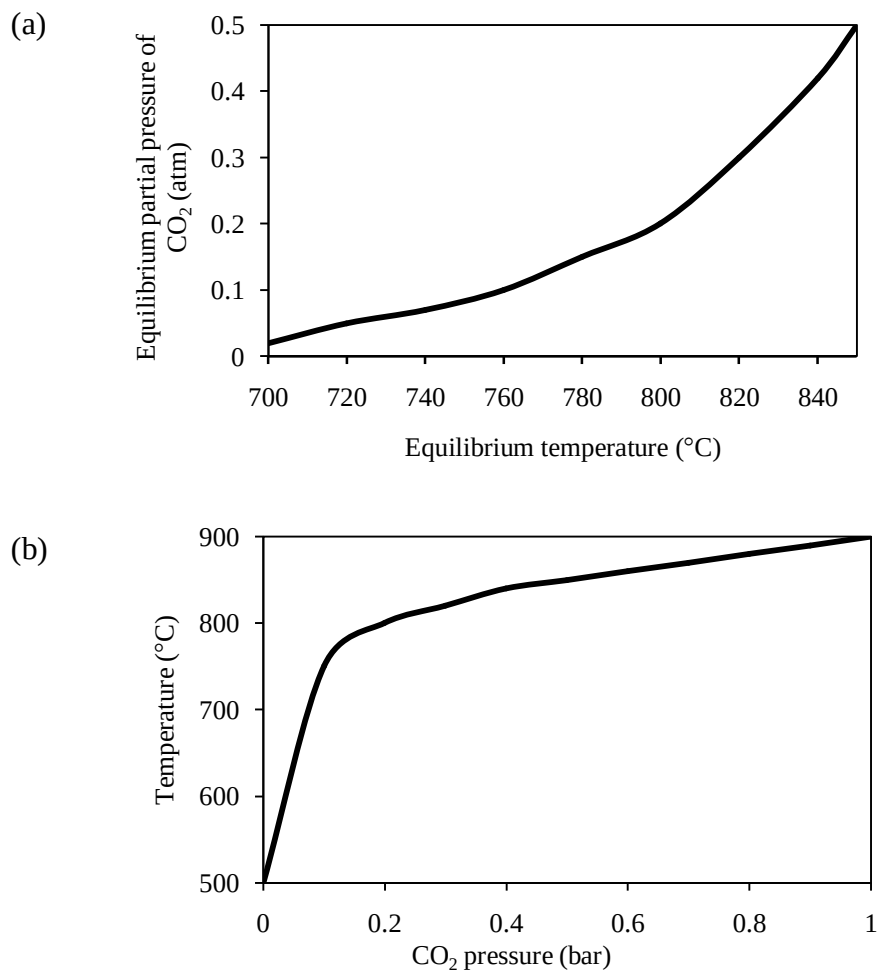

Figure 2-12: Influence of temperature towards equilibrium CO_2 partial pressure (a) Sakadjian et al. [34]; (b) Senthoorselvan et al. [44]

Iyer and Fan [38] apply chicken eggshell as the CO_2 adsorbent and modified it structured by adding acetic acid. The study was conducted using TGA where calcination was set at temperature 700°C for 60 minutes in N_2 and carbonation started once the gas was switched to 10% of CO_2. The performance of eggshell in capturing CO_2 was tested once different types of adsorbent shape were applied (pellet and fines). The results in Figure 2-13 showed that fines types of adsorbent are able to

capture more CO_2 compared to other form of adsorbent. The study also found that reactivity of fine adsorbent is much higher than the pellet adsorbent. However, "the pellets adsorbents were observed to posses better kinetics since mass transfer characteristics is more improved due to thinner diffusional length" [38]. Shorter diffusional length enables the adsorbent to have uniform heat transfer within the particle to initiate carbonation reaction and ease the adsorption of CO_2 by CaO.

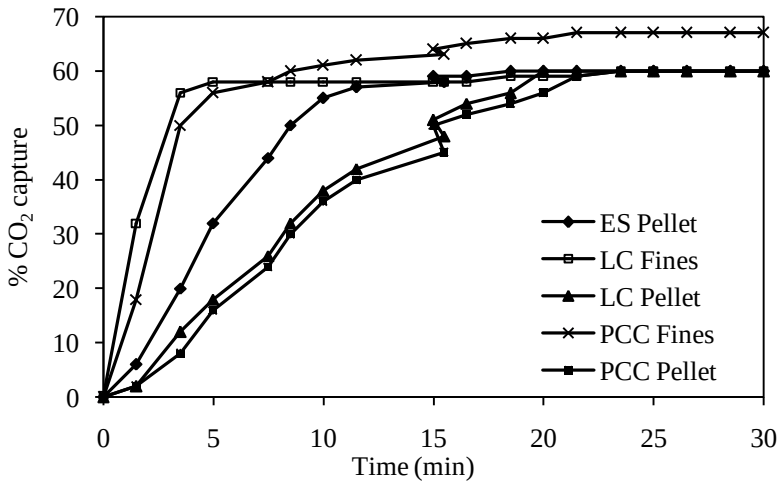

Figure 2-13: Amount of CO_2 captured for different types of CO_2 adsorbent (ES: Eggshell; LC: Linwood carbonate; PCC: Precipitate $CaCO_3$) [38]

Senthoorselvan et al. [44] study on CO_2 separation from flue gases using dolomite and limestone in a number of calcination and carbonation cycles. The performance of the adsorbent was tested at different calcination temperature in 4 cycles. Using TGA to determine the reactivity of the adsorbent, Figure 2-14 shows the results of the amount of CO_2 captured at respective calcination temperature. In the first cycle, highest conversion was experienced by the sample that been calcined at 750°C but not much different with the one that been calcined at 800°C. CO_2 was least been captured by the adsorbent that been calcined at highest temperature (930°C) and the trend is the same but decreasing profile once number of cycle was increased.

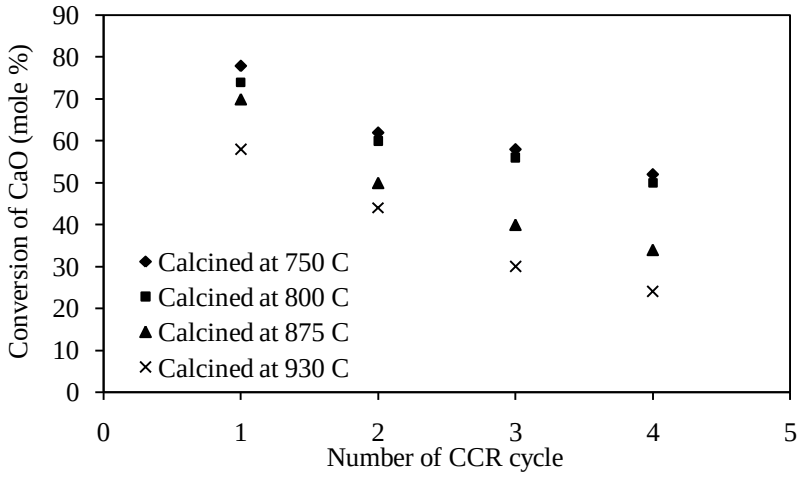

Figure 2-14: Carbonation conversion for the sample that been calcined at different temperature [44]

Bonquet et al. [18] conducted a study on the efficiency of calcination and carbonation cycles using CaO as the adsorbent. The study was conducted in TGA and classical fixed bed reactor for comparison purposes. Calcination was conducted at 850°C for 40 minutes at 20K/min under N_2 flow of 100N *l*/h. The reactivity of CaO was also studied at different calcination temperature and time. Figure 2-15 below shows the results of carbonation conversion that been conducted in a number of calcination carbonation cycles with respect to different calcination temperature and calcination time.

The results show the same behavior obtained by Senthoorselvan et al. [44]. Higher calcination temperature reduce the carbonation conversion of the adsorbent hence smaller amount of CO_2 can be captured. Yet the conversion between the calcined sample at 750°C and 850°C are almost the same. The value keep decreasing as the cycles continues. At 850°C, carbonation was favored when calcination time was 40 minutes yet for 750°C, to achieve highest carbonation conversion, calcination should be hold for 3 hours. As illustrated in Figure 2-15 (b) carbonation is favored once calcination is hold at shorter time length especially when higher calcination temperature (850°C and 950°C) is applied. Therefore, suitable calcination temperature and time should be applied to the synthesized adsorbent in order to achieve better carbonation conversion and higher amount of CO_2 captured.

(a)

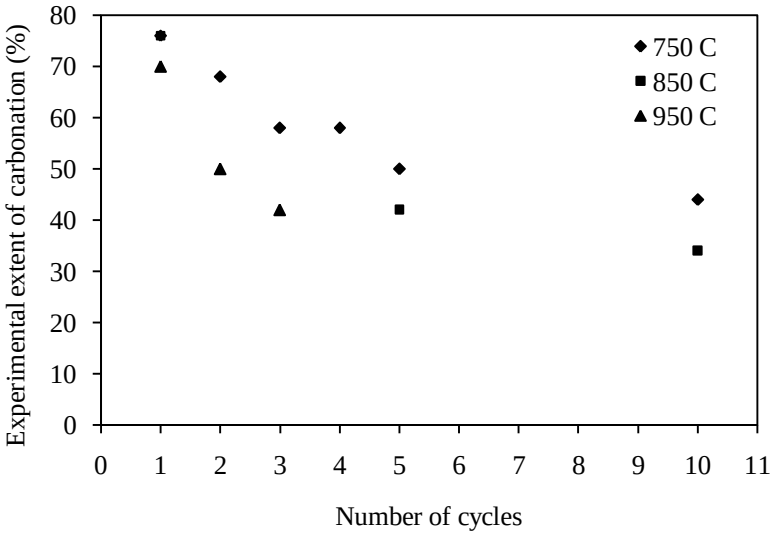

(b)

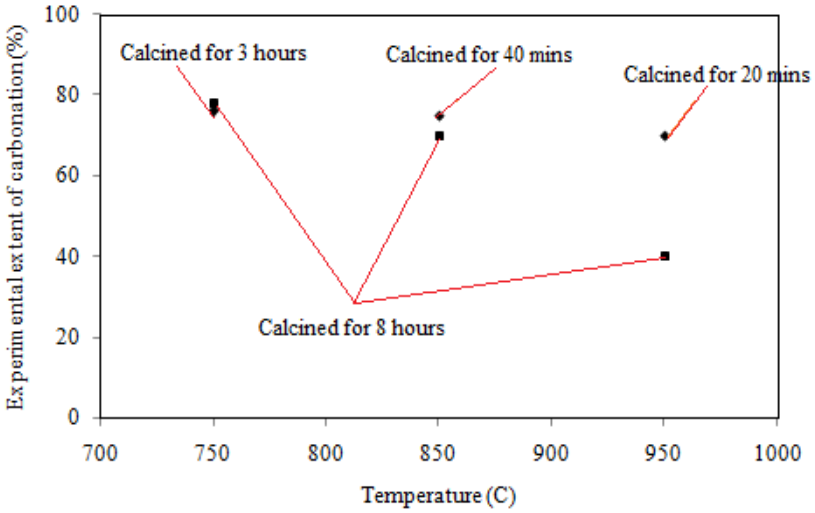

Figure 2-15: Carbonation conversion at different (a) calcination temperature and (b) calcination time [18]

The summary on the effect of calcination condition towards carbonation as conducted by previous study is described in Table 2-7. Based on the literature that been discussed before, calcination conditions such as temperature, particle sizes and shapes can have a major impact on the adsorbent performance. Smaller particle sizes and high calcination temperature (less than 950°C) are favored by most of the researchers. The stated conditions are able to produce high capacity CO_2 adsorbent.

Table 2-7: Summary on previous research on the effect of calcination conditions on carbonation performance of the adsorbents.

Author	Material	Condition varied	Outcome
Bonquet et al. [18]	Mexican limestone	Calcination temperature, calcination time	Higher calcination temperature reduce the carbonation conversion of the adsorbent hence smaller amount of CO_2 can be captured. Carbonation is favored once calcination is hold at shorter time length especially when higher calcination temperature is applied.
Senthoorselvan et al. [44]	Limestone, dolomite	Calcination temperature	Highest conversion was experienced by the sample that been calcined at lower temperature. CO_2 was least been captured by the adsorbent that been calcined at highest temperature (930°C) and the value is decreasing once number of cycle is increased.
Iyer and Fan [38]	Chicken eggshell	Particle size or shape	Adsorbent in powder form is able to capture more CO_2 compared to pellet form of adsorbent. Reactivity of powder adsorbent is much higher than the pellet adsorbent. Pellets adsorbent posses better kinetics than powder form since mass transfer characteristics is more improved due to thinner diffusional length.

2.7 Kinetic study

According to Karagiannis et al. [29], the combination of various experimental conditions such as temperature, mass sample and heating rate, cause the kinetic values to be in different ranges. For instance, high temperature may reduce the activation energy yet at larger particle size, the value may be changed. There is several

limitation factors involve once the reaction of calcination and carbonation occurred which is normally involve gas diffusion factor, chemical reaction or ash layer. The concentration changes are shown in the diagram below (Figure 2-16).

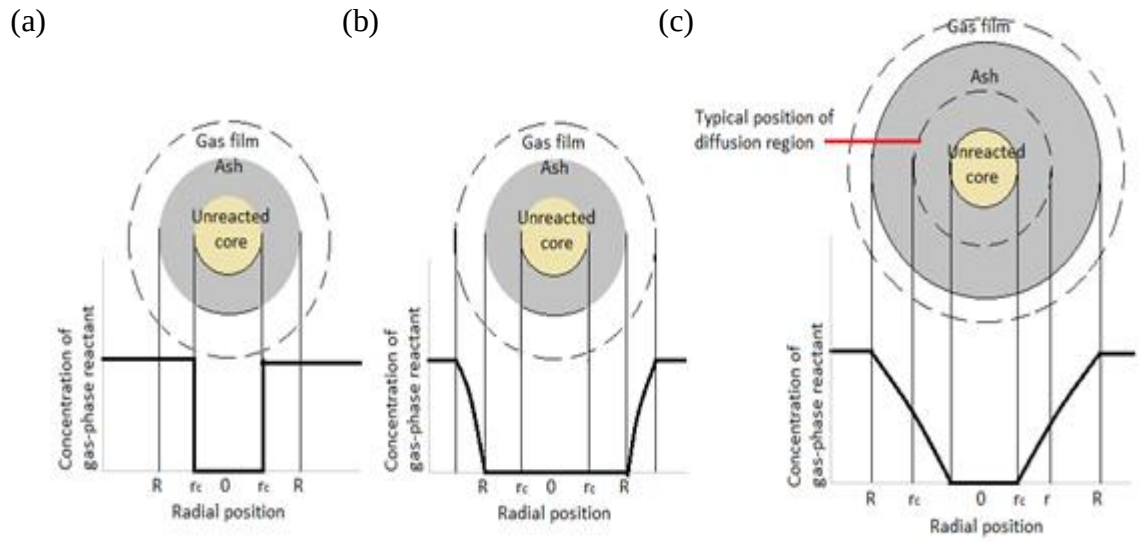

Figure 2-16: Behavior of reacting particle at different limiting factor (a) chemical reaction; (b) gas film (c) diffusion through ash layer [11]

Figure 2-16 provides the illustration on the behavior of the gas and solid during the carbonation once possible limiting steps take place [11]. The mechanism is described based on Shrinking Core Model approach. As shown, the concentration of the gas phase is varied according to the radius of the particle of the sample. Figure 2-16 (a), (b) and (c) illustrate the early, intermediate and final stage of carbonation which involves chemical reaction kinetic control and product layer diffusion control respectively. At early stage of carbonation, reaction between CaO and CO_2 occur where kinetic of chemical reaction take place and the CO_2 gas that build up at the outer layer of CaO adsorbent may produce gas film kinetic control. After a while, the reaction of CaO with CO_2 will form $CaCO_3$ (product/ash layer) at the outer layer of the adsorbent which may cause diffusion kinetic control to turn on.

Overall kinetics of calcination and carbonation for a solid is largely affected by procedural variables and external factors such as heating rate, particle size, sample weight, velocity and pressure of purge gas and composition of the atmosphere. Stanmore and Gilot [15] simplify that kinetics of calcination is complicated by:

1. CO_2 concentrations which inhibit the reaction.

2. Particle size which introduced thermal and mass transfer limitations.

3. Catalysis or inhibition by impurities.

2.7.1 Kinetics for calcination

In dealing with kinetic calculation of the reaction, the Arrhenius rate law is commonly applied. Arrhenius extended the idea by separating the expression according to forward or backward reaction and expressed the rate law as in Equation 2.3. A is known as frequency factor of the reaction while E is the activation energy which is the minimum amount of energy required to initiate the reaction.

$$k = Ae^{-E/RT} \tag{2. 3}$$

According to Gaur and Reed [39] van't Hoff mentioned that the logarithm of the specific rate of a reaction should be a linear function of the reciprocal absolute temperature as depicted in Equation 2.4 and 2.5:

$$\ln K = B - A^{'} / T \tag{2. 4}$$

$$\frac{dlnK}{dT} = \frac{A'}{T^2} = \frac{\Delta H}{RT^2} \tag{2. 5}$$

Since the equilibrium constant is equal to the ratio of k (forward reaction) and k' (reverse reaction), the overall heat of reaction then signifies an energy change for each direction. The above equation can be written as Equation 2.6:

$$\frac{dlnk}{dT} - \frac{dlnk^{'}}{dT} = \frac{E - E'}{RT^2} \tag{2. 6}$$

In Ozawa [46] developed a method using simple integral method that been widely applied for many purposes such as to study high polymer degradation. Based on Ozawa method, activation energy and reaction constant can be obtained by deriving it

at three heating rates. Ozawa claimed that the rate of decomposition must consist of Equation 2.7:

$$\frac{dW}{dt} = A \exp\left(-\frac{E}{RT}\right) W^n \tag{2. 7}$$

Ozawa [46] also mentioned that there are two different major method of analyzing the kinetics. The first part is Equation 2.8 is treated as the differential equation where the fraction of weight needs to be integrated with respect to the temperature. It requires derivation of complex quantities and trial-and-error fitting. The second method is by plotting the logarithm graph to get the kinetic constant where the weight-temperature curve needs to be differentiated graphically. Followings are the steps involved in kinetics analysis based on Ozawa method:

- W is basically the weight fraction of the reacting material which can be expressed in form of structural quantity (x).

$$W = f\ (x) \tag{2. 8}$$

- It is expressed as below where x change according to the ordinary kinetic equation:

$$-\frac{dx}{dt} = A \exp\left(-\frac{\Delta E}{RT}\right) g\ (x) \tag{2. 9}$$

- By integration, Equation 2.9 is expressed as below;

$$-\int_{x_0}^{x} \frac{dx}{g(x)} = A \int_{t_0}^{t} \exp(-\frac{\Delta E}{RT}) dt \tag{2. 10}$$

- At constant heating rate, a, the change in x is given as follow:

$$-\int_{x_0}^{x} \frac{dx}{g(x)} = \frac{A}{a} \int_{T_0}^{T} \exp(-\frac{\Delta E}{RT})\ dT \tag{2. 11}$$

- T_0 is the value of T at $t = t_0$. However, at low temperature, the reaction rate is very low. Thus, the right side of the Equation 2.11 is:

$$\int_{T_0}^{T} \exp(-\frac{\Delta E}{RT})\ dT = \int_{0}^{T} \exp\left(-\frac{\Delta E}{RT}\right)\ dT \qquad (2.\ 12)$$

Ozawa has defined the function of *f(x)*, *g(x)* and $\int dx/g(x)$ as in Table 2-8.

Table 2-8: Mathematical equation for each type of reaction order

Type of reaction	f (x)	g (x)	$\int dx/g(x)$
Zeroth order	*W*	*1*	*W*
First order	*W*	*W*	*ln W*
Second order	*W*	W^2	*-1/W*
Third order	*W*	W^3	$-2/W^2$
Random degradation	$(1-x)^{L-1}\left\{1+x\frac{(N-L)(L-1)}{N}\right\}*$	*-(1-x)*	*-ln(1-x)*

*N: initial degree of polymerization and L is the least number of repeating units of polymer not volatized. The approximation for N>>L: $f(x) = (1-x)^{L-1}\{1+(L-1)\,x\}$.

Dollimore et al. [47] explained that in 1885, Hood recorded the first logarithmic relation between specific reaction rates with respect to the temperature which is as follows:

$$\log k = \frac{A'}{T} + Constant \qquad (2.\ 13)$$

k = rate constant; A' = preexponential factor

T= Temperature

Then Arrhenius then restated the relationship as follows:

$$\ln k = -\frac{E}{RT} + ln\ A \qquad (2.\ 14)$$

E = activation energy; R= gas constant

Or :

$$k = Ae^{-E/RT} \quad (2.\ 15)$$

However, in 1995, Harcout and Esson put an alternative to the equation by assigning *C* and *m* is to be constant and positive constant respectively, as below:

$$k = CT^{m} \quad (2.\ 16)$$

According to Dollimore et al. [47] concentration term is "meaningless" for solid state reaction. Instead, the extent of reaction or fraction decomposed, denoted by α, is significant for the process. Since there are various types of solid state reaction mechanism exist as described in Table 2-9, the determination on the suitable mechanism is based on following steps;

Specific reaction rate constant then is defined as:

$$\frac{d\alpha}{dt} = k\, f(\alpha) \quad (2.\ 17)$$

$f(\alpha) =$ function of α according to reaction mechanism

For non-isothermal kinetic studies, the usual method of analysis is simply to utilize the following relationships. The first is to relate temperature, T, with the rate of heating, b.

$$T = T_0 + bT \quad (2.\ 18)$$

T = temperature (°C); T_0 = Initial temperature (°C)

b = heating rate (°C/min)

By combining Equation 2.17 and 2.18, kinetic expression will lead to:

$$\frac{d\alpha}{dT} = \frac{d\alpha}{dt}\ x\ \frac{dt}{dT} = \frac{k\, f(\alpha)}{b} \quad (2.\ 19)$$

Or

$$k = \frac{\left(\frac{d\alpha}{dT}\right) b}{f(\alpha)} \tag{2. 20}$$

By following the Arrhenius equation, the expression will be:

$$\ln\left(\frac{\left(\frac{d\alpha}{dT}\right) b}{f(\alpha)}\right) = \ln A - \frac{E}{RT} \tag{2. 21}$$

$$g\ (\alpha) = \int_0^{\alpha} \frac{d\alpha}{f(\alpha)} = \frac{A}{b} \int_{T_i}^{T} e^{-\frac{R}{T}}\, dT \tag{2. 22}$$

Table 2-9: Classification of mathematical expressions of reaction mechanism [47]

Mechanism	$g(x) = \int \frac{d\propto}{f(\propto)} = k\,t$	$f(\propto) = \frac{1}{k}\left(\frac{d\propto}{dt}\right)$
1) *Acceletory α-t curves*		
P_1 Power law	$\alpha^{1/n}$	$n(\alpha)^{(n-1)/n}$
E_1 Exponential law	$\ln \alpha$	α
2) *Sigmoidal α-t curves*		
A_2 Avrami-Erofeev	$[-\ln (1-\alpha)]^{1/2}$	$2(1-\alpha)[-\ln(1-\alpha)]^{1/2}$
A_3 Avrami-Erofeev	$[-\ln (1-\alpha)]^{1/3}$	$2(1-\alpha)[-\ln(1-\alpha)]^{2/3}$
A_4 Avrami-Erofeev	$[-\ln (1-\alpha)]^{1/4}$	$2(1-\alpha)[-\ln(1-\alpha)]^{3/4}$
B_1 Prout-Tompkins	$\ln[\alpha/(1-\alpha)] + C$	$\alpha(1-\alpha)$
3) *Deceleratory α-t curves*		
3.1 Geometrical models		
R_2 Contracting area	$1-(1-\alpha)^{1/2}$	$2(1-\alpha)^{1/2}$
R_3 Contracting volume	$1-(1-\alpha)^{1/3}$	$3(1-\alpha)^{2/3}$
3.2 Diffusion mechanisms		
D_1 One-dimensional	α^2	$\frac{1}{2}\alpha$
D_2 Two-dimensional	$(1-\alpha)\ln(1-\alpha) + \alpha$	$[-\ln(1-\alpha)]^{-1}$
D_3 Three-dimensional	$[1-(1-\alpha)^{1/3}]^2$	$3/2(1-\alpha)^{2/3}[1-(1-\alpha)^{1/3}]^{-1}$
D_4 Ginstling-Brounshtein	$(1-2\alpha/3)-(1-\alpha)^{2/3}$	$3/2\,(1-\alpha)^{-1/3} - 1]^{-1}$
3.3 Order of reaction		
F_1 First order	$-\ln(1-\alpha)$	$1-\alpha$
F_2 Second order	$(1-\alpha)^{-1}$	$(1-\alpha)^2$
F_3 Third order	$[(1-\alpha)]^{-2}$	$\frac{1}{2}(1-\alpha)^3$

A plot of [(dα/dT)b/f(α)] against 1/T can allow the determination of activation energy (E) and frequency factor (A). Figure 2-17 demonstrates the method of identifying all of the parameters involved in calculation using the developed model. By identifying the parameters described in Table 2-9 and Table 2-10, will enable a kinetic mechanism to be identified or narrowed down the option for mechanisms. Once the value of Ti and Tf is obtained, such a scheme is presented in flowchart of Figure 2-18 can be used to finalized the reaction mechanism that can be applied in the analysis [47]. Type of reaction mechanism is determined based on the value of conversion, α, $\Delta L_oT/\Delta H_i T$ and characteristics of T_i and T_f.

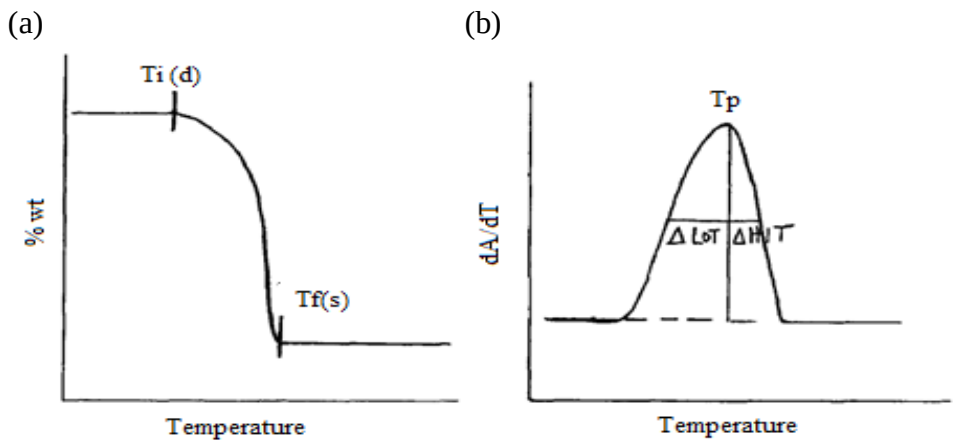

Figure 2-17: (a) Typical TGA plot showing Ti diffuse and Tf sharp and (b) typical dTG plot showing the half plot [47]

Table 2-10: Characterization of kinetic mechanisms based on the shape of TG plots [47]

Group	Mechanism	Characteristics features of T_i and T_f	$\Delta L_oT/\Delta H_i T$
A	A_2, A_3, A_4	T_i sharp, T_f sharp	≈1
B	R_2, R_3, D_1, D_2, D_3, D_4	T_i diffuse, T_f sharp	>>1
C	F_1, F_2, F_3	T_i diffuse, T_f diffuse	≈1

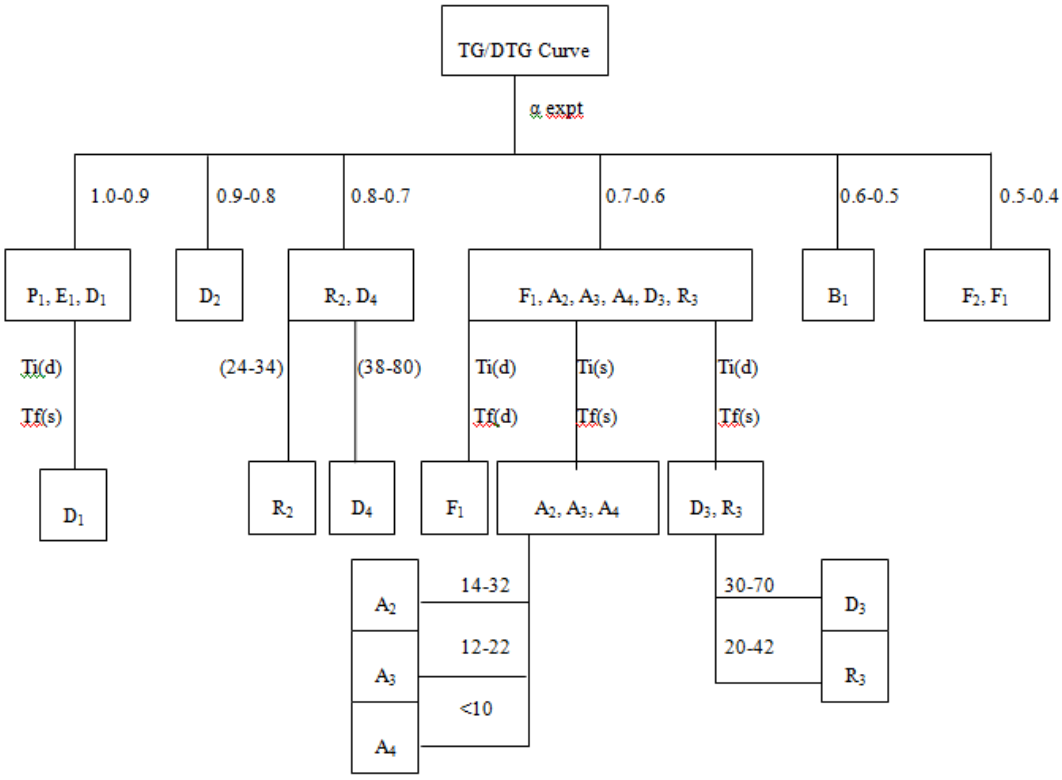

Figure 2-18: Flow chart showing the procedures in recognizing the kinetic mechanisms [47]

Samtani et al. [7] apply Arrhenius equation in analyzing the kinetics of solid state calcination. Fraction of the sample reacted during the calcination is denoted by α, represents the weight loss of the sample at the current temperature with respect to the overall weight loss.

$$\alpha = \frac{w_i - w_t}{w_i - w_f} \tag{2. 23}$$

α: fraction decomposed ; w_i: initial weight (mg)

w_t: current weight (mg); w_f: final weight (mg)

Where the differential form of the equation will be as follows:

$$\frac{d\alpha}{dt} = -\frac{\left(\frac{dw_t}{dt}\right)}{w_i - w_f} \tag{2. 24}$$

$\frac{d\alpha}{dt}$: differential rate of decomposed fraction;

$\frac{dw_t}{dt}$: differential rate weight loss (dTG)

Thus, the rate of reaction is represented by dα/dt as follows:

$$\frac{d\alpha}{dt} = kf(\alpha) \tag{2. 25}$$

$$k = \frac{d\alpha/dt}{f(\alpha)} \tag{2. 26}$$

k: rate of reaction constant (1/min)

$f(\alpha)$: function of α according to reaction mechanism

Arrhenius equation that to be fitted for this process is as follows:

$$\ln k = \ln A - \frac{E}{RT} \tag{2. 27}$$

By combining equation (5) in (6):

$$\ln \frac{d\alpha/dt}{f(\alpha)} = \ln A - \frac{E}{RT} \tag{2. 28}$$

The values of dw_t/dt are obtained from the differential thermogravimetric plot (derivative weight). This value is substituted into Equation 2.27 which is then can be used to plot the Arrhenius graph of dα/dt versus 1/T. The slope of the graph will yield activation energy, E, of the process and the intercepts of y axis represents exponential A which is the value on ln k, rate constant. The value of f (α) is given in Table 2-11. The right applied model is determined based on the best fit linear line that been plotted [7].

Basically, the methods discussed are using the same principle of kinetic analysis for solid decomposition. The same reaction mechanism is used which is acceleratory, sigmoid and decelerator α-t curve. Table 2-12 give out the summary of the methods for kinetic analysis that been explained in this section. Based on the literatures, all of the methods used are applying the basic equation of Arrhenius. Yet, some modification is made to suit the process under studied such as steady and non-steady

state reaction. Besides, the approach of choosing reaction mechanism of the process is various, either by best fitting points or value of temperature gradient and dTG area ratio. Therefore, the selection of suitable approach to do kinetic analysis will depend on the process condition and available data in the study.

Table 2-11: Classification of mathematical model for reaction mechanism [7]

Kinetic classification	f(α)
1) *Acceletory α-t curves*	
P1 Power law	$n(\alpha)^{(n-1)/n}$
E1 Exponential law	α
2) *Sigmoidal α-t curves*	
A_2 Avrami-Erofeev	$2(1-\alpha)[-\ln(1-\alpha)]^{1/2}$
A_3 Avrami-Erofeev	$2(1-\alpha)[-\ln(1-\alpha)]^{2/3}$
A_4 Avrami-Erofeev	$2(1-\alpha)[-\ln(1-\alpha)]^{3/4}$
B_1 Prout-Tompkins	$\alpha(1-\alpha)$
3) *Deceleratory α-t curves*	
3.1 Geometrical models	
R_2 Contracting area	$2(1-\alpha)^{1/2}$
R_3 Contracting volume	$3(1-\alpha)^{2/3}$
3.2 Diffusion mechanisms	
D_1 One-dimensional	$\frac{1}{2}\alpha$
D_2 Two-dimensional	$[-\ln(1-\alpha)]^{-1}$
D_3 Three-dimensional	$3/2(1-\alpha)^{2/3}[1-(1-\alpha)^{1/3}]^{-1}$
D_4 Ginstling-Brounshtein	$3/2\ (1-\alpha)^{-1/3} - 1]^{-1}$
3.3 Order of reaction	
F_1 First order	$1-\alpha$
F_2 Second order	$(1-\alpha)^2$
F_3 Third order	$\frac{1}{2}(1-\alpha)^3$

Table 2-12: Summary of previous research on kinetic analysis of calcination process

Author	Method
Dollimore et al., [47]	• The options of various reaction mechanisms are narrowed down using the value of T_i and T_f of TG and dTG curve. • Considering heating rate in the developed model. • Plotting $\ln\left(\frac{\left(\frac{d\alpha}{dT}\right)b}{f(\alpha)}\right)$ against 1/T to yield linear plot and obtain activation energy and reaction constant. $$\ln\left(\frac{\left(\frac{d\alpha}{dT}\right)b}{f(\alpha)}\right) = \ln A - \frac{E}{RT}$$
Ozawa [46][39]	• An expression of g(x) is introduced to cater the function of conversion involved in the process. • The right applied model is determined based on the best fit linear lime that plotted $$-\frac{dx}{dt} = A\exp\left(-\frac{\Delta E}{RT}\right)g\ (x)$$
Samtani et al., [7]	• Plotting $\ln\frac{d\alpha/dt}{f(\alpha)}$ against 1/T to yield linear plot and obtain activation energy and reaction constant. • The right applied model is determined based on the best fit linear line that plotted $$\ln\frac{d\alpha/dt}{f(\alpha)} = \ln A - \frac{E}{RT}$$

2.7.2 Kinetics for carbonation

Lee [48] developed a model on determining the kinetic of carbonation of CaO with CO_2 by utilizing the results obtained by Bhatia and Permutter [19] and Gupta and Fan [27]. The model stated that carbonation rate is rapid at low conversion level of different initial heating rate which depends on temperature. Ultimate conversion, X_u, reached once no more significant conversion attained and the conversion rate is approaching zero. Rate of conversion is expressed as below:

$$\frac{dX}{dt} = k\left(1 - \frac{X}{X_u}\right)^n \tag{2. 29}$$

k = reaction constant (min-1)

X= conversion

X_u = ultimate conversion

N= reaction order

By integrating Equation 2.30 with n=1 and n=2, the following conversion expressions can be obtained respectively:

$$X = X_U\left[1 - \exp\left(\frac{-k}{X_u}t\right)\right] \tag{2. 30}$$

$$X = \frac{X_U t}{\left(\frac{X_u}{k}\right) + t} \tag{2. 31}$$

In Equation 2.31, if a constant b is the time taken to get half ultimate conversion, *then* $X = X_u/b$ at $t = b$. By substituting this expression, the equation is defined as:

$$X_u = kb \tag{2. 32}$$

Substituting Equation 2.32 in Equation 2.31 will yield below equation:

$$X = \frac{kbt}{b + t} \tag{2. 33}$$

If molar rate of CO_2 removal is interested, assuming no external mass transfer limitation of CO_2 to CaO particles will yield another expression as below:

$$rCO_2 = \frac{1}{M_{CaO}}\left(\frac{dX}{dt}\right) \tag{2. 34}$$

$$\mathrm{M_{CaO}} = \text{Molecular weight of CaO } \left(\frac{\mathrm{g}}{\mathrm{mol}}\right)$$

To determine the kinetic parameters by data fitting, Equation 2.33 can be written in linear form as follows:

$$\frac{1}{X} = \frac{1}{k}\left(\frac{1}{t}\right) + \frac{1}{kb} \tag{2. 35}$$

Figure 2-19 indicates the plots of *1/X* against *1/t* in order to obtain the value of *k* and *b* and differentiate the value with respective controlling regions. Therefore, the final value will provide the activation energy and reaction constant for each regime.

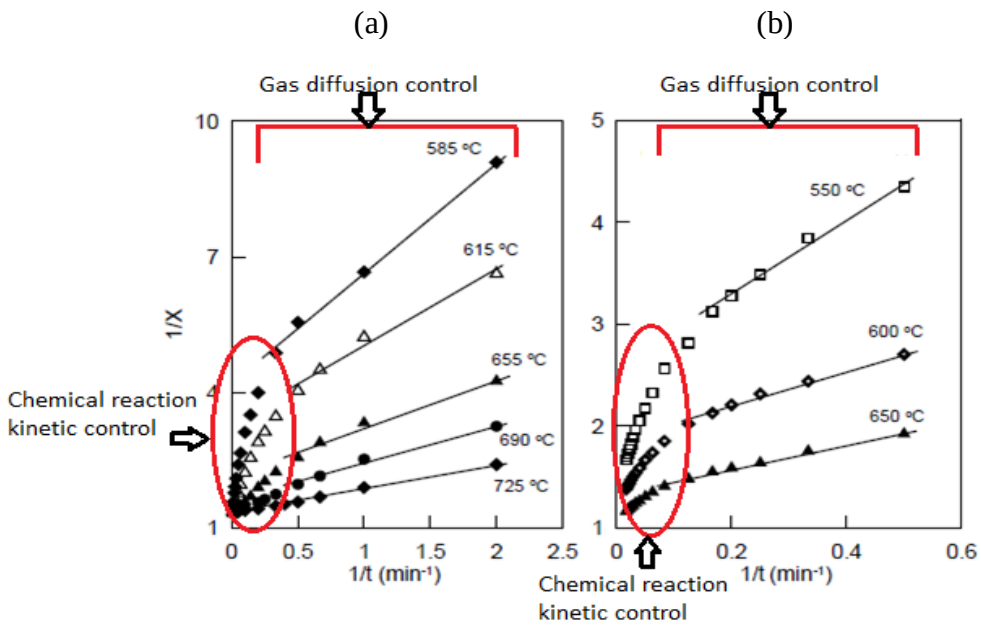

Figure 2-19: Plot of *1/X* against *1/t* using conversion data of (a) Bhatia and Perlmutter; (b) Gupta and Fan [48]

Sun et al. [49] also conducted the study on determining the rate constant for carbonation using atmospheric thermogravimetric analyzer (ATGA) and pressurized thermogravimetric analyzer (PTGA). The analysis on carbonation kinetic is based on gas solid reaction model. Grain model under kinetic control was used to determine the kinetic-controlled region and the equation is provided as below:

$$\frac{dX}{dt\,(1-X)^{2/3}} = 3r \tag{2. 36}$$

In integral form:

$$\left[1-(1-X)^{\frac{1}{3}}\right] = r\,t \tag{2. 37}$$

Using Equation 2.37, a plot of $1-(1-X)^{\frac{1}{3}}$ against t should illustrate a straight line of slope r which indicates the reaction is under kinetic control as shown in Figure 2.20. The slow-down stage is controlled by both surface reaction and product layer diffusion, showing a lower slope. Thus, constant value of r in kinetic controlled region is chosen to expand and to represent the rate of conversion at zero point *(r_0= r)*. Table 2-13 described the summary of the previous work on kinetic for carbonation which been explained in this section.

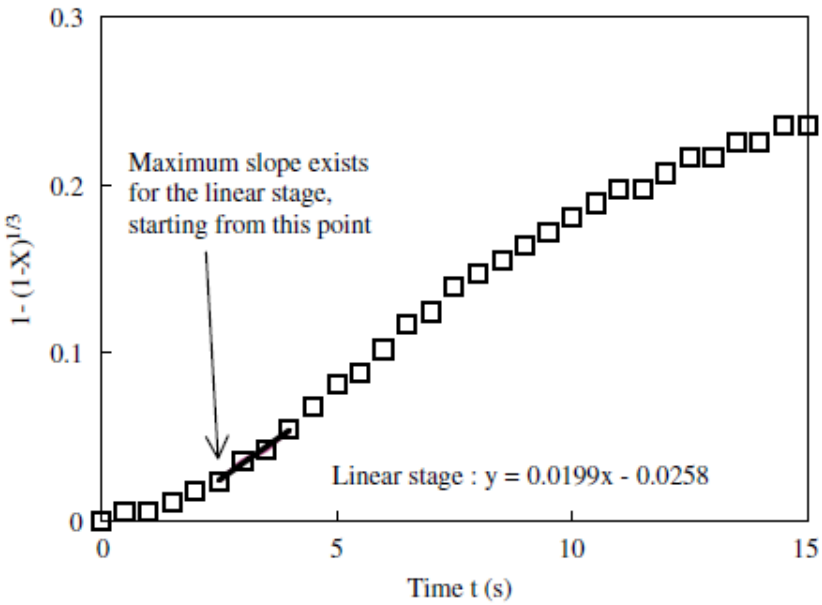

Figure 2-20: "Slope extraction with the aid of the grain model during early stages of carbonation for 38–45 µm Strassburg limestone particles at 700 °C with 15% CO_2 and 85% He" [49]

Table 2-13: Summary on kinetic analysis by previous research for carbonation

Author	Method
Lee [48]	Conversion is determined as : $X = kbt/(b+t)$ Rate of carbonation conversion as follows: $dX/dt = k(1 - X/X_u)^2$ Fitting the data to the linear model according to the regions to obtain reaction constant, k.
Sun et al. [49]	Grain model for gas solid reaction kinetic model is applied. Integral form for the reaction: $$\left[1-(1-X)^{\frac{1}{3}}\right] = r\,t$$ $1-(1-X)^{\frac{1}{3}}$ against t illustrate straight line of slope r which indicates the reaction is under kinetic control.

2.8 Summary

The chapter described the reliability of waste cockle shell as the potential natural occurrence source for CaO based adsorbent. By discussing on the production rate experienced of the country and future development regarding culturing and cultivating the cockle, it can be seen as abundant source in Malaysia. Thus, it has the potential to be the source of biomass for CO_2 capturing purpose and it is a promising option.

The chapter also explained the definition and mechanism involved in synthesizing the adsorbent which is called calcination and the process to capture CO_2 which is known as carbonation reaction. These processes can be done using many types of equipment either fluidized or fix bed circulation bed concept using fuel, inert gases, air or even solar energy as the source of heat. Reactivity of the reaction normally been studied using TGA.

In addition, the chapter also includes the study on CO_2 removal conducted by previous researchers using CaO based adsorbent. Till date the application of natural occurrence resources such as egg shells, limestone, dolomite, clam shells and mussel shells as the precursor of CaO based adsorbent shows a promising future and

comparable efficiency. Besides, the study on the effect of different operating conditions on CO_2 capture capacity by previous researchers was also described. Literature provides insight of the crucial part that ready to be understood regarding the optimum operating condition to synthesize and capture CO_2 so that the process is efficient and economical.

A number of kinetic models were developed by previous studies to analyze the kinetics of synthesizing process and its capturing reaction. The kinetic analysis for synthesizing the adsorbent (calcination) involves solid state reaction while carbonation is based on gas solid reaction. The analysis is based on Arrhenius equation in order to obtain activation energy and reaction constant at each phase. Carbonation is mostly involving chemical reaction kinetic control at initial stage and gas diffusion control at the end of the reaction.

Based on the literature review, application of waste shell as the main source for CO_2 adsorbent is widely applied. Yet no application of cockle shell as the CO_2 adsorbent can be found. Therefore, the utilization of waste cockle shell as the adsorbent in CO_2 removal field is perhaps can be a novel and good initial point for future CaO based adsorbent development especially in capturing CO_2. By understanding the influence of operating condition on the efficiency of the synthesis process and carbonation, it is expected that waste cockle shell can be an efficient and economical potential as the alternative adsorbent. In addition, kinetic model by Samtani et al. [7] has been adapted in this study to determine the kinetic properties for calcination of cockle shell while model developed by Lee [48] is applied for kinetic analysis during carbonation reaction of the synthesized CaO.

CHAPTER 3

METHODOLOGY

3.1 Chapter Overview

This chapter described the overall research methodology and procedures to synthesize CaO from waste cockle shells. It explained the procedures to study the performance of the material by using TGA and the suitable characterization approaches that been adopted in this study.

3.2 Overall Research Procedures

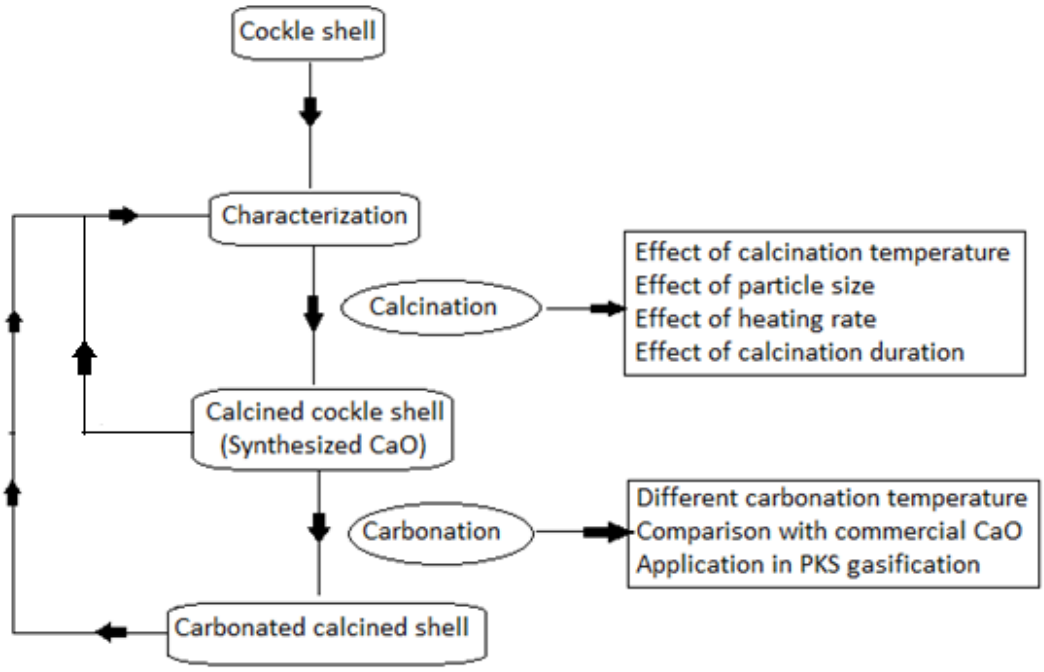

Figure 3-1: Flowchart of overall process involved in the study (PKS: Palm kernel shell)

Figure 3-1 illustrates the overall research procedures that been used for the completion of the study. After thorough literature review on the adsorbent development using natural resources and reliability of the sources, cockle shell is selected to be the raw material of the adsorbent. Since, the source is a waste and biomass material, the sample need to be carefully prepared. Material characterization is a crucial step to ensure the characteristics and properties of the sample chosen are comparable to the standard adsorbent and suitable for CO_2 adsorption.

Once the characterization analysis shows that $CaCO_3$ contained in the sample, calcination is conducted at different calcination condition to simulate their effects on carbonation reaction of the synthesized CaO. Once the condition for maximum carbonation is obtained, the behavior and capability of synthesized CaO is examined under different reaction temperature. The performance of the sample is compared once commercial $CaCO_3$ is used for calcination and carbonation at the same condition. In addition, synthesized CaO is used as CO_2 adsorbent during pyrolysis and steam gasification of palm kernel shell (PKS) where the performance of synthesized CaO is also been compared with commercial CaO.

3.3 Raw material

Chemical used in this study include Sigma Aldrich calcium carbonate (99+% purity), Sigma Aldrich calcium oxide (98% purity) and cockle shell powder from size ranges of less than 0.125mm to 4mm (~97% purity). Cockle shells were obtained from a stall that purchased cockles originated from the cultivation center in Perak. Therefore, the species of the cockle shell used in this study is a type of *Anadara Granosa,* a common species that grew well in southern east region. The gases involve are inert Nitrogen (N_2) gas with purity of 99.999% and Carbon Dioxide (CO_2) with purity of 99.8% which are supplied by MOX-Linde Gas Berhad.

3.3.1 Material Preparation

Cockle shells were washed with raw water to remove dirt and been dried under the

sun for two consecutive days and also using oven at 110°C for 2 hours. Shells were crushed using pestle and mortar which was then been ground into the powder form using Rocklabs rotation grinder. The shell powder was sieved in the shaker sieve for 10 minutes to ensure the powder was segregated well into various particle size groups (less than 0.125mm- 4mm).

Figure 3-2: Preparation of cockle shell powder to be used in this study

3.4 Material Characterization

By referring to Dann [50], material characterization is a crucial part of a research study as the approaches managed to discover the characteristics of the developed material including chemical and physical properties, reactivity or magnetic properties and structure. Four different types of chemical and structural analysis has been conducted for analysis of chemical composition, crystal types of the compound, surface morphology, and the pore properties of the samples. The characterization methods include x-ray fluorescence (XRF), x-ray diffraction (XRD), scanning

electron microscopy (SEM), energy dispersive x-ray (EDX) and physisorption analyzer.

The chemical composition of cockle shell was analysed using x-ray fluorescence, XRF (Bruker S4 Pioneer) while the crystal structure of the sample were estimated using x-ray diffraction, XRD (Bruker d8 Advance), which was run in 2 theta range 1 to 80° with step size of 0.05 and step time of 1s. SEM (Oxford Leo 1430) is useful in order to visualize the surface changes of the sample during the process. The result of EDX and SEM which estimate elemental composition and surface morphology respectively, are verified using XRD. In addition, Physisorption Analyzer (Micromeritics ASAP 2020 Accelerated Surface Area and Porosimetry Analyzer) is used to examine the pores property of the sample of different material types, surface area and porosity.

3.4.1 Thermal Gravimetric Analyzer (TGA)

TGA is a common thermal method used in many areas of chemistry to determine both phase changes as a function of temperature and to determine unknown quantities such as levels of hydration or oxygen content. It measures the property of a material as a function of temperature. Thermogravimetry analyses were carried out at desired heating rate (10-50°C/min) under N_2 (50 ml/min), over the whole range of temperature (50-950°C). EXSTAR 6000 TGA Analyzer is used to study the reactivity of the synthesizing process and its CO_2 capturing capability during carbonation.

The samples (~10 ±2 mg) were placed in the ceramic crucibles. The data on the effect of experimental conditions (particle size, heating rates, calcination temperature and period) on carbonation ability of cockle shell was recorded using Muse TA Rheo System. Sample mass and gas flow rate are kept constant throughout the reaction.

3.4.2 X-ray Diffraction (XRD)

In order to estimate the position of atoms in a solid, Dann [50] claimed that, XRD analysis can give the best estimation among other method and it is extensively

applied. Position of the atoms can determine the structure of the solid since the x-ray beam will scatter due to the atom position of the sample and normally, the typical wavelength used is 0.6-1.9 Å.

In this study, XRD (Bruker d8 Advance) is used to analyze the samples powder of raw cockle shell, synthesized CaO, carbonated cockle shell and the standard calcium oxide and calcium carbonate of Sigma Aldrich. The main objective is to determine the compound contained in the sample, and also the structure of the sample through its crystal morphology changes. Thus, the analysis were done at the standard operating condition which is 2 theta range 1 to 80° with step size of 0.05 and step time of 1s. Diffraction of a powder sample which contains enormous small size crystallites (10^{-7}-10^{-4} m) can recognize various range of the x-ray beam orientation.

3.4.3 X-ray Fluorescence (XRF)

The samples of pure cockle shell, synthesized CaO, calcium carbonate and calcium oxide were analyzed to get the comparison of each chemical composition. The sample was in powder form and 20 g each is needed for the testing using Bruker AXS, XRF S4 Pioneer.

3.4.4 Scanning Electron Microscopy (SEM)

The surface morphology structures were observed and analyzed by SEM Oxford Leo 1430. The changes of the sample surface structures can be illustrated, before and after the reaction is carried out. It is also important to conduct SEM to describe the pore destruction of formation after carbonation is done. An energy dispersive x-ray spectroscopy (EDX) was used to analyze the elemental composition in the samples during carbonation and calcination.

3.4.5 Physisorption Analyzer

Physisorption analyzer (Micromeritics ASAP 2020 Accelerated Surface Area and

Porosimetry) analysis helps to determine pore properties of the sample. Type of sample material (microporous, mesoporous, macroporous) can be determined using this analyzer. In addition, it also provides the value for surface area, pore volume and pore diameter of the samples. In this study, cockle shell, synthesized CaO, carbonated cockle shell and the standard adsorbents are among the samples that been analyzed. Using 3 ±0.1g sample weight, it is being degassed in liquid nitrogen at temperature of 77K for 4 hours before being analyzed.

3.4.6 Energy Dispersive X-ray (EDX)

Since XRF is unable to count in the elements which have very small proportion in a sample, while EDX is used to compensate with this disability. The comparison on the analysis results is included in Section 4.2.

Table 3-1: Summary on the characterization approach that adopted and the sample involved.

Characterizing approach	Model	Objective	Sample
X-Ray Fluorescence (XRF)	Bruker S4 Pioneer	Chemical analysis (Oxides & Elements)	Cockle shell, synthesized CaO, carbonated shell, Aldrich CaO.
Scanning Electron Microscopy (SEM)	LEO Model 1450	Surface morphology	Cockle shell, synthesized CaO, carbonated shell, Aldrich CaO+synthesized CaO.
Energy Dispersive X-ray (EDX)	Oxford-Inca Energy 200 Premium	Chemical analysis (Elements)	Cockle shell, synthesized CaO, carbonated shell.
Physisorption Analyzer	Micromeritics ASAP 2020 Accelerated Surface Area and Porosimetry	Pore properties	Cockle shell, synthesized CaO, carbonated shell, Aldrich CaO.

3.5 Effect of calcination conditions on carbonation

The study of calcination and carbonation was done by means of TGA. Small amount of sample (~10 ± 2 mg) is used to possibly eliminate the effect of thermal resistance due to sample mass. Atmospheric gas can be distributed evenly and minimized temperature gradient between sample and the sample holder. In addition, heating process will be more linear although the exothermic process may cause in-homogeneities or irregularities [51].

Table 3-2 summarizes the experimental conditions used to study the effect of each parameter. The selection of desired parameters to study are based on the literature reviews on the common factors that regularly been studied by previous researchers. Followings are the steps for calcination and carbonation that been used in this research which is generally applied in most of the related studies during previous work:

- Initially, nitrogen gas was set to flow at 50 ml/min.
- Then 5-10mg of cockle shell powder in desired particle size was placed in ceramic sample crucible.
- N_2 flow was set to continuously flow until the concentration reading for all gas is 0%. This step is considered as purging step.
- TGA was heated up at 110°C for 10 minutes to remove moisture content in the sample.
- The heating was proceed to desired calcination temperature and been hold for certain period.
- Then, the sample was cooled down to carbonation temperature.
- Finally, CO_2 gas was switched on while N_2 gas was shut down for carbonation to occur.
- The conditions were hold until no significant weight change was observed from the TG curves.

Table 3-2: Experimental condition to study the effect of calcination conditions on carbonation

Temperature Calcination (°C)	Calcined Duration (min)	Particle size (mm)	Heating rate (°C/min)	Temperature Carbonation (°C)
750	30	< 0.125	20	650
850	30	< 0.125	20	650
950	30	< 0.125	20	650
850	40	< 0.125	20	650
850	60	< 0.125	20	650
850	30	0.5-1.0	20	650
850	30	2.0-4.0	20	650
850	30	< 0.125	10	650
850	30	< 0.125	50	650

3.6 Comparison study on the performance of synthesized CaO with commercial adsorbent

The steps were done using TGA (EXSTAR 6000). Carbonation took place in atmosphere of CO_2 which was switched on once carbonation temperature is reached and the process condition was held constant until there is no weight change observed. The run was repeated for a minimum of two times to reduce the error that might occur during the testing. Table 3-3 describes the experimental conditions used for the experiment to study the effects of calcination condition on the synthesis of CaO process and its CO_2 capturing ability at different carbonation temperature.

Table 3-3: Experimental condition for carbonation of synthesized CaO

Temperature Calcination (°C)	Calcined Duration (min)	Particle size (mm)	Heating rate (°C/min)	Temperature Carbonation (°C)
850	30	< 0.125	20	500
				650
				850

The ability of synthesized CaO from cockle shell also been tested to adsorb CO_2 during gasification with and without steam of palm kernel shell (PKS). The performance of the sample is compared with commercial CaO (Aldrich CaO). The performance is measured based on concentration of CO_2 in the outlet gas flow which been analyzed by Gas Chromatography (GC Agilent 7890). The unit is equipped with two thermal conductivity detectors (TCD) and a flame ionization detector (FID). H_2, CO and CO_2 were measured using TCD detectors fitted with Molsieve 5A and Hayesep Q columns. Lower concentration of CO_2 in the outlet gas signifying that CO_2 been adsorbed well by the adsorbent and vice versa. Followings are the procedures applied during the reaction which was conducted using TGA.

- Initially, nitrogen gas was set to flow at 50 ml/min.
- Then mixed of ~5±0.2 mg of PKS and ~5±0.2 mg adsorbent powder was placed in ceramic sample crucible.
- N_2 flow was set to continuously flow until the concentration reading for all gas except N_2 is 0%. This step is considered as purging step.
- TGA was heated up at to reaction temperature (900°C)
- For gasification with steam, the flow was switched on at 110°C and the flow rate was kept constant at 0.005 ml/min.
- The heating is preceded to 900°C and been hold for 10 minutes to provide enough time for the reaction to occur.
- Then, the sample was cooled down to ambient temperature.

Table 3-4: Experimental conditions for PKS gasification

Particle size of PKS (mm)	Particle size of synthesized CaO and Aldrich CaO (mm)	Heating rate (°C/min)	Reaction temperature (°C)	Calcined Duration (min)
0.25-0.5	< 0.125	20	900	10

Calcination process of cockle shell and the ability of synthesized CaO during carbonation also been compared to commercial carbonate source (Aldrich $CaCO_3$) and mix of cockle shell and Aldrich $CaCO_3$ (1:1 weight ratio). The procedures are the same with the step explained in Section 3.5, yet the operating conditions were different as displayed in Table 3-5. The conditions were chosen based on the conditions where CaO synthesized from cockle shell performance carbonation behavior to be the best.

Table 3-5: Experimental condition using different carbonate sources

Temperature Calcination (°C)	Calcined Duration (min)	Particle size (mm)	Heating rate (°C/min)	Temperature Carbonation (°C)
850	40	< 0.125	20	650

3.7 Chapter Summary

Overall, this chapter has described all of methods and approached that been applied in this study. It covered the steps of characterizing the samples using XRF, XRD, physisorption analyzer, SEM and EDX. Besides, the methods of understanding the reactivity of synthesized adsorbent (CaO) from cockle also has been described in this chapter. Procedures of testing CO_2 capture ability of the synthesized CaO via carbonation were also described. Calcination and carbonation methods described in this chapter have been established and implemented by most of the previous studies. The novelty involve since raw material of this research are a waste and biomass resources. Overall, using the described methods, TGA has demonstrated its ability to illustrate the reactivity of synthesizing adsorbent and performance of the adsorbent by using it to conduct carbonation reaction.

CHAPTER 4

RESULTS AND DISCUSSION

4.1 Chapter Overview

This chapter illustrates and elaborates the results gained throughout the study. It is divided into four main sections which are material characterization, carbonation behavior under various calcination conditions, comparison of carbonation performance among cockle shells and commercial adsorbent, and kinetic analysis of calcination and carbonation reaction. Calcination is a process of synthesizing calcium oxide (CaO) from cockle shell while carbonation is referring to carbon dioxide (CO_2) capturing reaction using the synthesized CaO.

Material characterization section discloses the outcome of the analysis done to the sample using XRF, XRD, EDX, SEM and physisorption analyzer. The results display chemical and physical properties of the samples used in this research such as chemical composition, surface morphology and type of crystallization in the sample. The transition occurred to the sample after undergoing the reaction is better visualized and understand through this analysis.

Behavior of cockle shell during calcination and carbonation under various calcination conditions is demonstrated using TGA. TG and dTG curves record weight change in the sample with respect to time and temperature, which enable the demonstration of phase transitions of the sample throughout the reaction. For instance, calcination is indicated by weight lost and carbonation is denoted based on weight gain. Besides, exothermic and endothermic region of the reaction can also be determined using dTG curves.

In addition, the performance of cockle shell in capturing CO_2 is tested at different

carbonation temperature in order to visualize the capability of the material to withstand high temperature process. The performance of cockle shell also been compared with Aldrich $CaCO_3$ (less 0.125 mm with 99% purity) which is calcined at same condition to yield CaO. In addition, cockle shell is utilized as CO_2 adsorbent during gasification of palm kernel shell. The capability of the shell is measured based on the concentration of CO_2 gas at the outlet gas stream detected by the installed Gas Chromatography (Model: Agilent GC 7890). The results are also compared with the commercial adsorbent.

The final section of this chapter is discussing on kinetics analysis for calcination and carbonation reaction. Since calcination of cockle shell involve only solid decomposition reaction, therefore, the analysis is based on solid reaction mechanism as been described by most of the researchers previously explained in Chapter 2. Carbonation is a gas solid reaction and therefore a developed model that fit to its reaction mechanism is implemented.

4.2 Material Characterization

A number of characterization methods have been conducted in order to verify the characteristics of the developed material. The analysis was conducted before and after the calcination and carbonation reaction. Material characterization is important to confirm the nature of physical morphology and disclose the characteristics of the involved material. In addition, the analysis helps to visualize the structure changes occurred of the sample which influences the efficiency of the synthesized adsorbent.

4.2.1 X-Ray Fluorescence Analysis (XRF)

In order to estimate the composition of the sample, analysis of XRF is conducted. XRF is able to provide estimation based on metal oxide or metal compound of the sample. Based on the chemical analysis done using XRF, the major element of cockle shell is found to be Calcium which is approximately 70%wt. The percentage

composition is similar to the commercial adsorbent, synthesized CaO and carbonated shells.

As described in Table 4-1, there are presence of other metal elements in the cockle shell and synthesized CaO. However, the amount is relatively very small and due to this small amount, it is assumed that these elements will not affect the calcination and carbonation reaction. XRF analysis indicates the amount of the compound contained in the cockle shells and synthesized CaO are almost the same with the commercial calcium oxide (Aldrich CaO). Thus the application of cockle shell as the alternative source of calcium based material or precursor is acceptable.

Table 4-1: Elemental analysis of raw cockle shell using XRF

Element	Cockle shell (%wt)	Synthesized CaO (%wt)	Aldrich calcium oxide (% wt)	Carbonated cockle shell (%wt)
Ca	69.99	70.22	70.12	70.99
O	29.00	29.00	29.00	29.00
Al_2O_3	0.65	-	-	-
Mg	0.27	0.48	0.87	-
Fe, Sr, Cl, Si	<1.00	<1.00	-	-

4.2.2 X-Ray Diffraction Analysis (XRD)

In order to determine the crystal structure of the sample and to verify the outcome of XRF analysis, XRD characterization method was conducted for cockle shell, synthesized CaO and commercial adsorbents samples. XRD analysis required the sample amount to be not less than 1g. The calcined samples were prepared using horizontal tube furnace. 5 grams of cockle shell was placed in the ceramic sample boat and calcined at 850 °C for 30 minutes in nitrogen atmosphere. The flow rate of nitrogen and heating rate of the process was kept constant at 0.5 l/min and 20 °C/min respectively. CO_2 infrared gas analyzer (Model 7500, Teledyne Analytical

Instrument) was installed at the outlet of the unit to monitor CO_2 concentration at the outlet gas.

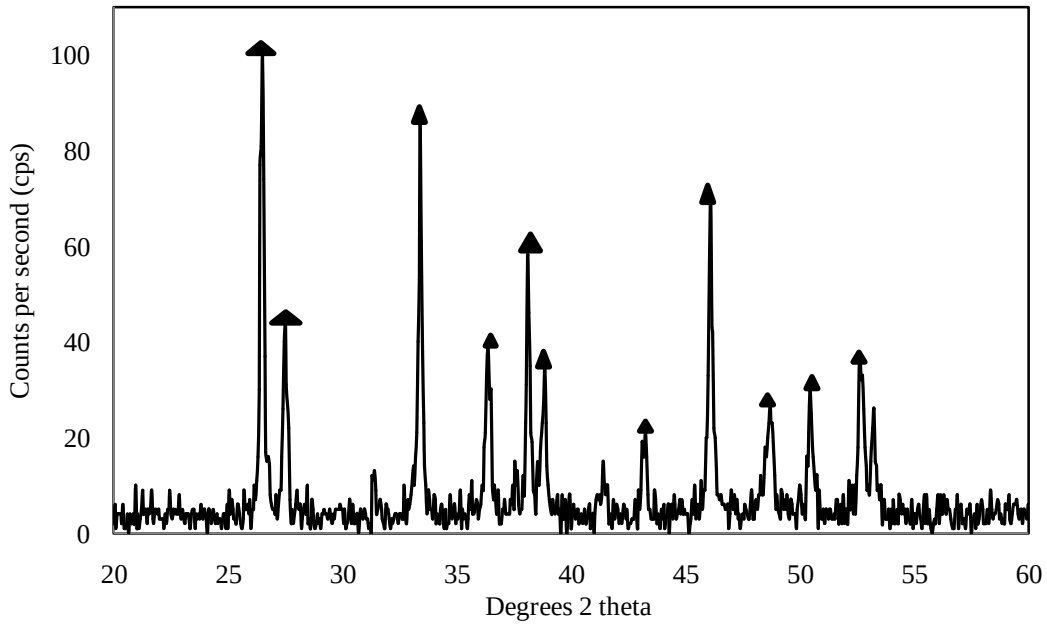

Figure 4-1: XRD spectra of the raw cockle shell (▲ = $CaCO_3$)

Based on the XRD spectrum which is illustrated in Figure 4-1, it is found that cockle shell is made up of aragonite, a type of calcium carbonate ($CaCO_3$) polymorph other than calcite and vaterite [43]. Aragonite ($CaCO_3$) is the least abundant of calcium carbonate crystal and has smaller range of physico-chemical condition as it is able to transform into calcite [52]. Even though calcite is the most stable polymorphism of calcium carbonate, aragonite has higher density and hardness which make it very suitable material in plastic, paper, glass fiber and other industry [53]. Aragonite can be good filler for paper and polymer material since it can improve the mechanical properties of the material [52] [43]. Thus, the finding has shown its existence as constituent of calcium carbonate in the shell.

XRD analysis for synthesized CaO was conducted to ensure the calcination done was able to convert calcium carbonate contained in the shells into calcium oxide as stated in the Equation 2.1. From the analysis, it is evident that calcium oxide has been produced by calcining the shell at 850 °C for 30 minutes in inert atmosphere. Figure 4-2 illustrated the spectra for synthesized CaO and found that CaO compound was

present in the sample. Therefore the approach and methodology of calcining cockle shells at high temperature in inert atmosphere was able to decompose calcium carbonate into calcium oxide.

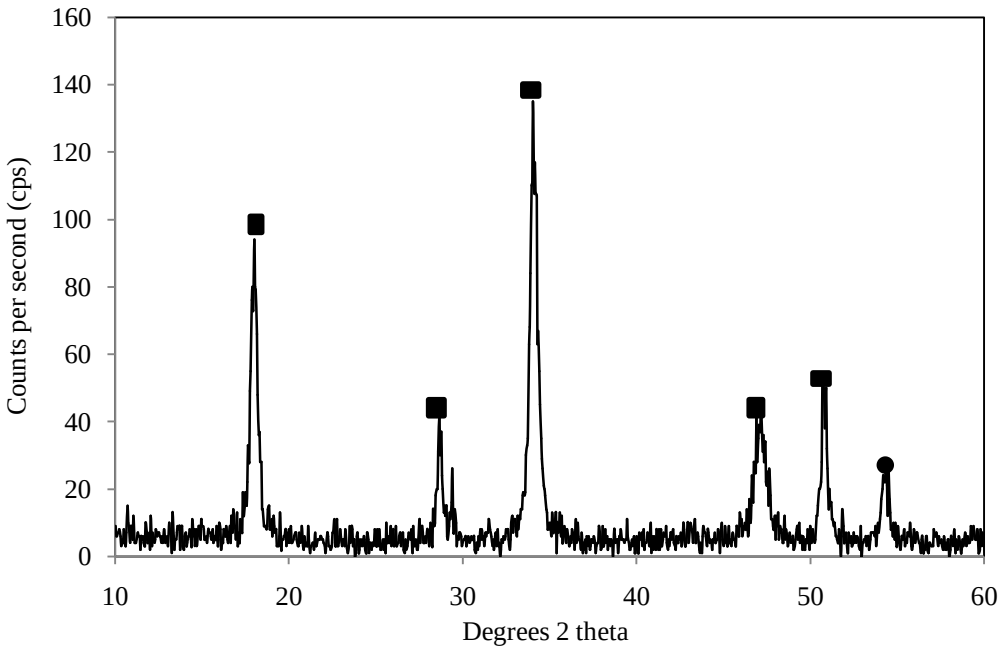

Figure 4-2: XRD spectra of synthesized CaO (■ = CaO; ● = impurity)

The analysis of XRD has also been conducted using commercial sample of Aldrich calcium carbonate at purity of 99%. To ensure the comparison is acceptable, the particle size of cockle shell powder and Aldrich calcium carbonated used, was selected to be in the same ranges of particle sizes approximately 0.1mm. Figure 4-3 illustrates the spectra of Aldrich calcium carbonate. As can be observed, the spectrum of Aldrich calcium carbonate is smoother than cockle shell spectrum where the peak is sharper and less broad.

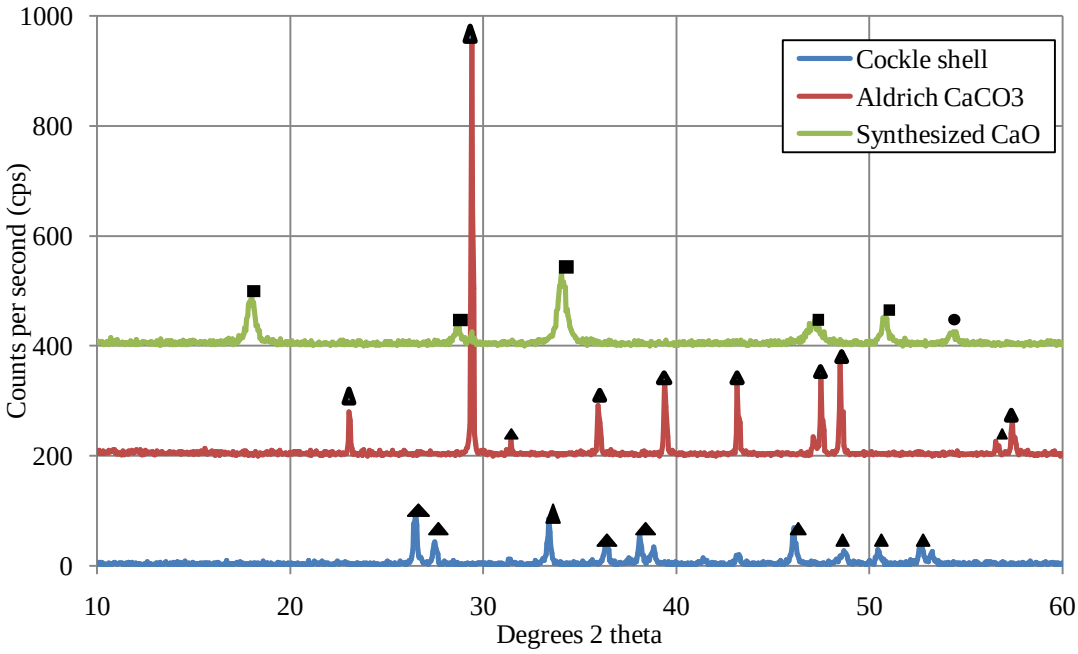

Figure 4-3: XRD spectra of commercial calcium carbonate (▲ = $CaCO_3$; ■ = CaO; ● = Impurity)

According to the Manual of Basic XRD of Scintag [54], sharp and narrow diffraction peak indicates the crystallinity of the sample while very broad peak shows the sample is amorphous. Connoly [55] mentioned that intensity of a peak represents the total scattering of the beam from the plane of crystal structure and it depends on the distribution of atoms in the material. In this case, cockle shell and synthesized CaO have broad peak compared to the commercial $CaCO_3$. Plus, the peak intensity of commercial $CaCO_3$ is higher compared to the one observed for cockle shell.

The difference in peak intensity and peak broadness might due to the difference in type of crystal own by the natural resources of cockle shell which is aragonite polymorph and its crystal type is orthorhombic. Inversely, commercial $CaCO_3$ polymorph is calcite where its crystal type is rhombohedron as observed in SEM analysis. Difference in crystal structure create changes in ray diffraction during the analysis hence influence its peak intensity and broadness.

In addition, Dann [50] claimed that relative intensity of each phase in a mixture of compounds indicates its amount and it depends on crystal class, lattice types, symmetry, unit cell parameter and distribution and type of atom in unit cell. However

in this case, there is only one compound presents in the each sample and the spectrum for all of the samples illustrates relatively narrow and sharp peaks. Thus, based on the intensity and shapes of the peaks, the samples involved in this study are crystalline type of material.

4.2.3 Scanning Electron Microscopy Analysis (SEM)

SEM is a method of getting the images of the surface structure of the sample. The electrons beam will be attracted to the atoms and creates the patterns and images of the structure. Theoretically, aragonite has a needle like structure while calcium oxide has more uniform, well distributed and sphere like structure [56]. Thus, to visualize this image, SEM analysis was conducted for the samples of cockle shell, synthesized CaO, commercial calcium oxide, commercial calcium and mix of synthesized CaO and commercial oxide.

Figure 4-4 illustrates the structure of cockle shell obtained in this study where it is commonly known as needle-like structure. According to Wang and Thomson [52], the natural occurrence of needle-like or whisker structure of aragonite is due to biogenic origin and mineral organisms. However, there are some research being conducted to produce this kind of structure and the process relies on temperature, solution pH and additives [56]. Hu et al. [56] synthesized the aragonite using limestone and Figure 4-4 illustrates the images of the needle like aragonite obtained during the study. This observation is almost the same (long and sharp end) with the work done by Hu et al. [56] who did the study to synthesis aragonite.

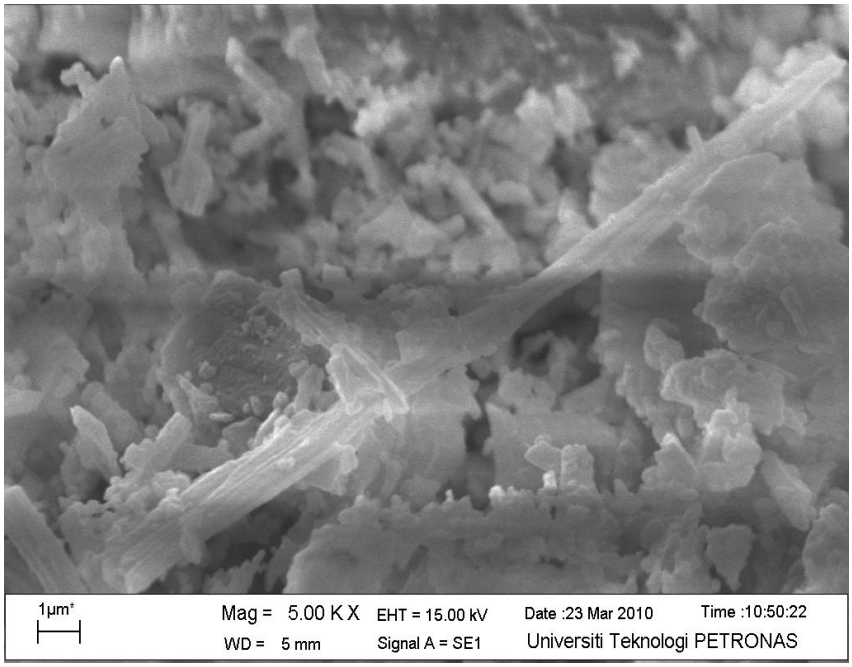

Figure 4-4: SEM image of aragonite in cockle shell obtained for the study

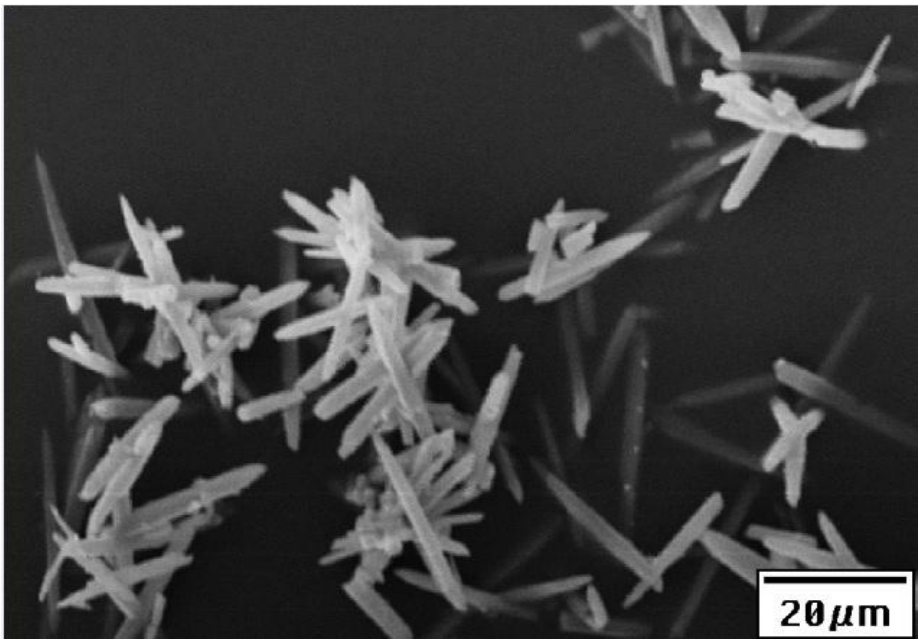

Figure 4-5: SEM image of aragonite obtained from limestone by Hu et al. [56]

Figure 4-6 shows the surface morphology of the synthesized CaO. By comparing the image in Figure 4-7, SEM analysis on calcined limestone done by Sun et al. [49], the structure of the synthesized CaO is almost the same. Sun et al. [49] claimed that the grain shape are almost spherical but with some evidence of initial grain-neck

growth due to early stage of sintering and this behavior indicates that grain model is a suitable model to describe the calcination process and determine the kinetic analysis of the process, although the grains are not perfectly spherical.

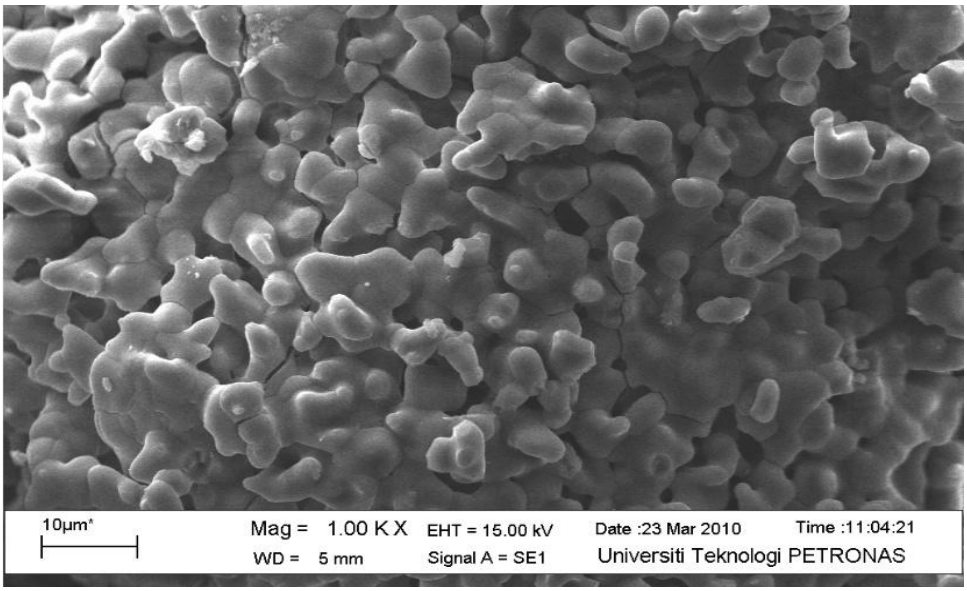

Figure 4-6: SEM image of synthesized CaO under inert condition at 850°C obtained in the study

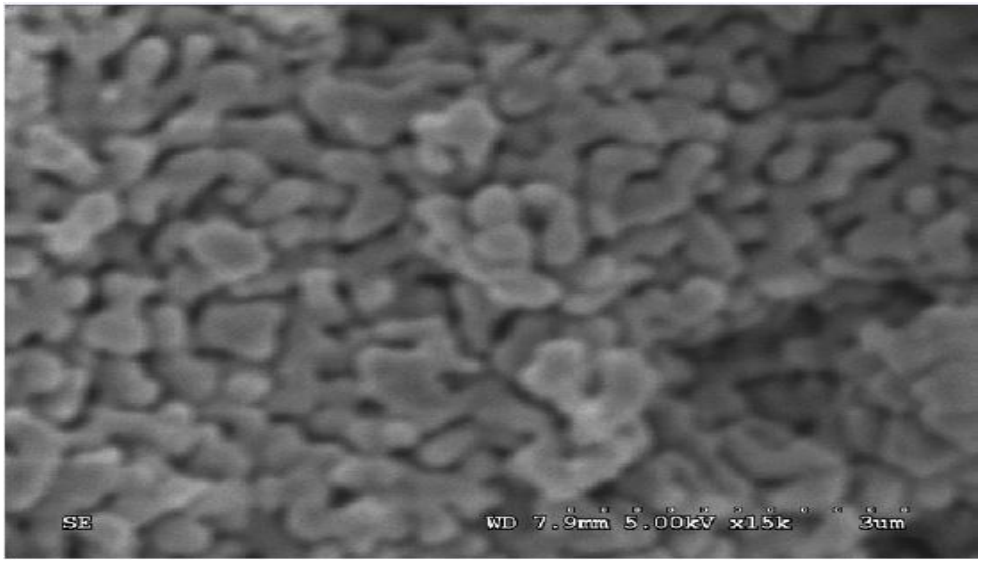

Figure 4-7: SEM images of calcined limestone under inert condition at 850°C, found by Sun et al [49]

Figure 4-8 show the image of the synthesized CaO that had been mixed with Aldrich calcium oxide. Aldrich CaO and $CaCO_3$ are made up of the calcite (polymorph type of $CaCO_3$) which in this case it provides the rhombohedron crystal structure as shown in the figure. The presence of Aldrich calcium oxide has varied the shape and structure of the adsorbent and theoretically it should provide more surface area for the reaction to take place. Thus the action of mixing the adsorbents in this study is hoped to increase the performance of the adsorbent during carbonation. Till date, development of mixing adsorbent with cockle is hardly to be found.

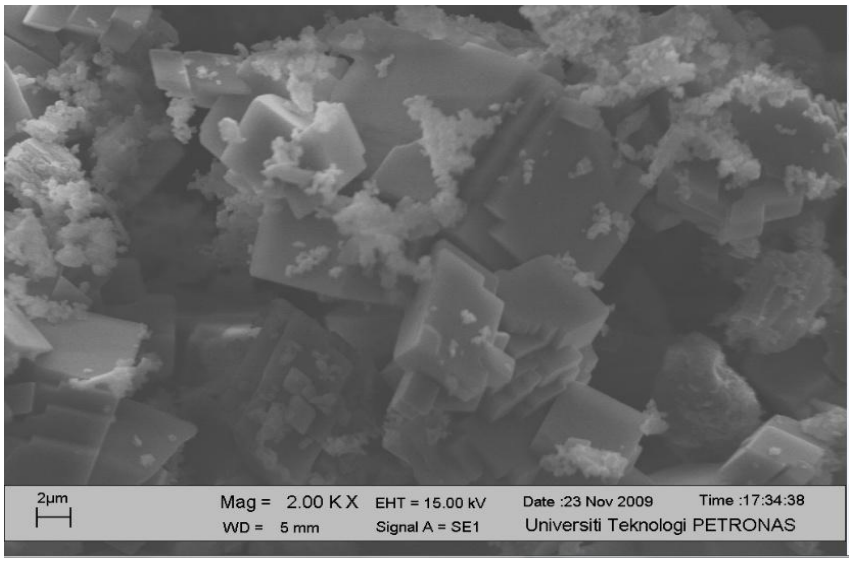

Figure 4-8: SEM image of synthesized CaO in inert condition at 850°C for 30 minutes which is mixed with Aldrich calcium oxide

Figure 4-9 illustrates the surface structure of the carbonated shell, the synthesized CaO after carbonation at 650°C. The surface of the adsorbent shows like a saturated adsorbent since not much open pores can be observed at the surface. CO_2 that fills in the pores of the adsorbent and react with CaO cores, cause the adsorbent to granulate and coarsen. Product layer of $CaCO_3$ caused the grain size to be relatively increased and having less pore compared to the previous images before capturing the CO_2. The same observation was found by Abanades and Alvarez as depicted in Figure 4-10 which indicates the surface changes of calcium oxide adsorbent after calcination-carbonation process. Abanades and Alvarez [17] provide carbonation atmosphere of composition 15% CO_2 and 85%N_2, while this study apply 100% CO_2 atmosphere.

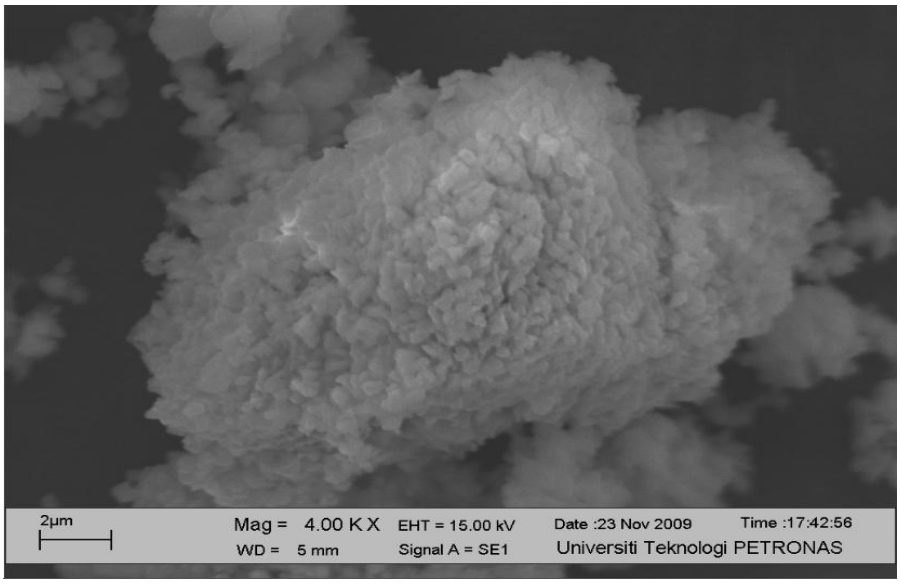

Figure 4-9: SEM image of synthesized CaO after carbonation at 650°C in 100% CO_2

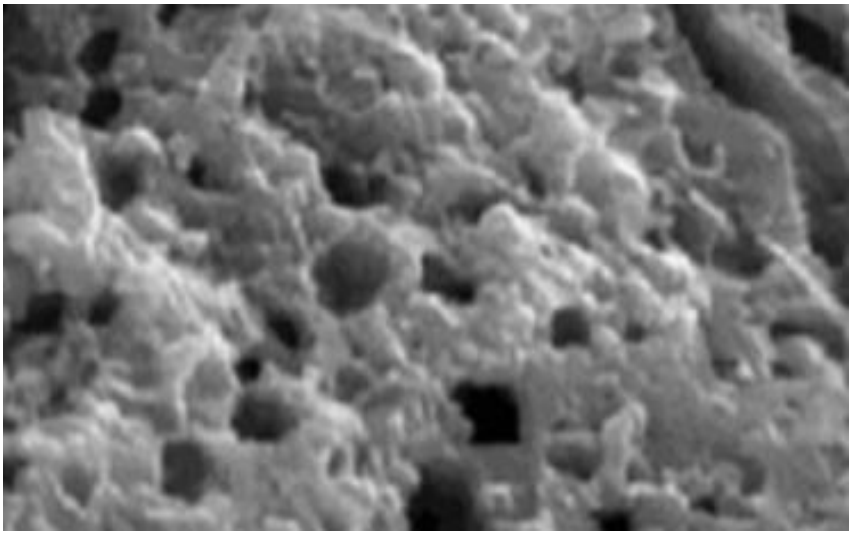

Figure 4-10: SEM image of carbonated calcium oxide as studied by Abanades and Alvarez [17]

4.2.4 Energy Dispersive X-ray Analysis

EDX is a technique used to identify the elements contained in a material. It is also a way of determining the efficiency of the reaction that has been conducted. Besides, the content of the elements in the sample like $CaCO_3$ and CaO also were tested. At

different calcination condition, the elements that present in the sample are analyzed to ensure the calcination and carbonation conditions used in the study is able to synthesis CaO. Thus, this analysis is aimed to ensure the calcination condition used is correct and also to confirm the findings of other analyzer like XRF.

Figure 4-11 indicates the maps of EDX analysis for cockle shell. The results show the presence of carbon, oxygen and calcium elements in the sample. The content of the elements were analyzed based on the weight percent where raw cockle shell contained 15.77% (C), while oxygen is 55.39% (O), and calcium 28.85% (Ca) by weight as shown in Figure 4-12. Thus this analysis confirmed the presence of the carbon in the sample.

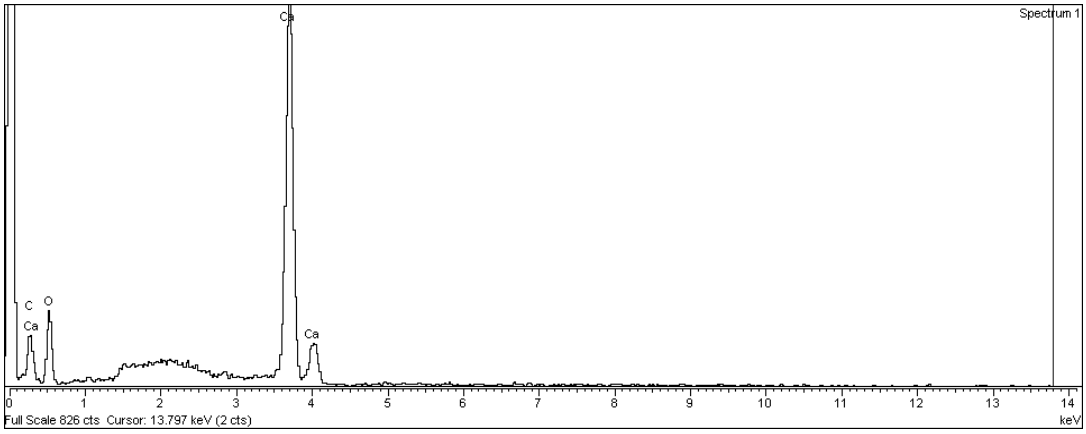

Figure 4-11: EDX spectrum of raw cockle shell

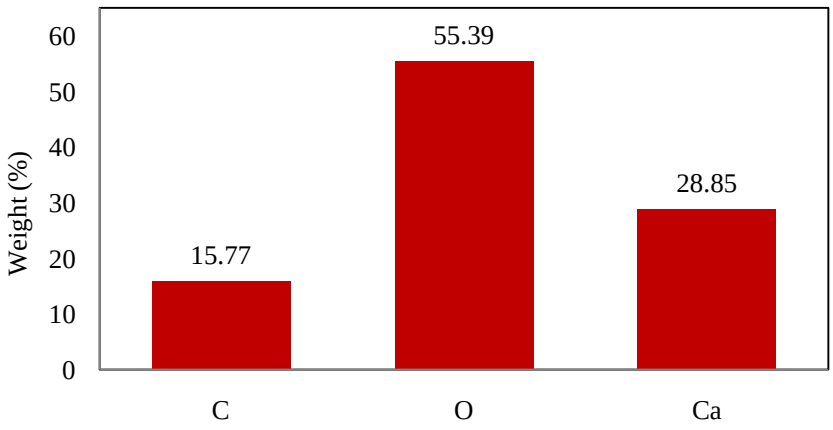

Figure 4-12: Elemental content in raw cockle shell through EDX analysis

EDX analysis was also conducted for the calcined samples at different calcination conditions, in order to find out the elemental content of the sample with respect to different calcination condition. The analysis is to verify whether the calcination condition used in the study is able to eliminate the carbon source and producing the metal oxide. Table 4-2 describes the amount of each elements contained in the sample once various calcination condition are applied. Based on this analysis, carbon still exists although the calcination was already conducted at 850°C for 20 minutes. However, when the calcination duration was increased to 40 minutes, there are increment in the amount of Ca and O while no presence of carbon elements can be observed.

Table 4-2: EDX analysis of synthesized CaO at different calcination duration

Calcination duration (min)	Calcination temperature (°C)	Element weight (%)		
		C	O	Ca
20	850	11.62	48.27	40.11
40	850	-	45.19	54.81
20	950	-	47.56	52.64
40	950	-	53.64	46.36

The same observation of absence of carbon and only calcium and oxygen exist occurred when calcination was conducted for 20 minutes at 950°C or 40 minutes at the same calcination temperature. However, with longer calcination time will reduce the amount of calcium in the sample. Therefore, based on this analysis, the changes of the elemental weight can be observed once the experimental variables are changed. Presence of carbon indicates that calcination conducted at holding time of 20 minutes is not enough for a complete carbonate conversion into CaO. C element is eliminated faster (20 minutes calcination duration) once calcination temperature is raised to 950°C yet at lower temperature the calcination duration needs to be longer (850°C in 40 minutes).

4.2.5 Physisorption Analysis

As the study is about synthesizing and developing an adsorbent, thus, physisorption analysis is crucial to determine the surface area and porosity properties of the sample. In this study, physisorption analysis has been conducted for five samples which are the commercial calcium carbonate and calcium oxide (Sigma Aldrich), raw cockle shell, the synthesized CaO and carbonated sample. The purpose of this analysis is to enable comparison between the involved samples based on pore sizes, area and volume of the sample and to illustrate the changes occur to the sample after undergone calcination and carbonation. In addition, surface area is an important factor that influences synthesis process and carbonation reaction

The sample preparation for raw cockle shell, synthesized CaO and carbonated sample are prepared according to procedures that been described in Chapter 3. To ensure a reasonable comparison, the properties of samples are kept within standard. For example, the particle size of commercial calcium oxide and calcium carbonate used in the comparison study are less than 0.125 mm. Therefore, the particle size for the cockle powder and synthesized CaO prepared are controlled within this range. In addition, XRF analysis also indicates that the almost similar composition among these carbonate sources. Therefore, the comparison of the samples is reliable.

As shown in Table 4-3, cockle shell contained higher surface area and pore width (size) compared to Aldrich $CaCO_3$. In addition, surface area, pore volume and average pore diameter of synthesized CaO is higher than the commercial adsorbents (Aldrich CaO). During physisorption analysis process, nitrogen molecules act as the adsorbate [57]. Nitrogen molecule will fill in and resides on the pores and covers all the areas of the sample in order to measure the surface area and porosity of the sample [57].

Through isotherm log plot of the analysis, the type of the adsorbent material that been developed can be estimated. Basically, there are 6 typical types of isotherm log plots had been developed by Brunaeuer. Figure 4-13(a) shows the isotherm log plot for commercial calcium oxide (Aldrich calcium oxide) while Figure 4-13(b) and Figure 4-13(c) shows the log plot for cockle shell and synthesized CaO respectively.

The isotherms normally follow six forms of shape which is developed by Brunauer [58].

Table 4-3: Summary of physisorption analysis using sample with particle size less than 0.125mm

Sample	BET surface area (m^2/g)	Single point adsorption total pore volume of pores less than 1.24×10^{-7} m width at P/P_o is 0.984 (m^3/g)	Adsorption average pore width (4V/A by BET) (m)
Aldrich $CaCO_3$	3.44	1.28×10^{-9}	1.5×10^{-9}
Aldrich CaO	2.18	6.17×10^{-9}	1.1×10^{-8}
Cockle shell	1.56	4.92×10^{-9}	1.3×10^{-8}
Synthesized CaO	9.63	2.34×10^{-8}	9.7×10^{-9}

Isotherm plots for all of the samples show the similarity with the adsorption isotherm of type 2. According to Webb and Orr [58] type 2 indicates the material to be either nonporous adsorbent or the adsorbents have relatively large pores. However, there are hysteresis loop on every curves of the samples. Webb and Orr [58] described the samples with this behavior is typical of mesoporous (2-50 x 10^{-9}m) and microporous (> 50 x 10^{-9}m). As shown in Table 4-3, average pore diameters for all of the involved samples falls in the range of 2-50 x 10^{-9}m, which indicates the samples are mesoporous material.

Stanmore and Gilot [15] mentioned that the porosity fraction that is associated to small macropores and mesopores are an important factor that controls the carbonation conversion. It is due to the inhibition of $CaCO_3$ in small pores or any large voids, which is formed during the carbonation. Gupta and Fan [27] also agreed that mesoporous structure favored high conversions for carbonation reactions. Since the pores of the synthesized CaO from cockle shell is clarified to be mesoporous, thus, utilizing cockle shell as adsorbent source is very encouraging.

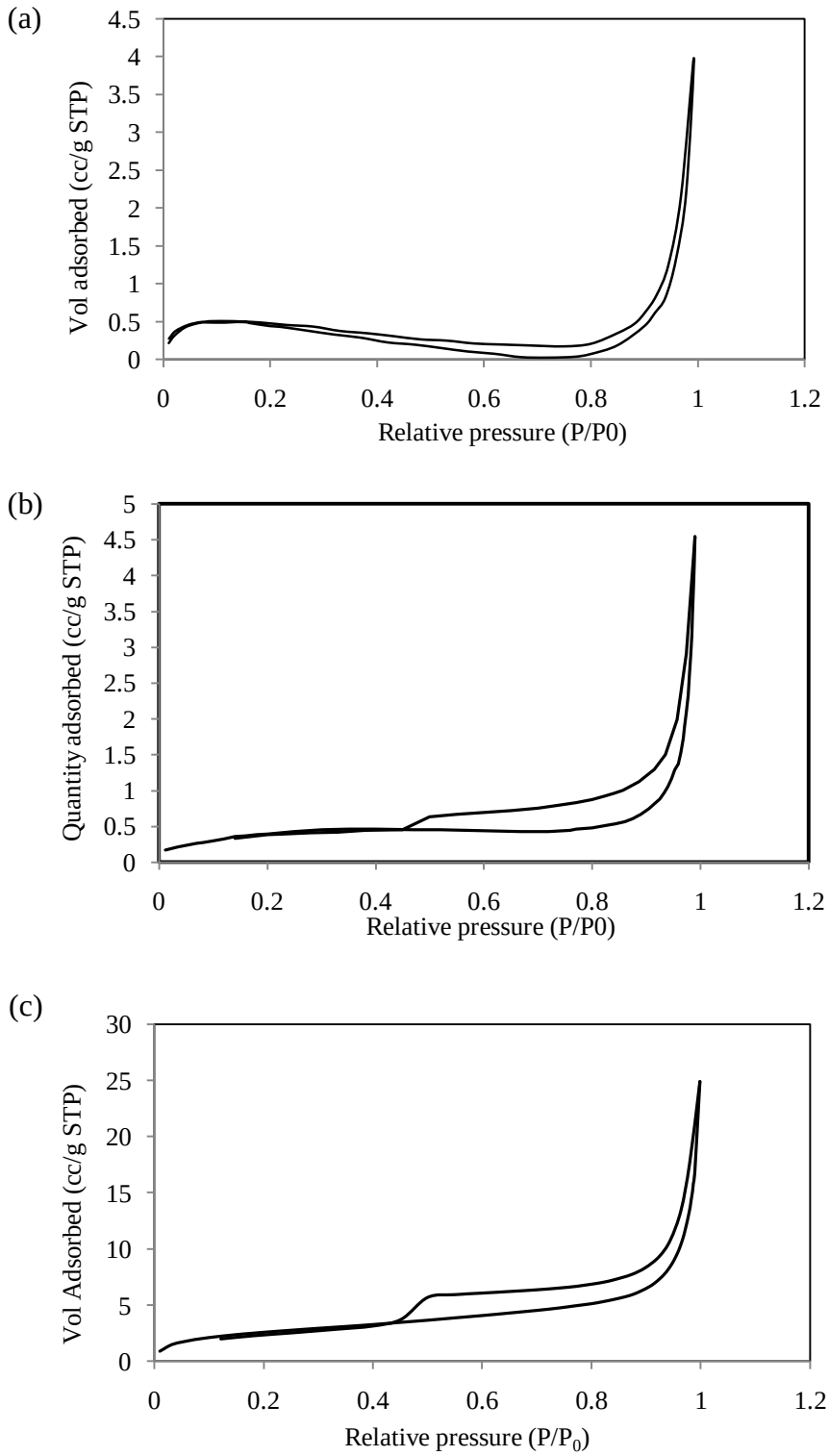

Figure 4-13: Isotherm log plot of (a) Aldrich calcium oxide, (b) raw cockle shell and (c) synthesized CaO

4.3 Thermal Gravimetric Study on Behavior of Calcination and Carbonation Reaction of Cockle Shell

Basically, calcination is conducted in inert atmosphere. The known mass sample is placed in the ceramic crucible and heated up to calcination temperature at certain heating rate. Carbonation is then conducted once the temperature is brought down to carbonation temperature and CO_2 gas is switched on. The recorded weight change and weight change with respect to time then can be observed using TG and DTG curves respectively.

In this study, calcination and carbonation are conducted in pure nitrogen and pure CO_2 atmosphere respectively in order to eliminate the potential of selectivity factor to occur. Besides, same amount of sample (~5 mg) for every run is used to minimize the influence of mass and heat transfer to the reaction. Flow rate of each purge gas is maintained to be constant throughout the process (50 ml/min).

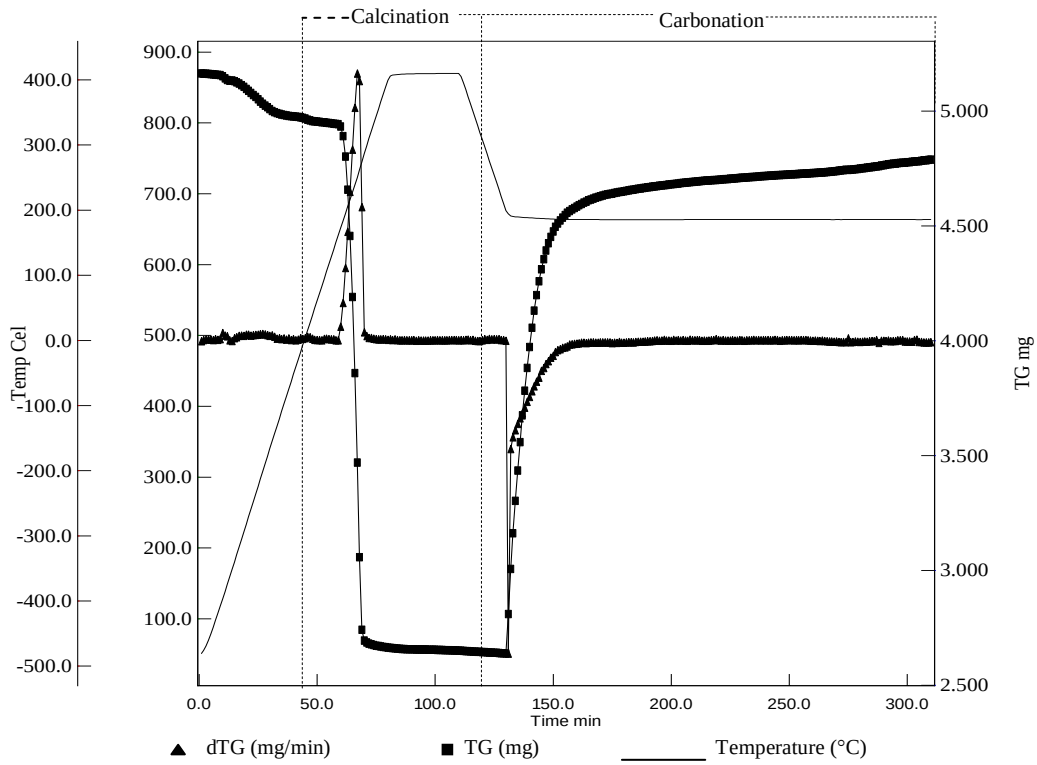

Figure 4-14: TG and dTG curves obtained for calcination and carbonation in TGA by using MUSE software (Calcination T; 750°C; Carbonation T: 650°C; Heating rate: 20°C /min; Particle size: < 0.125mm, Calcined duration: 60 min)

Overall, based on TG curves obtained, calcination of cockle shell took place in three phases as shown in Figure 4-14. The first phase was where a very small weight loss at temperature around 400-600°C occurred in which might be due to dissociation of volatile component in the sample. Then the mass was rapidly decreased once the temperature is above 700°C and finally became constant when the temperature reached 800°C. Section 4.4 illustrates that cockle shell retained ~ 55% of its initial sample weight regardless the differences in particle sizes, heating rates, calcined duration and calcined temperature applied. As described in Chapter 2, amount of weight loss represents the amount of CO_2 that been desorbed by carbonate contained in the shell and the remaining weight belongs to the amount of the product.

Barros et al. [9] mentioned that $CaCO_3$ started to disintegrate into CaO at the temperature range of 700-900 °C and Khinast et al. [16] mentioned that at high temperature, CO_2 is released and CaO is formed. Ar and Dogu [22] also agree that the weight loss of the sample is wholly results of $CaCO_3$ decomposition since other compound is at negligible weight. Therefore it can be stated that synthesis of CaO from cockle shell can be obtained once the temperature is above 700 °C and the process is stable or complete after 800 °C as shown by constant weight, as indicated in Figure 4-14. Minimum two runs of experiment is conducted in this study which shows standard deviations of each run of data falls in the range of less than 5%.

The observation of above behavior also can be explained based on the description by Barros et al. [9] which is as follows: weight loss of the initial part (100-140 °C) is due to the moisture trap inside the material, once the temperature is increased (250-410 °C), the volatile organic material started to dissociate and release that occur at 500-540 °C, the resistance organic material also started to be released and finally at 650°C, the sample started to rapidly loss the weight as the sample started to disintegrate into CaO. No significant weight loss at the end of the process indicates the calcination was already complete.

The weight loss and retained weight achieved during calcination in this study is observed to meet the reaction stoichiometry as represents in Equation 2.1. Molecular weight of CaO, CO_2 and $CaCO_3$ are 56, 44, and 100 g/mol respectively. Therefore if

the amount of weight retain, weight loss and initial weight is 55 -56%, 43-44% and 100% respectively, the amounts seemed to satisfy the stoichiometry balance of each species and the reaction equation itself.

$$CaCO_3\,(s) \rightarrow CaO\,(s) + CO_2\,(g) \qquad (4.1)$$

In addition, Borgwardt [42] claimed that weight loss depends on the type of micrograin array of the sample. It is believed that if micrograin has a face centered array of uniform spheres, it will have certain value of diameter and molar volumes that control the amount of micrograin and the percent of weight loss that can be experienced by the sample. CaO, CO_2 and $CaCO_3$ have their specific relative molar volume and micrograin array, therefore this property is perhaps another reason for the observed behavior.

Carbonation involved the reaction between synthesized CaO with CO_2. As illustrated, carbonation occurs in two regimes. The first regime involves a rapid weight gained experienced by the sample until it reached the second regime where the weight gained was slowed down until no significant weight change happened, as indicated by TG curve in Figure 4-14. As described in Chapter 2, initially carbonation is controlled by chemical reaction where most of calcium oxide get reacted with carbon dioxide and producing the calcium carbonate. But then, as the time goes on, the product layer that build-up has introduced resistance to the reaction and cause the overall reaction to be controlled by CO_2 gas. Due to product layer limitation and less pores available, the reaction is slower and insignificant.

In this study, carbonation was conducted at 650°C at 20°C/min in atmosphere of 100% carbon dioxide. The process was hold at certain carbonation temperature for 180 minutes to ensure carbonation became saturated and no significant weight change occur can be observed. Calcination was conducted before carbonation under certain conditions that been described previously to demonstrate the effects on carbonation. A number of calcination conditions were varied to understand this behavior.

Overall, synthesized CaO experienced carbonation rapidly in the temperature range of 650-700°C before become almost constant throughout the reaction. The time taken for rapid carbonation is around 30-60 minutes. This observation indicates that

carbonation was favorable at the stated temperature and can be prolong for almost 60 minutes before becoming saturated. However, the ability relies on the calcination conditions. Other carbonation temperature also been tested to understand its capture capacity which has been portrayed by carbonation conversion and amount of CO_2 that been captured per kilogram of synthesized CaO utilized.

4.4 Effect of Calcination Conditions towards Carbonation of Cockle Shell

4.4.1 Particle sizes

The right particle size of the sample used in synthesizing the adsorbent is important since the factor can influence the heat distribution in the sample during the reaction. Besides, the factor also can determine the calciner size that needs to be used for the calcination process to ensure the right heat distribution to occur. According to Stanmore and Gilot [15], particle size of less than $5x10^{-3}$mm is not recommended due to the cost of grinding and it may cause the destruction to pore volume of the adsorbent. Inversely, large particle size may introduce transport limitations. Stanmore and Gilot [15] also claimed that sample at particle size of 1-2 $x10^{-3}$mm can cause the limited effect on conversion but it has no resistance in pore diffusion. Due to the above reasons, the smallest size for this study is selected to be less than 0.125mm and the largest were less than 4mm.

Table 4-4: Calcination and carbonation condition to study the effect of particle sizes

Calcination temperature (°C)	Calcined period (min)	Carbonation temperature (°C)	Particle size (mm)	Heating rate (°C /min)
850	30	650	< 0.125 0.5-1 2-4	20

Calcination was conducted in inert atmosphere (N_2) at 850 °C and hold for 30 minutes before the temperature was reduced to 650°C for carbonation. 20°C/min is

the chosen heating rate since most of the studies conducted by the researchers are within this range. Too low heating rate can be uneconomical to the process yet too high heating rate may introduce inhomogeneous effect to the process. Other calcination conditions are described in Table 4-4. Figure 4-15 (a) illustrates the thermal-gravimetric (TG) curves obtained.

Sample weight loss indicates calcination reaction where calcium oxide being synthesized and weight gained represents the occurrence of carbonation reaction. As illustrated, calcination is initiated at temperature above 700 °C for all of the particle sizes and the process seemed to become constant once reaching 850 °C. Carbonation started rapidly once the temperature reached 650°C and the sample rapidly gained weight for 30-60 minutes, depend on particle sizes, before reaching another region of insignificant weight change.

TG curves in Figure 4-15 (a) show that all of the samples experienced 44-45% of weight loss during calcination, regardless of different particle sizes. However, during carbonation, different particle sizes take different time length to reach a constant or saturated point. Sample with particle size of 0.5-1 mm reached the fastest saturation point which is about 30 minutes after carbonation started.

Although sample with particle size 2-4 mm experience longer time to become saturated, the final weight gained by the sample was similar with particle size of 0.5-1mm which is approximately 90%. Sample with smallest particle sizes exhibits longer time to reach saturated point which was around 40-60 minutes besides gaining highest weight during carbonation which was about 94%. This behavior describes the ability of small particle size to capture more CO_2 compared to sample with larger particle sizes.

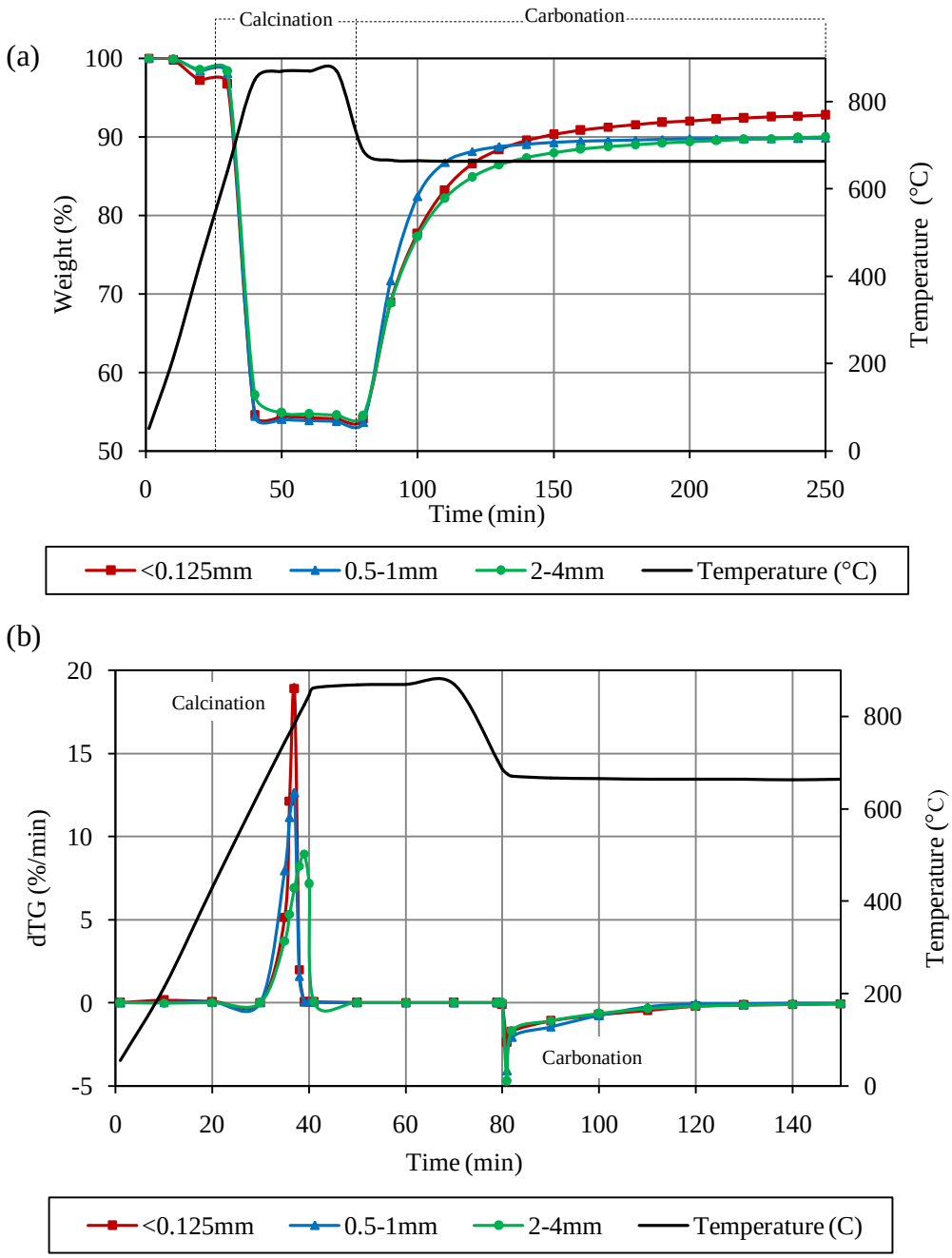

Figure 4-15: (a) TG curves and (b) dTG curves for calcination and carbonation reaction using samples with different particle sizes.

By looking at dTG curves (Figure 4-15 (b)), calcination reaction is represented by sharp positive peak which represents an endothermic reaction. The curves also display the calcination rate of the shells. Highest peak value demonstrates by the sample with particle size <0.125 mm which denotes that it experienced highest calcination rate. The lowest peak is illustrated by the sample with particle size of 2-4mm. In addition,

dTG peak become broader once particle size is larger since it require more time to decompose the sample.

DTG peak that pointing down as illustrated in Figure 4-15 (b) during carbonation signifies that it is an exothermic reaction. Based on the curve, carbonation rate for smaller particle size sample is higher compared to carbonation rate experienced by larger particle size. According to Borgwardt [42], maximum calcination rate can be reached when particle size of the sample is minimized because no transfer limitation presents [16]. Hence, wider surface area owned by the sample with smaller particle size which contributes to better heat distribution in the sample that enable higher and faster uptake of the heat to promote the calcination and carbonation process.

Smaller grain size has lower minimum temperature to initiate calcination and carbonation since the heat transfer is much better once the sample size is smaller [59]. Hu and Scaroni [43] agreed that the smaller particle size experienced uniform heat and mass transfer since the heat transfer from the external (bulk gas) into the sample core and surface occurs at less limitations. As described by Ye et al. [40], smaller particle size provides less pore diffusion resistance and thus mass transfer of CO_2 gas through the sample core can be improved.

In addition, the analysis done by physisorption analysis also shows that specific surface area of particle size less than 0.125 mm is greater than the one with particle size of 0.5-1mm range. Larger surface area, offers better heat distribution, and lesser resistance owned by synthesized CaO with smaller particle size, leads to better carbonation performance as monitored in this study. The analysis of the findings is described in Table 4-5.

Table 4-5: Physisorption analysis for sample with different particle sizes

Particle size	< 0.125mm	2-4mm
BET surface area (m^2/g)	9.63	4.18

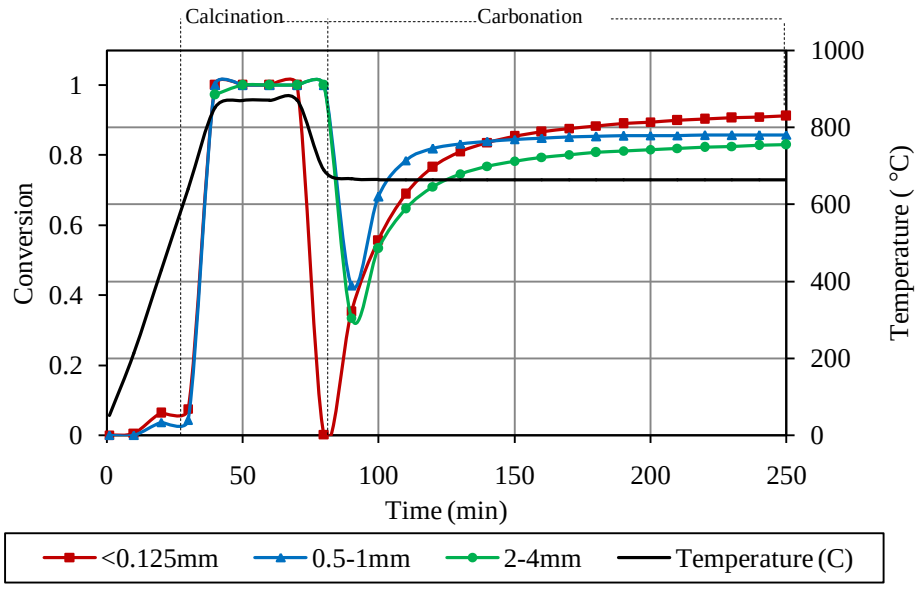

Figure 4-16: Conversion plot for calcination and carbonation reaction using samples with different particle sizes

Mole conversion in Figure 4-16 illustrates that the entire sample is almost completely converted into calcium oxide since the value of around 1 is attained during calcination. However, as expected, carbonation conversion of the sample with smallest particle size was the highest. It captures the highest amount of CO_2 which is about 0.72 kg of CO_2 per kilogram of synthesized CaO as shown by Figure 4-17. Ives et al. [37] studied on CO_2 removal by eggshells, mussel shells and limestone in 750°C fludized bed (N_2 atmosphere, 2g of 0.6mm particle size) shows that limestone has highest CO_2 capacity (99%) compared to mussel shell and egg shell (95%) at the first cycle of calcination and carbonation. To compare, the adsorption capacity of synthesized CaO is lower than the one obtained by Ives et al. [37]. The observation may due to different synthesis and operating condition.

According to Jeon and Yeom [60], adsorbent with smaller particle size has wider surface area that contributes to higher adsorption capacity. For instance Jeon and Yeom [60] whose research on crab shell as adsorbent in phosphate removal, shows that shell particles less than 1mm in diameter removed more than 85% of 500 mg/L phosphate in 24 h while particles 3.35 mm in diameter exhibited only 50% removal efficiency. Yet, too fine adsorbent size is still unfavorable for packed bed type of

reactor as it may cause clogging problem. Therefore, the application of the adsorbent needs to suit the purposes and involved processing units.

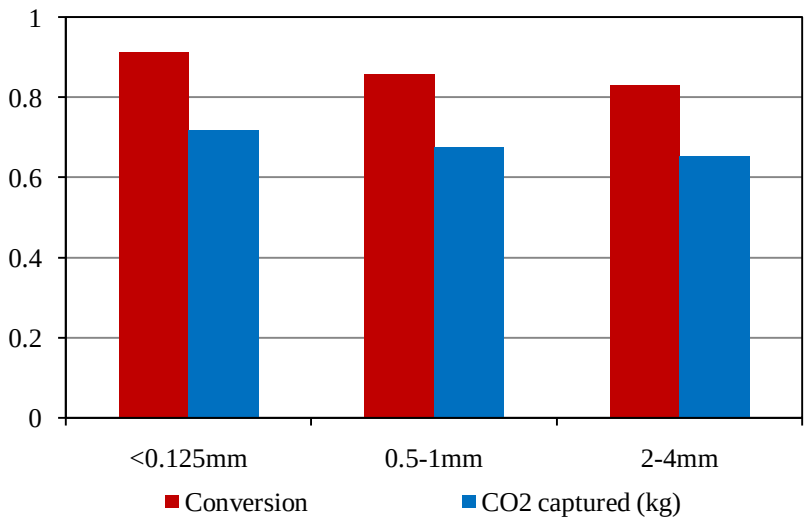

Figure 4-17: Amount of CO_2 captured by shell with different particle size during carbonation

Overall, particle sizes of the sample influence the calcination rate of the cockle shell which affects the process of synthesizing CaO and also the performance of carbonation in its ability to capture CO_2. In this case, sample with smallest particle size (less than 0.125mm) demonstrates the best calcination and carbonation behavior compared to the other two large particle sizes (0.5-1mm, and 2-4mm). By having highest calcination rate, endured longer time to become saturated and high CO_2 capture capacity, cockle shell with particle size less than 0.125 mm are favorable to be used for further calcination and carbonation study.

4.4.2 Calcination temperature

Calcination which is an endothermic process, is favored by high temperature in order to own better adsorption effect [60]. Therefore, by calcining the cockle shell at high temperature, it can be an additional advantage in synthesizing the CaO. However, very high calcination temperature (> 1100°C) may lead to the sintering and attrition effect [15] [61]. Therefore, to avoid a severe sintering effect, this study used 950°C as the maximum temperature for calcination.

Table 4-6: Calcination and carbonation condition to study the effect of calcination temperature on carbonation

Calcination temperature (°C)	Calcined period (min)	Carbonation temperature (°C)	Particle size (mm)	Heating rate (°C/min)
750 850 950	30	650	<0.125	20

Figure 4-18 describes the TGA curves for calcination and carbonation when the calcination temperature was varied. As described, calcination was conducted in inert atmosphere under constant flow rate of nitrogen (50 ml/min) and the process was hold for 30 minutes to ensure the completion of the process. Then carbonation started once CO_2 gas was switched at 650°C at the same flow rate as nitrogen. The detail of the process condition is described in Table 4-6.

As illustrated in the figure, calcination which was demonstrated by rapid weight reduction in TG curve was observed to start at 700°C for about 20 minutes regardless the set up of calcination condition and the weight was almost constant at 55% for 30 minutes at each calcination temperature. During carbonation, sample weight increased due to the capture of CO_2 by the synthesized CaO. At lowest calcination temperature (750 °C), saturated point is achieved earlier than the sample that been synthesized at 850 °C and 950 °C.

This behavior suggests that adsorbent that been synthesized at higher temperature took longer time to become saturated and can be used for time consuming process before being put for regeneration purposes. However, the final weight gained during carbonation for all of the samples were almost the same (92-95%). Therefore, CO_2 adsorption capacity of each synthesized adsorbent is expected to be the similar although they had been synthesized at different calcination temperature.

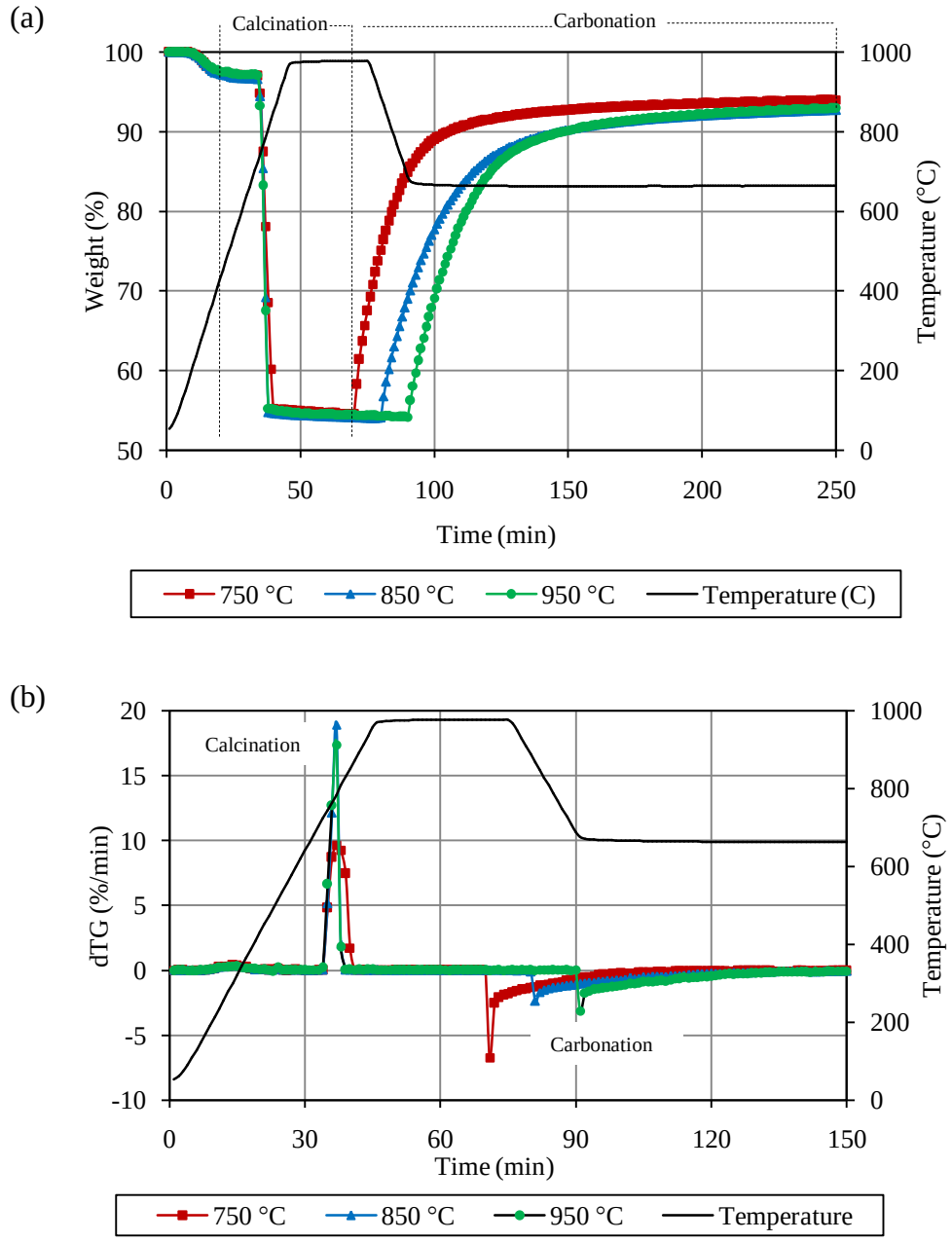

Figure 4-18: (a) TG curves (b) dTG curve during calcination and carbonation of cockle shell at different calcination temperatures

DTG plot in Figure 4-18 (b) signifies the calcination and carbonation rate at three calcination temperatures. High calcination temperature promotes higher calcination rate since significant heat is supplied to decompose the sample and thus accelerates the synthesis process. In this study, CaO is synthesized at highest calcination rate once been calcined at 850°C compared to the other calcination temperature. Yet the

carbonation rate experienced by this sample is lower than the sample that been calcined at 750°C. However, as indicated in Figure 4-18 (a), synthesized CaO at 750°C will saturated faster than the sample that been synthesized at 850°C. Therefore, 750°C is yet an ideal temperature to synthesis a durable CO_2 adsorbent.

In addition, synthesized CaO at calcination temperature of 950°C also showed higher carbonation rate compared to the sample that been calcined at 850°C although its calcination rate is lower. However, due to sintering effect, synthesizing the adsorbent at high temperature is unfavorable since the structural changed can affect the performance of the adsorbent. Li et al. [62] also stated that when CaO-based adsorbent is calcined at high temperature, sintering will reduce specific area and porosity of CaO and lessen its capture capacity. In addition, it is uneconomical for the operation.

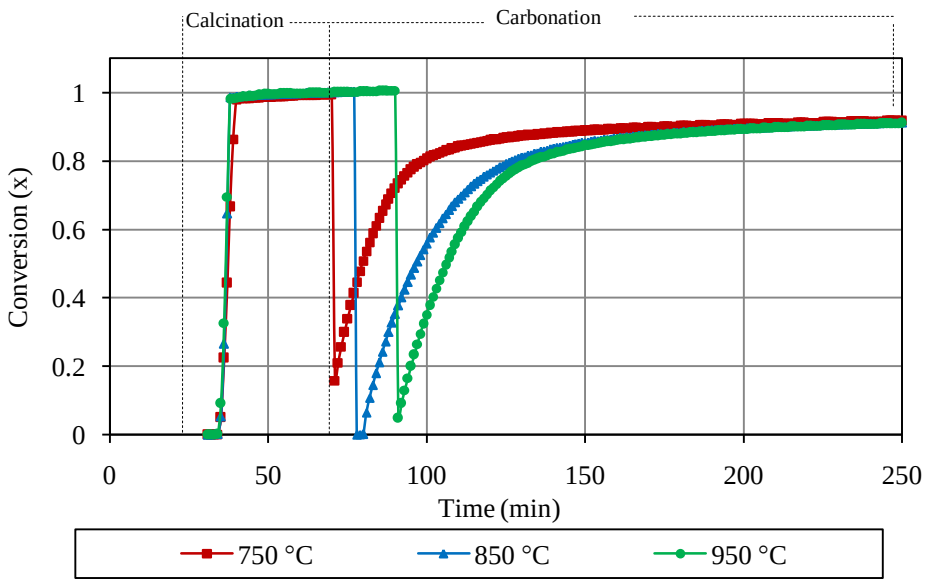

Figure 4-19: Conversion plot for calcination and carbonation at different calcination temperature

Figure 4-19 shows the plot of conversion for the sample during calcination and carbonation of the shell that been calcined at 3 different calcination temperatures. The sample reached conversion of almost 1 during calcination which suggesting the sample were completely been converted into calcium oxide. Calcination at high temperature however does not affect much the carbonation conversion of the sample and the amount of CO_2 that can be captured per kilogram of the synthesized CaO. As

indicated in Figure 4-20, the amount of CO_2 captured by the samples that been calcined at different temperature are almost the same which is about 0.72kg of CO_2 per kilogram of synthesized CaO while the conversion achieved is 0.91.

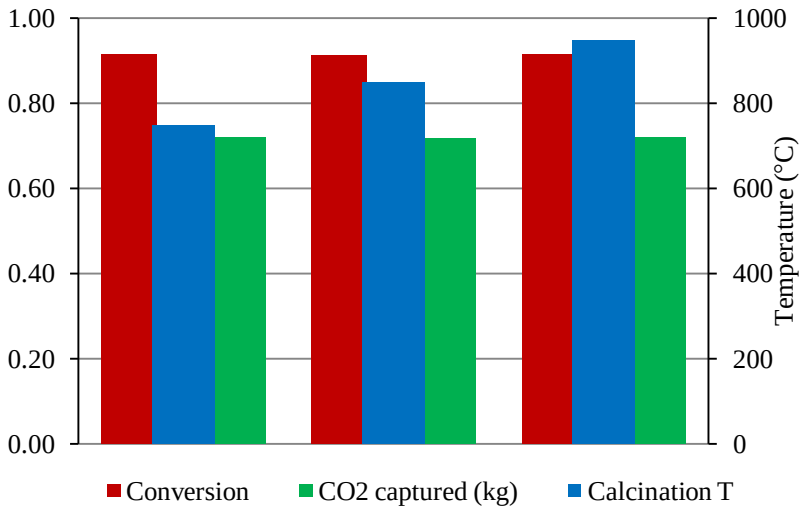

Figure 4-20: Amount of CO_2 captured per kilogram of synthesized CaO at different calcination temperature

Overall, based on this study, calcination temperature of 850 °C demonstrates the best behavior of both calcination and carbonation process. It recorded the highest calcination rate and the synthesized CaO is not easily saturated. At lower temperature (750 °C), the synthesized CaO illustrates lower calcination rate and earlier saturation point. In addition, too high calcination temperature is costly to the operation, time consuming and a disadvantage for the sample structure. Therefore, the medium temperature of 850 °C for calcination process is selected for the next study to synthesis the sample and conduct the carbonation reaction.

4.4.3 Heating rate

Heating rate can influence the rate of decomposition of sample in an interval of time and the cost of operating the calciner. Singh et al. [59] mentioned that heat transfer can be improved once heating rate is raised higher. Hatakeyama and Liu [51] described that heating rate can influence the temperature distribution inside the sample. It can shift the lower temperature range of the chemical reaction region to

higher temperature region and this influences the kinetics of the reaction. At high temperature, high heating rate cause the reaction to be at greater speed which will narrow the temperature interval and enhance the occurrence of sharp derivative curve.

Table 4-7: Condition for calcination and carbonation of cockle shell to study the effect of different heating rate

Calcined temperature (°C)	Calcined period (min)	Carbonation temperature (°C)	Particle size (mm)	Heating rate (°C /min)
850	30	650	<0.125	10 20 50

Calcination of cockle shell was conducted in TGA for the same particle size (less 0.125mm), in inert atmosphere at calcination temperature of 850°C, to demonstrate the effect of different heating rates on calcination and carbonation. The detail of the process condition is described in Table 4-7. Figure 4-21(a) and (b) illustrate TG and dTG curves respectively, obtained during calcination and carbonation once different heating rate was applied.

Figure 4-21 (a) indicates that high heating rate enables the calcination to complete in shorter time range as it managed to elevate the temperature cause the reaction to be faster than at slow heating rate. The effect of heating rate probably results structural change since CO_2 is expelled more vigorous at high heating rate [62]. Therefore, calcination occurred rapidly once higher heating rate was applied. As portrayed in Figure 4-21 (b), dTG curve become narrower and sharper once heating rate is increased as claimed by Hatakeyama and Liu [51]. This denotes that higher heating rate will increase the calcination rate and rapid synthesis of CaO can be obtained.

The behavior signifies that calcination rate can be increased once heating rate is increased since the heat transfer is improved. Besides, the maximum calcination rate also can be achieved. This factor is an advantage if the operation aims to reduce the production time or gaining more adsorbent in short period of time. However, the

drawback can be severe regarding energy penalty or cost to the operation since high heating rate also cause higher apparent temperature of reaction [30].

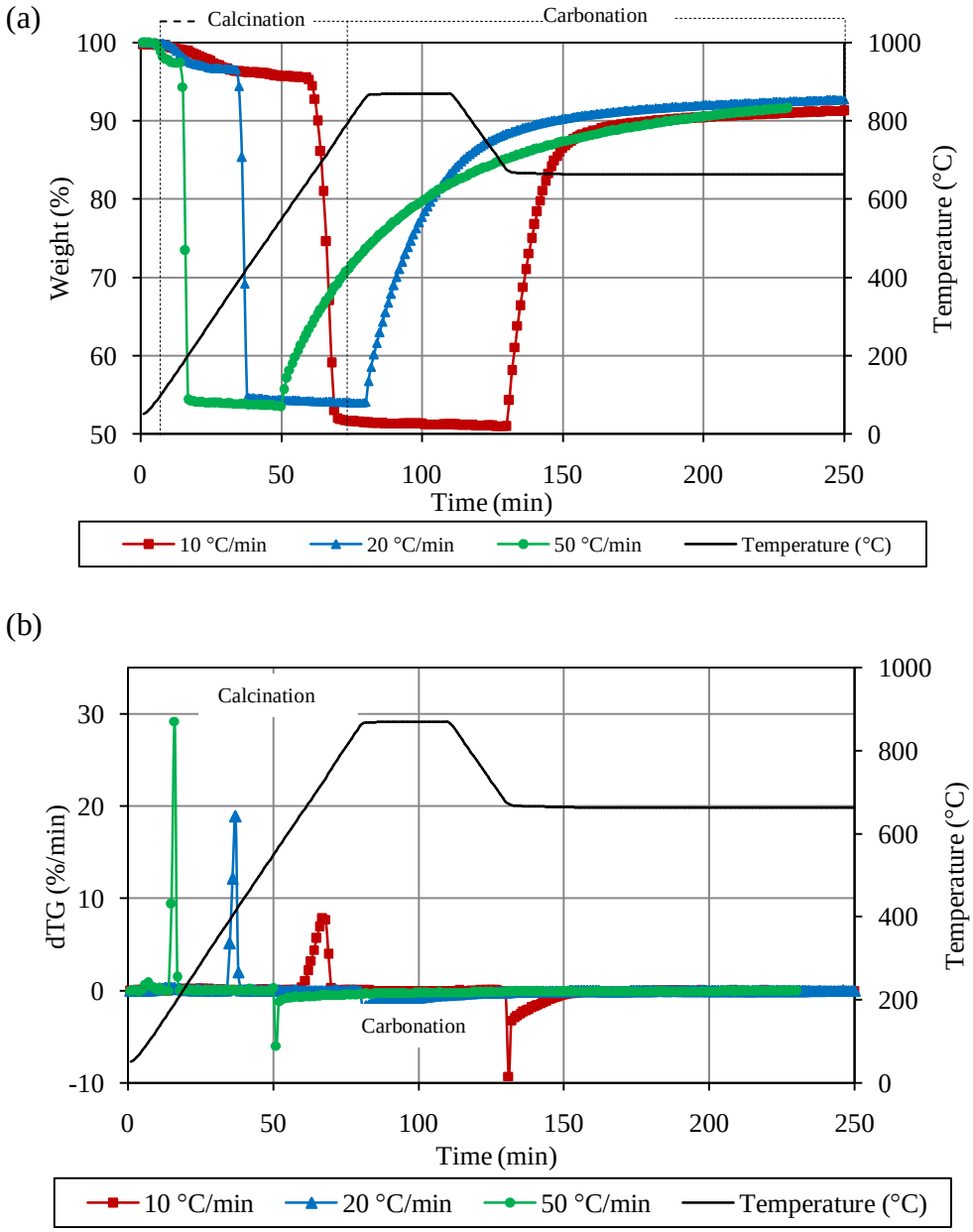

Figure 4-21: (a) TG curves (b) dTG curves for calcination and carbonation for cockle shell at different heating rate

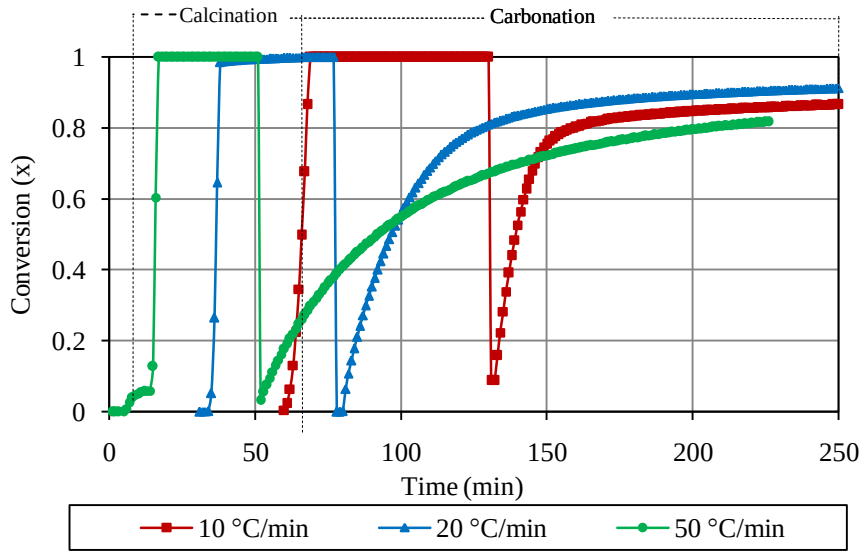

Figure 4-22: Conversion of cockle shell during calcination and carbonation at different heating rate

Figure 4-22 shows the conversion plot of the cockle shell during calcination and carbonation at different heating rate. The entire sample reached calcination conversion of almost 1 during calcination in different time length. The behavior of synthesized CaO indicates the ability of the synthesized CaO in capturing CO_2 is independent of the heating rate. However, the time taken to reach carbonation saturated point for the synthesized CaO at higher heating rate is longer compared to the other sample. As illustrated, sample that been calcined at heating rate 10°C/min reached saturated point (~0.85 conversion) around 20 minutes after carbonation started but for the sample that been calcined at heating rate 50°C/min reached saturated point (~0.80 conversion) after 150 minutes of carbonation period.

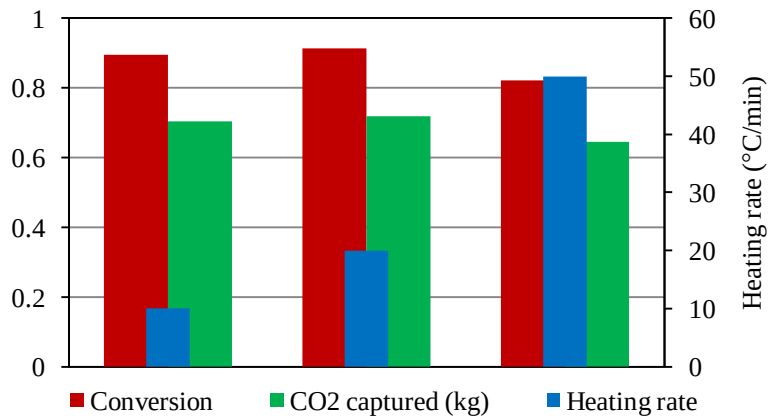

Figure 4-23: Total conversion and amount of CO_2 captured by synthesized CaO at different heating rate

Figure 4-23 shows carbonation conversion and amount of CO_2 that been captured by synthesized CaO at different heating rate. Compared to 50 °C/min, the results show that the synthesized CaO at 20°C/min has the highest carrying capacity since it demonstrates the highest conversion and amount of CO_2 capture per kilo of synthesized CaO. Low heating rate is possible to eliminate or minimize the irregularities of endothermic temperature within solid reactant and temperature difference between the gas phase and solid sample. It helps to minimize the potential mass and heat transfer intrusions in the reaction [61].

However, Li et al. [62] found that higher heating rate will increase calcium utilization efficiency once calcination is at 850 °C. Therefore, more CO_2 gas is able to be captured by the sample. So in this study, 20°C/min is the optimum heating rate since at the stated heating rate, calcination and carbonation rate is based on proper time consumed, conversion achieved and amount of CO_2 that can be captured per kilogram of synthesized CaO.

4.4.4 Calcined duration

At constant calcination temperature, synthesis of an adsorbent and its performance during carbonation also depend on the duration of calcination. Time and temperature of calcination act vice versa in producing a quality adsorbent. Hassibi [63] claimed that holding time needs to be sufficient to allow for heat to penetrate the particles and desorb the CO_2. Therefore calcination can be done either at high temperature and at low residence time or vice versa. In this case, calcination temperature is already been fixed at 850°C to enable the study on the effect of calcined duration.

Calcination duration also can be a reason for sintering to occur which reduce the efficiency of synthesized adsorbent. Therefore, suitable calcination period is crucial to synthesize an efficient adsorbent. Most of the research conduct calcination for more than 20 minutes to ensure the sample is being calcined completely. In this study, the effect of calcined duration is study for three different periods (30-60 minutes). The detail of calcination and carbonation conditions is described in Table 4-8.

Table 4-8: Conditions of other parameters during calcination and carbonation reaction to study the effect of calcined period

Calcined temperature (°C)	Calcined period (min)	Carbonation temperature (°C)	Particle size (mm)	Heating rate (°C /min)
850	30 40 60	650	<0.125	20

Figure 4-24 (a) demonstrates the TG curves for calcination and carbonation at different calcination period. Calcination was conducted at 30, 40 and 60 minutes at 850°C in inert atmosphere. Then the temperature was reduced to 650°C and the carbonation started once CO_2 gas was switched on. As illustrated, holding calcination period to a longer time does not change the total amount of weight loss experienced by the sample during calcination. Yet, holding the calcination at 30 minutes does increase the weight gained of the synthesized CaO during carbonation and the total weight is reduced as the holding time is increased to 60 minutes.

The sample that was hold at shorter duration, reach saturation point later than the one that been held longer. For example, sample that been hold at 30 minutes during calcination reached the saturated point (85wt %) around 40 minutes after carbonation started but for the sample that been hold for 40 minutes during calcination it took 20 minutes to reach the saturated point. Therefore sample that been hold for 30 minutes during calcination can endure longer time to capture CO_2 before becoming saturated.

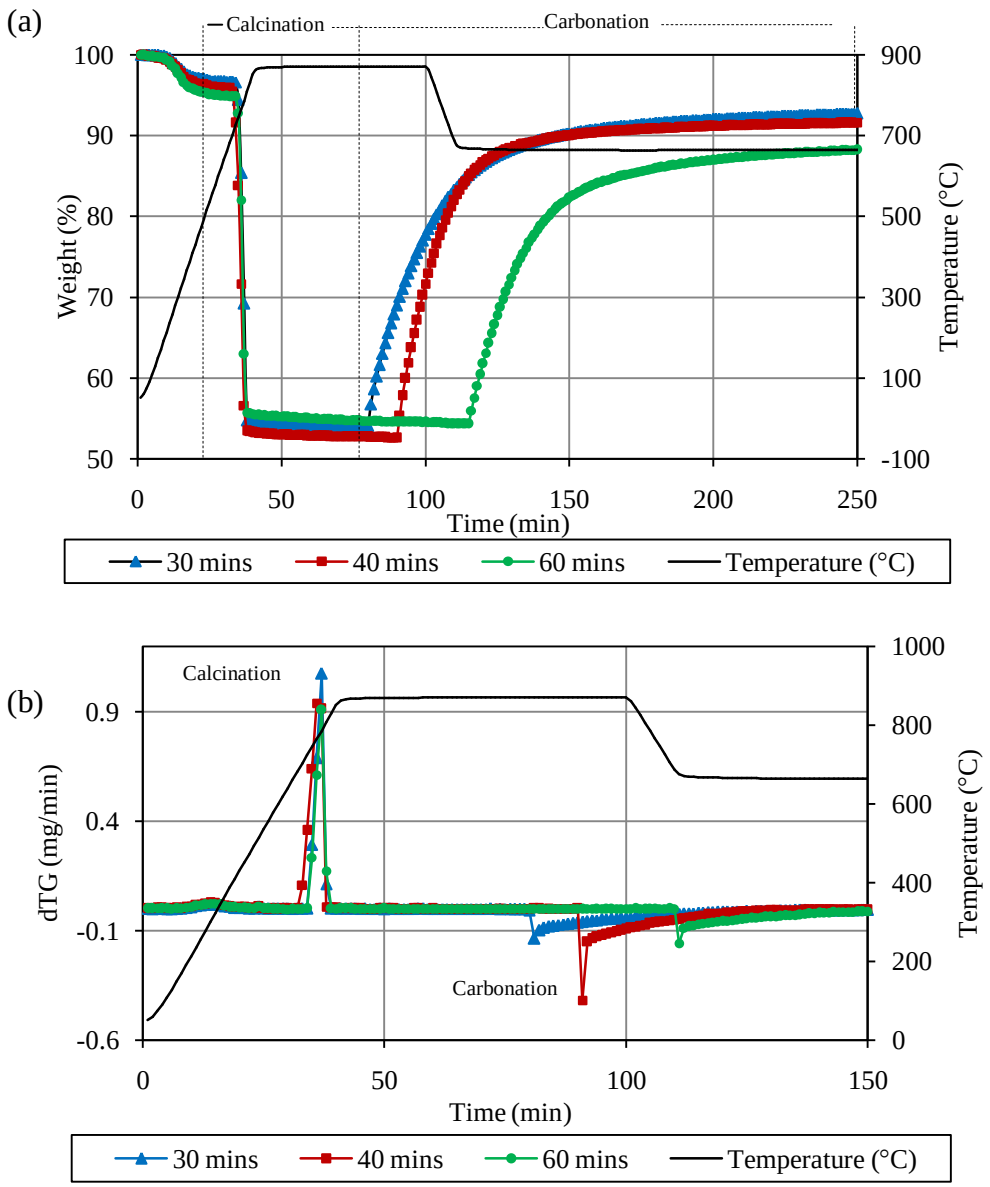

Figure 4-24: (a) TG curves (b) dTG curves for calcination and carbonation of cockle shell at different calcination duration

According to Gilot and Stanmore [15], longer calcination time cause the sample to experience sintering effect and surface area distruction. Since calcination temperature was kept constant, calcination time is the domain factor towards inefficiency of the adsorbent. Due to sintering and reduction of surface area, not much CaO surfaces and pores can be accessed by CO_2 during carbonation and hence reduce the adsorption capability of synthesized CaO.

Figure 4-25 shows the conversion of the shell during calcination and carbonation reaction at different calcination holding time. It shows that the sample is fully converted into CaO at each calcination duration since the conversion for calcination reached the value of 1. However, carbonation conversion reacted differently at different calcination duration. It was observed that calcining the sample for 40 minutes enable the sample to experience highest carbonation conversion. It signifies the carrying capacity of the sample is higher compared to the other sample of synthesized CaO. Calcining the sample at 60 minutes was unfavorable for carbonation since it reduced carbonation conversion.

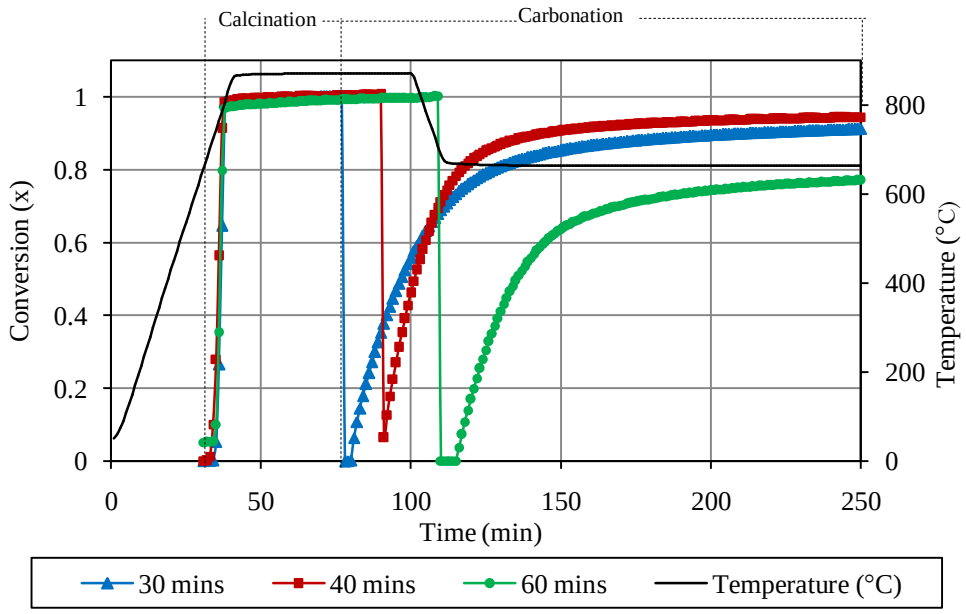

Figure 4-25: Conversion plot of cockle shell during calcination and carbonation reaction

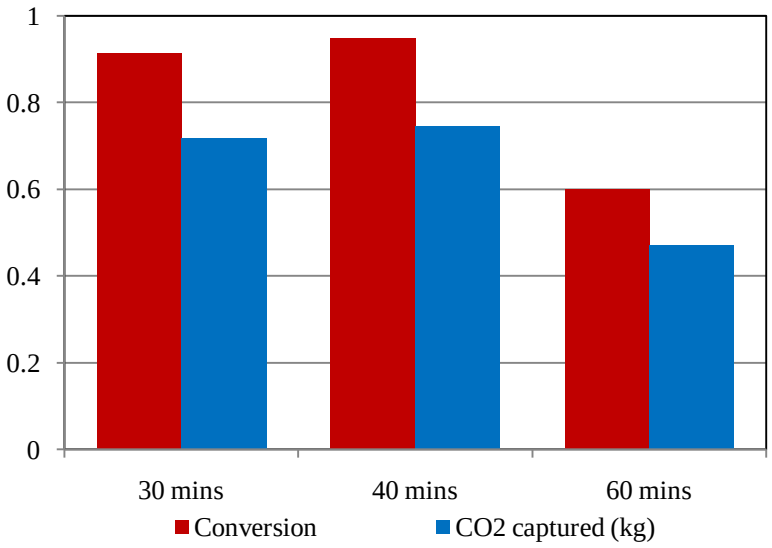

Figure 4-26: Carbonation conversion and amount of CO_2 captured at different calcination duration

Carbonation conversion was applied to analyze the capability of synthesized CaO to capture CO_2. Figure 4-26 indicates the estimated amount of CO_2 that can be captured by one kilogram of synthesized CaO at different calcination duration. The amount of CO_2 captured by the synthesized CaO at holding time of 40 minutes shows the highest value compared to others while the sample that been calcined for 60 minutes captured the lowest value as expected. Therefore, the overall behavior of carbonation reaction of the synthesized CaO is dependent toward the calcination holding time. The factor may influence the aggressiveness of sintering activity which affecting the efficiency of the adsorbent. Therefore, in this case, at calcination temperature of 850°C, using particle size of less than 0.125mm, 40 minutes is the optimum holding time to synthesis CaO since it can experience highest the carbonation conversion and adsorb more CO_2.

4.5 Performance of Synthesized CaO

4.5.1 Carbonation temperature

This section emphasizing the capability of the synthesized CaO, obtained during calcination of cockle shell, to adsorb CO_2 at different reaction temperature. In this case three carbonation temperatures have been tested which are in the range of 500-950°C. Table 4-9 described the detail conditions for calcination and carbonation experienced by cockle shell. The conditions were determined based on the optimum carbonation behavior (carbonation rate, carbonation conversion and amount of CO_2 captured) as observed in Section 4.4. Carbonation was conducted in 100% CO_2 atmosphere for 180 minutes when N_2 gas flow was shut down at carbonation temperature and CO_2 gas was switched on into TGA.

Table 4-9: Conditions of calcination and carbonation reaction to test the performance of cockle shell at different carbonation temperature

Calcined temperature (°C)	Calcined period (min)	Carbonation temperature (°C)	Particle size (mm)	Heating rate (°C /min)
850	30	500 650 850	<0.125	20

By referring to TG curve in Figure 4-27 (a) and conversion plot in Figure 4-28, cockle shell experienced highest weight gained (~93%) and conversion (~0.9) once carbonation being conducted at 650°C. Once carbonation temperature was increased to 850°C, synthesized CaO experienced rapid carbonation reaction. It reached saturated point faster yet gained lower weight increment compared to the sample at carbonation temperature of 650°C. Synthesized CaO is monitored to hardly reach its saturation point when carbonation temperature is 500°C since the weight of the sample keep increasing. Same observation noted by Bhatia and Perlmutter [19] and

Gupta and Fan [27] reported by Lee et al. [48]. Figure 4-30 illustrates the finding and indicates that carbonation perform better at temperature more than 600°C.

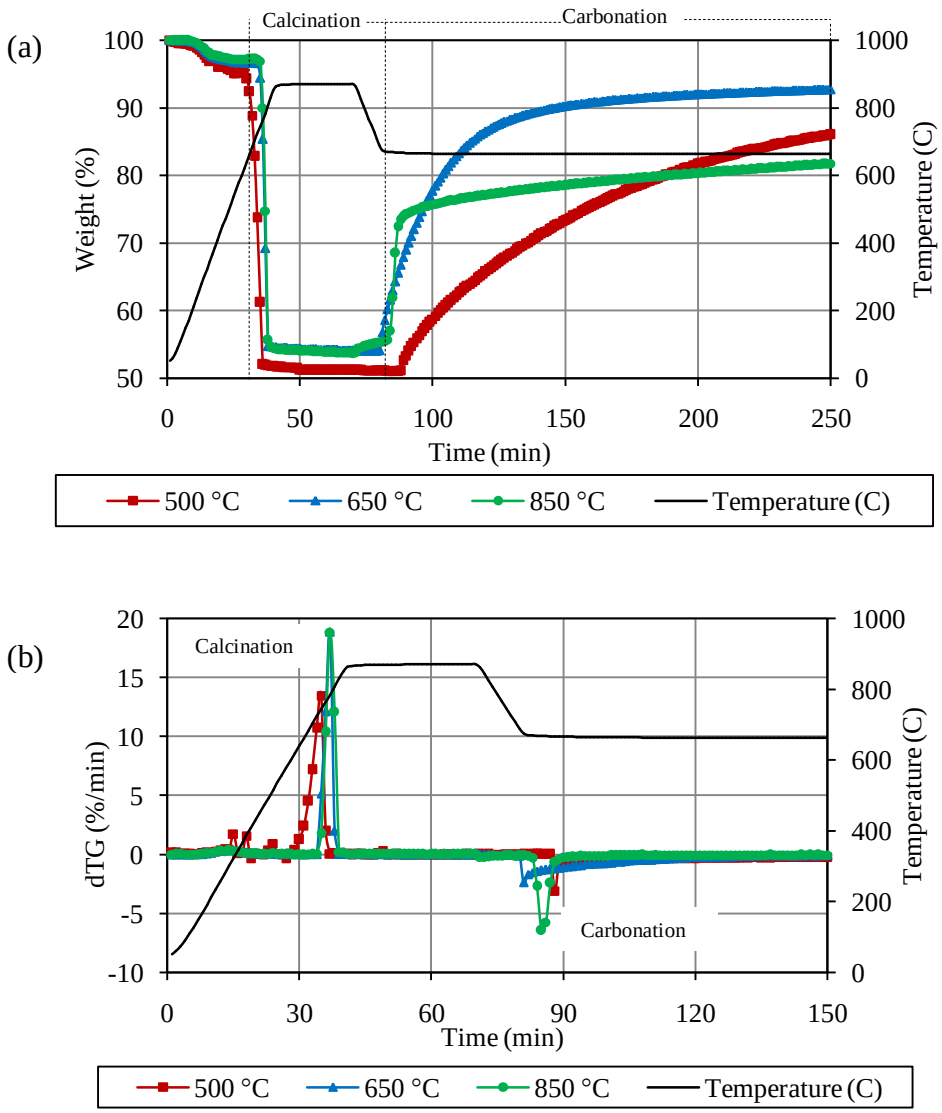

Figure 4-27: (a) TG (b) dTG curves during calcination and carbonation of cockle shell at different carbonation temperature

dTG plot in Figure 4-29 (b) shows that the synthesized CaO experienced highest carbonation rate at reaction temperature of 850°C although it obtained lowest carbonation conversion. The behavior signifies that at high reaction temperature, synthesized CaO able to capture CO_2 rapidly yet not able to sustain at longer time before become saturated. In addition, it only managed to capture small amount of CO_2 as shown in Figure 4-30 since at high temperature, CO_2 is hard to be kept on the layer of CaO and it undergoes the reaction due to equilibrium and partial pressure factor

[34] [44]. The gas tends to leave the surface faster since the pressure to keep it at the reacting surface is low and equilibrium does not favor the reaction forward (carbonation reaction).

Though, too low operating temperature (~500°C and lower) is also unable to favor carbonation since it increases the partial pressure of CO_2 which does not support carbonation reaction. In addition, very high temperature can introduce sintering effect that reduces the pores and volumes of the adsorbent thus lead to inefficient carbonation. In addition, as observed in Figure 4-30, the amount of CO_2 captured is the highest at 650°C. Therefore, overall, in this study, cockle shell can perform better to capture CO_2 at temperature around 650°C.

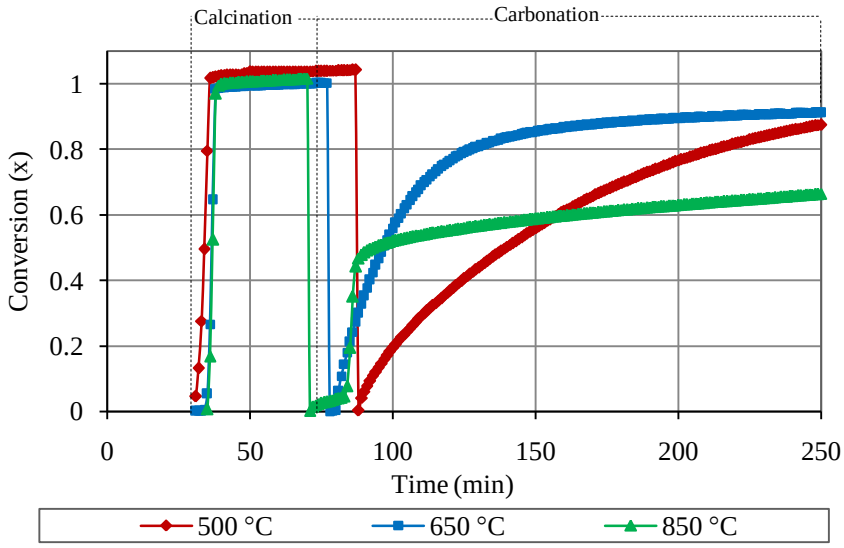

Figure 4-28: Conversion plot for calcination and carbonation of cockle shell at different carbonation temperature

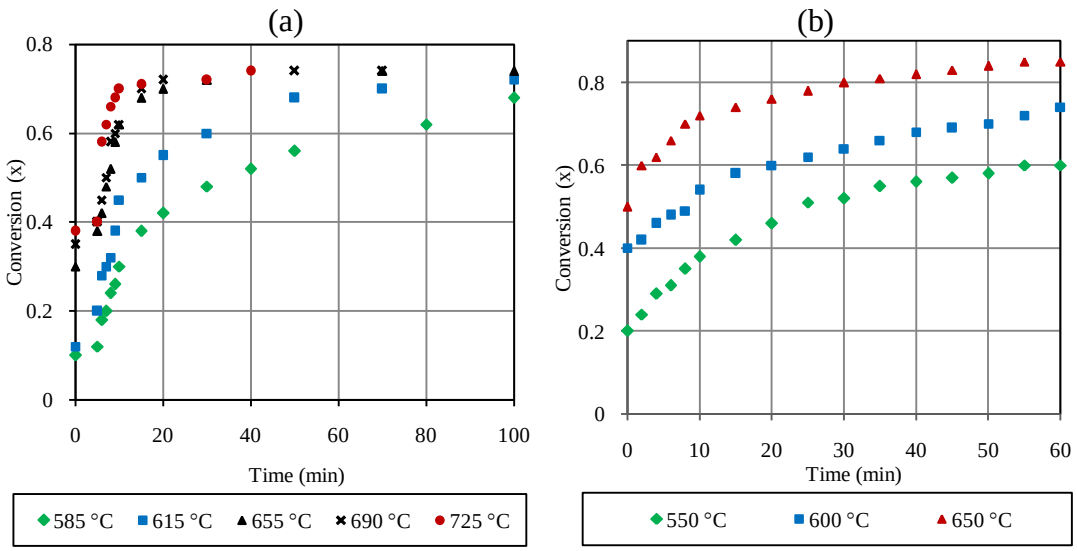

Figure 4-29: Carbonation conversion of (a) Bhatia and Perlmutter [19]and (b) Gupta and Fan [27] at different carbonation temperature [48]

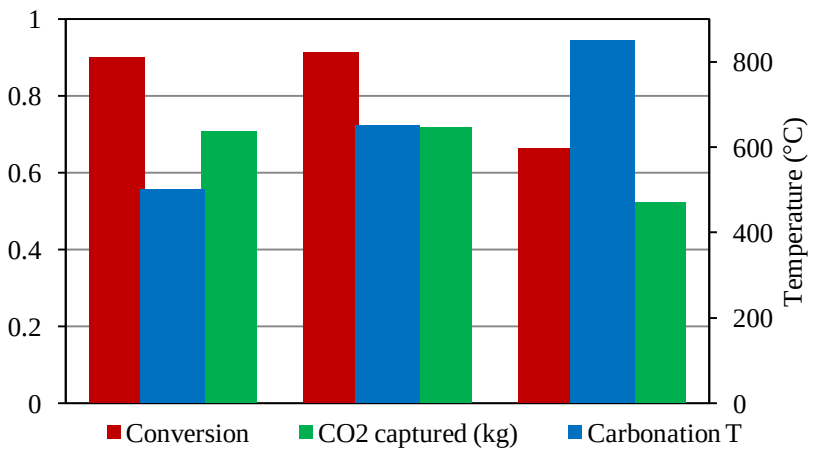

Figure 4-30: Carbonation conversion and amount of CO_2 captured at different carbonation temperature

Overall, this study simplifies that synthesized CaO from cockle shell performed best in reaction temperature range of 600-700°C. It can experience rapid carbonation reaction at higher temperature but will get saturated faster. Yet, too low reaction temperature (around 500°C and below) is unable for CO_2 to be captured since the temperature is not high enough to trigger the reaction and cause high pressure to build up during the reaction which is unfavorable in the carbonation reaction. Therefore the performance of synthesized CaO is dependent on the temperature of the reaction.

4.5.2 Comparison of carbonation capacity between synthesized CaO and commercial adsorbent

Performance of cockle shell in capturing CO_2 is being compared with commercial calcium carbonate (Aldrich $CaCO_3$) and a mixed composition of cockle shell and Aldrich $CaCO_3$. The portion of the two materials in the mixture was the same 1:1 ratio based on weight percent. The equal amount ratio is selected to minimize the influence of different material composition towards carbonation efficiency. The conditions of calcination and carbonation were fixed at the same condition to obtain CaO with highest carbonation efficiency from cockle shell. The details are described in Table 4-10.

Table 4-10: Calcination and carbonation condition to compare the performance of each adsorbent

T Calcined (°C)	Calcined period (min)	T Carbonation (°C)	Particle size (mm)	Heating rate (°C /min)
850	40	650	<0.125	20

Figure 4-31 illustrates TG and dTG curves obtained during calcination and carbonation of cockle shells, Aldrich $CaCO_3$ and mixed of Aldrich $CaCO_3$ and cockle shell. As illustrated in Figure 4-31 (a), rapid calcination of all carbonate sources occur at almost the same temperature and within equal time ranges which is around 650°C to 800°C for 20-30 minutes. However, carbonation reactivity of each carbonate sources was different.

Cockle shell experienced rapid carbonation compared to Aldrich $CaCO_3$ and mixed of Aldrich $CaCO_3$ and cockle shell. dTG plot in Figure 4-31 (b) also indicates the synthesized CaO from cockle shell experienced the highest carbonation rate. However, it also achieved saturation point faster than the other samples yet obtained lowest weight gained. Carbonate source from mixed composition of Aldrich $CaCO_3$ and cockle shell managed to obtained largest weight gained during carbonation which is about 95wt%. This behavior indicates high carbonation conversion and CO_2 capture capacity.

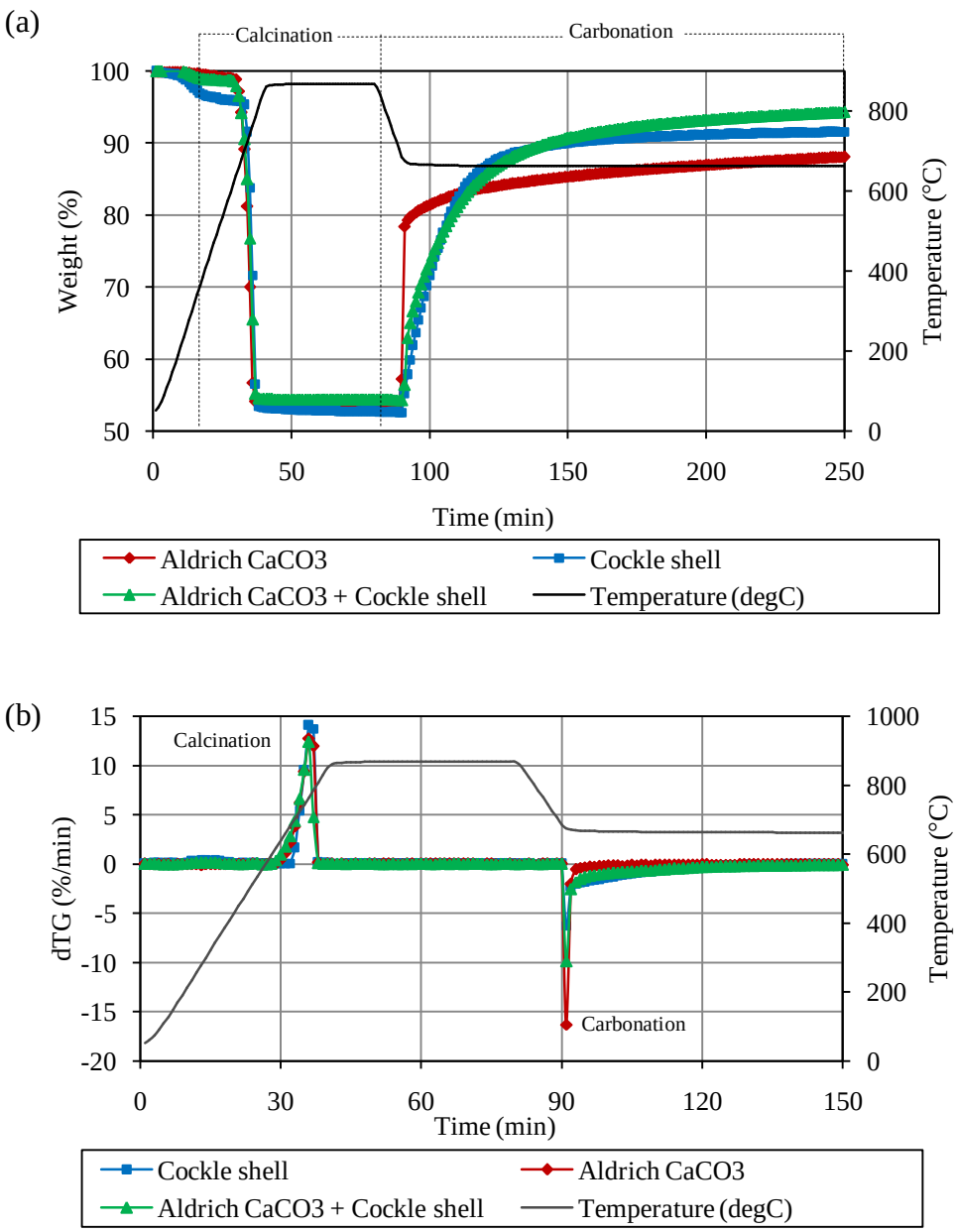

Figure 4-31: (a) TG curves (b) dTG curves during calcination and carbonation of each potential adsorbent material

Figure 4-32 shows the carbonation conversion experienced by each adsorbent during the study while Figure 4-33 indicates the estimated amount of CO_2 that can be captured per kilogram of synthesized CaO with respect to each carbonation conversion value. The conversion and amount of CO_2 captured by cockle shell and mixed composition of cockle shell and Aldrich $CaCO_3$ are almost similar while commercial adsorbent, Aldrich $CaCO_3$, shows lower conversion values and amount of

CO_2 captured. This result indicates that mixing the commercial adsorbent with cockle shell failed to provide significant improvement towards the capability of the sample in capturing CO_2. In addition, the performance of synthesized CaO from cockle shell was also comparable. Therefore, synthesized CaO from cockle shell is acceptable for CO_2 capture activity.

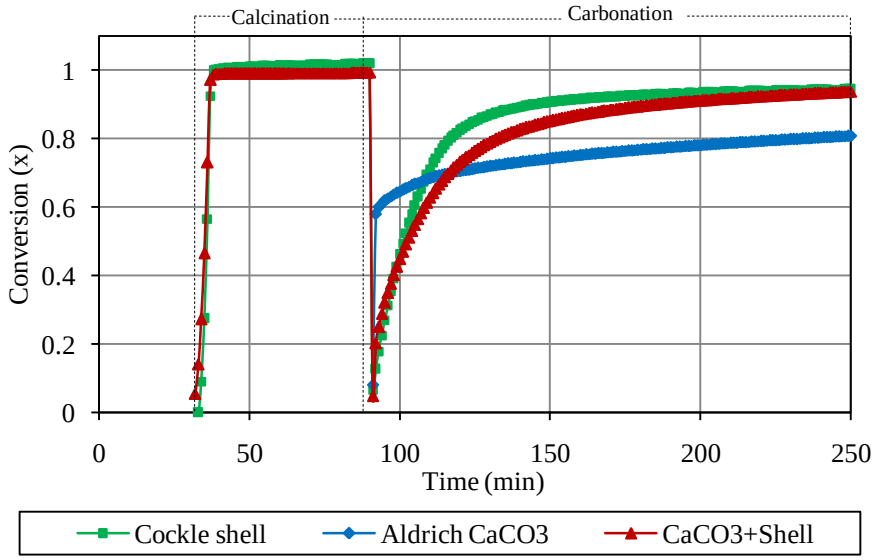

Figure 4-32: Conversion during calcination and carbonation experienced by different carbonate sources

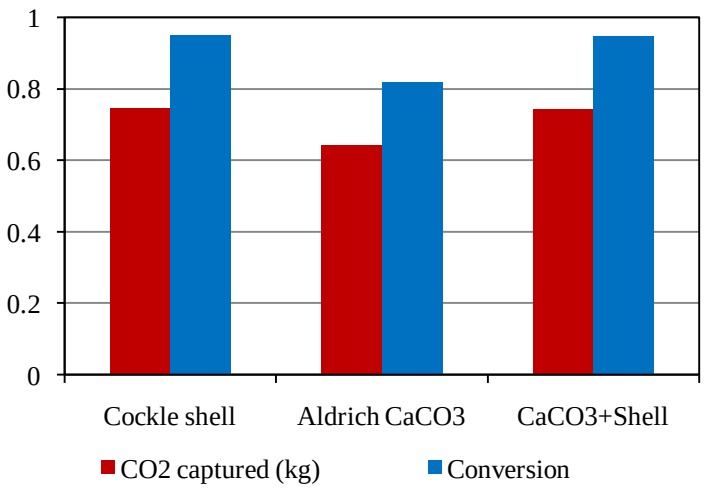

Figure 4-33: Amount of CO_2 captured and carbonation conversion experienced by each adsorbents

4.5.3 Application of synthesized CaO in pyrolysis and steam gasification of palm kernel shell (PKS)

Pyrolysis of PKS was conducted in TGA at heating rate of 20°C/minutes in inert atmosphere using N_2. The sample (~5 mg) together with the adsorbent (~5 mg) was heated up to 900°C and being hold for 10 minutes to ensure the completion of the process. CO_2 is one of the product gases during PKS pyrolysis reaction, other than hydrogen (the desired gas). The composition of outlet gas was measured using gas chromatography (GC) analyzer by Agilent Technologies.

Steam gasification of PKS with steam was conducted by switching on the steam line once the temperature reached 100°C. The flow rate of steam was kept constant at 0.005 ml/min. The capability of cockle shell as CO_2 adsorbent was tested and the results were compared with standard calcium oxide (Aldrich CaO) as demonstrated in Figure 4-34. It also demonstrates an example of the decomposition profile during PKS pyrolysis and steam gasification.

PKS experienced two stages of rapid weight loss which are at temperature range of ~400-500°C and 700-900°C. At temperature above 700°C, CO_2 concentration in the outlet stream started to deplete. In addition, synthesized CaO and Aldrich CaO recorded different temperature for maximum capture of CO_2. This behavior illustrates both adsorbent have different favorable carbonation temperature in order to capture more CO_2. In addition, the carbonation reactivity of adsorbent is normally low at temperature more than 700°C. As recorded by GC analyzer, the process released large concentration of H_2 and lesser amount of CO_2 at this stage.

For PKS pyrolysis, most of CO_2 rapidly released at 300-450°C and 500-600°C range once using synthesized CaO and Aldrich CaO respectively. For PKS steam gasification, most of CO_2 are rapidly released at 500-600°C and 200-450°C using synthesized CaO and Aldrich CaO respectively. The behavior occurred since carbonation temperature was not yet reached favorable temperature yet decomposition process occurred rapidly. Above the stated temperature range, it was observed that CO_2 was aggressively captured by the adsorbent since CO_2 concentration in the outlet gas was decreased.

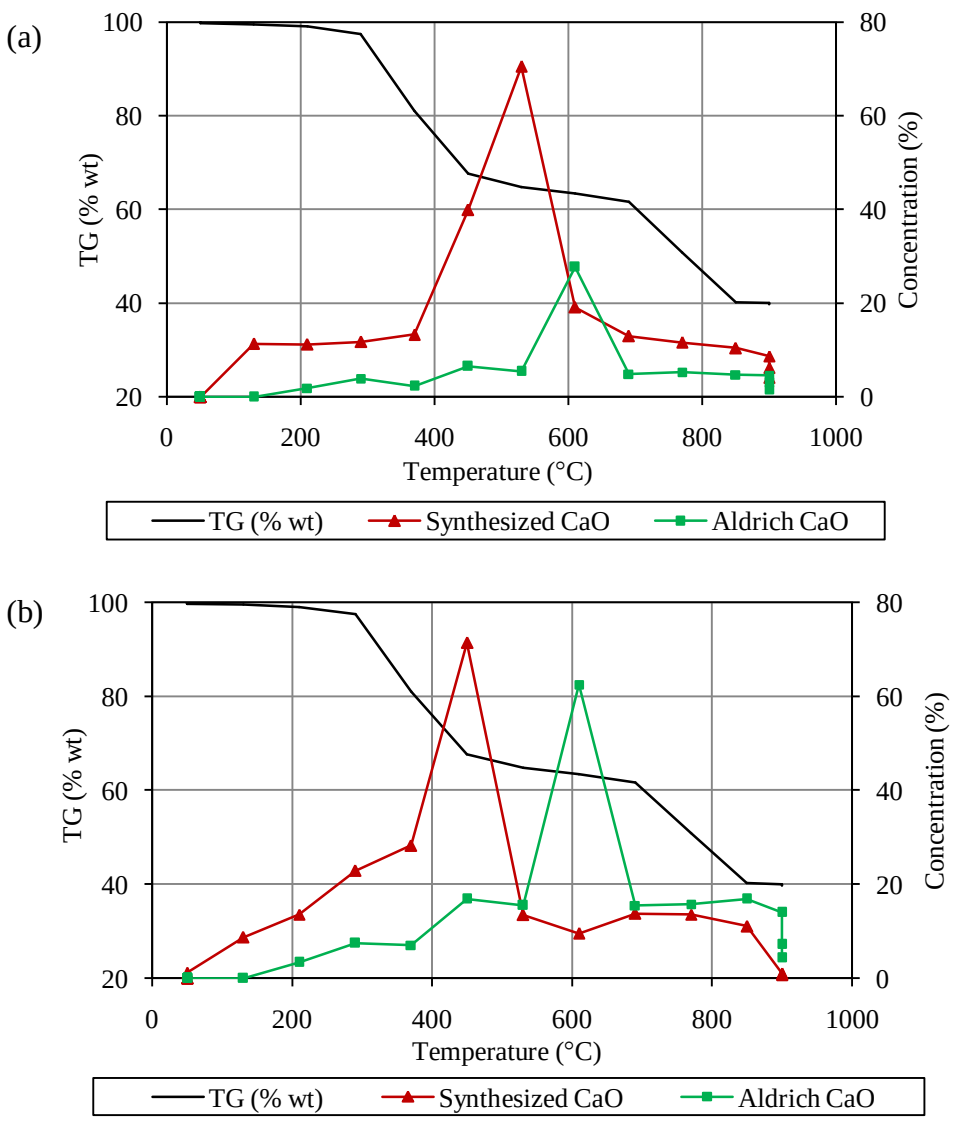

Figure 4-34: Concentration of CO_2 in the outlet gas during PKS gasification (a) pyrolysis (b) steam gasification

Table 4-11: Comparison of CO_2 amount in outlet gas during pyrolysis and steam gasification of PKS using synthesized CaO and commercial CaO as the adsorbent

Application	PKS pyrolysis		PKS steam gasification	
Adsorbent	Synthesized CaO	Aldrich CaO	Synthesized CaO	Aldrich CaO
CO_2 concentration (ppm)	2314.82	721.01	2103.29	1868.20
Fraction of CO_2 released (%)	52.99	29.05	23.38	39.12

Table 4-11 described the amount of the CO_2 in the outlet gas for every 5 mg of the sample and 5mg of adsorbent used at each run. The concentration in percentage displayed by Table 4-11 is calculated based on the concentration (ppm) of CO_2 with respect to total gas concentration in the outlet flow. The results indicate that Aldrich CaO able to capture CO_2 more than synthesized CaO during PKS pyrolysis. However, during steam gasification, synthesized CaO look more favorable since less CO_2 amount been detected in the outlet gas flow. Basically, steam helps to enhance reaction rate and hence also improve the adsorption capacity of the sample. Steam presence may introduce a preference towards the carbonation activity of the synthesized CaO.

4.6 Kinetic Analysis

Kinetics analysis is important to determine the ways in which the physical condition of the particles is related to the rate of particle reaction [64]. The analysis is divided into two parts which are calcination part and carbonation part. Each parts refers to different method of kinetic analysis which been explained previously in Chapter 2. 7.

The stated model is found to be compatible with the results found in this study since the model managed to construct linear plot of logarithmic reaction constant (ln K) against inverse absolute temperature (1/T). Kinetic analysis is conducted for calcination process under different calcination conditions such as particle size, temperature, holding time and heating rate. Kinetic analysis for carbonation part is also discussed based on three reaction temperatures using the same method described by Lee [48].

4.6.1 Calcination using different particle sizes of the sample

Particle size is one of the factors influencing the kinetics of calcination process since the energy motion of a particle depends on its size. Therefore, this research study on three ranges of particle sizes for the sample according to the size of adsorbent in the market as described in Chapter 2. The calcination conditions were described in Table

4-4. Calcination was conducted at 850°C for 40 minutes in N_2 using heating rate of 20 °C /min.

Figure 4-35 illustrates the linear log plot of ln K against 1/T in order to obtain the activation energy and the constants. The calculation is tested with three reaction orders to determine the type of reaction order that best fit the process. The result of the analysis is simplified in Table 4-12. Using regression analysis, reaction order is different with respect to the particle sized that been used. As described in Table 4-12, increase in particle sizes of the sample cause the activation energy to increase. In addition, increased in order of reaction caused activation energy and exponential factor of Arrhenius equation to increase. In this case, sample with particle size less than 0.125mm fit the best with zero order reaction mechanism while sample size of 0.5-1mm and 2-4mm fit best as first and second order reaction respectively.

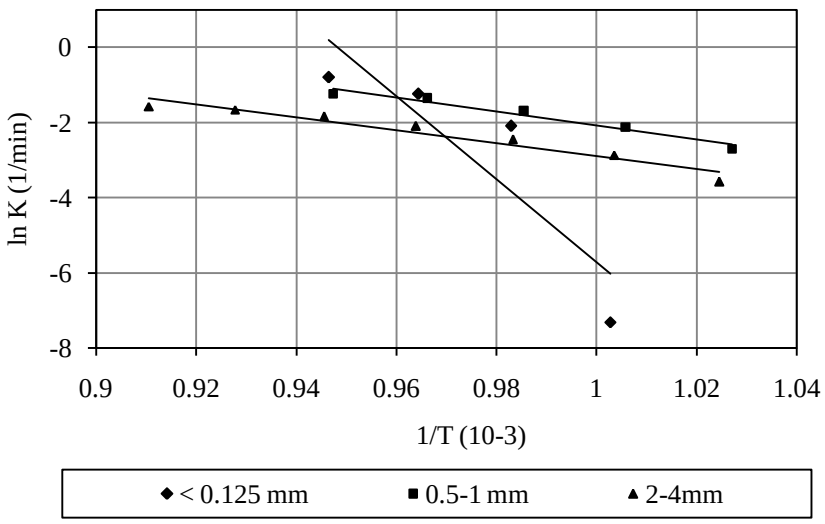

Figure 4-35: Plot of ln K against 1/T using reaction equation of zero order for different particle size during calcination

Theoretically, smaller particle size provides greater surface area which improves heat distribution within the sample and enhances better decomposition process. Thus, it reduces the resistance for the reaction to occur and minimize activation energy of the process. In addition, Table 4-5 already described the surface area of different particle sizes which indicates that surface area is greater for the sample with particle size of less 0.125 mm compared to the sample with particle size of 2-4mm. Therefore,

it can be concluded that smaller particle size provides greater surface area which reduces the activation energy for the process.

Table 4-12: Kinetic analysis using each order of reaction for samples at different particle sizes

Particle sizes (mm)	Reaction mechanism	Kinetic parameters		
		E (kJ/mol)	ln A (1/min)	R^2
<0.125	Zero order	297.39	33.13	0.999
	First order	527.36	60.7	0.989
	Second order	757.24	87.86	0.977
0.5-1	Zero order	154.47	16.5	0.960
	First order	312.27	35.83	0.984
	Second order	470.16	55.15	0.948
2-4	Zero order	142.67	14.27	0.939
	First order	236.53	25.63	0.972
	Second order	330.48	37.00	0.994

Using the kinetics analysis obtained in Table 4-12, the following kinetic constants are obtained. As described, kinetic constant increased for every increasing particle size.

Particle size = < 0.125mm; $K = 2.44 \times 10^{14} \exp(-297.39/RT)$ mol/m^{2}min

Particle size = 0.5-1mm; $K = 3.64 \times 10^{15} \exp(-312.27/RT)$ mol/m^{2}min

Particle size = 2-4mm; $K = 1.17 \times 10^{16} \exp(-330.48/RT)$ mol/m^{2}min

4.6.2 Calcination at different calcination temperature

Kinetics is very dependent on temperature since it influences the activation energy and reaction constant as portrayed by Arrhenius equation that been described in Chapter 2. The factors are crucial since it determines the condition of synthesis operation to be economical and efficient. Therefore, the analysis is conducted for three calcination temperature as described in Table 4-6. Carbonation is fixed at 650°C while using sample with particle size less than 0.125mm to minimize or avoid

possible limiting factors other than temperature. Heating rate and gas flow rate were also kept constant.

Figure 4-36 illustrates plot of ln K against inverse absolute temperature using reaction mechanism of zero order. The plot is used to analyze the activation energy and reaction constant of calcination process. Using regression analysis, the best fit curve is determined and it estimates the suitable reaction mechanism of the process. The outcome of the analysis is described in Table 4-13.

Kinetics analysis indicates that in calcination temperature range of 750-950°C, process of synthesizing CaO from cockle shell is best described by zero order reaction mechanism. As described in Table 4-13, using zero order reaction mechanism, regression value lies in the range of 0.990-0.999. In addition, the activation energy (E) also demonstrates the decreasing value once calcination temperature is raised higher. By referring to zero order mechanism, activation energy is 399.83kJ/mol when calcination temperature was 750°C and reduced to 297.39kJ/mol and 222.40kJ/mol when calcination temperature was increased to 850°C and 950°C respectively.

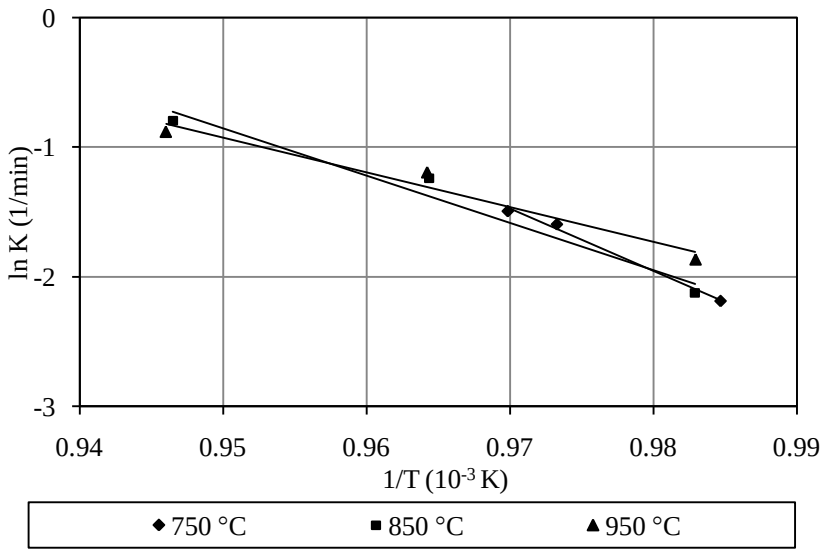

Figure 4-36: Plot of ln k against 1/T using reaction equation of zero order for different calcination temperature

Table 4-13: Kinetic analysis using each order of reaction for different calcination temperature

Calcination temperature	Order	Kinetic parameter		
		E (kJ/mol)	ln A	R^2
750 °C	Zero order	399.83	45.17	0.992
	First order	669.79	77.16	0.980
	Second order	939.50	109.10	0.947
850 °C	Zero order	297.39	33.13	0.999
	First order	527.36	59.00	0.989
	Second order	757.32	87.44	0.977
950 °C	Zero order	222.40	24.48	0.997
	First order	477.82	54.69	0.967
	Second order	733.31	84.89	0.983

Increasing temperature provides more energy and distributes more heat to the particle of the sample. It helps to accelerate kinetic energy of the particles to decompose and minimize required amount of energy to initiate the process. Hence, further increased in temperature will reduce the activation energy of the reaction. The followings are the kinetic expression according to calcination temperature using zero order reaction mechanism.

Calcination T= 750°C, $K = 4.14 \times 10^{19} \exp(-399.83/RT)$ mol/m^{2}min

Calcination T= 850°C, $K = 2.44 \times 10^{14} \exp(-297.39/RT)$ mol/m^{2}min

Calcination T= 950°C, $K = 4.28 \times 10^{10} \exp(-222.40/RT)$ mol/m^{2}min

4.6.3 Calcination at different holding time

Holding time is learned to affect the efficiency of synthesized CaO during carbonation but then it also may have influence on the kinetics of the synthesis process. According to Bonquet et al. (2009) [18] holding time can be a limiting factor for efficient calcination process given the reaction temperature is constant. In addition, finding from EDX analysis in Table 4-2 indicates that holding time plays important role in converting $CaCO_3$ into CaO. Therefore, in this study, the effect of holding time on the kinetics of calcination also been examined. Table 4-8 recorded the detail conditions.

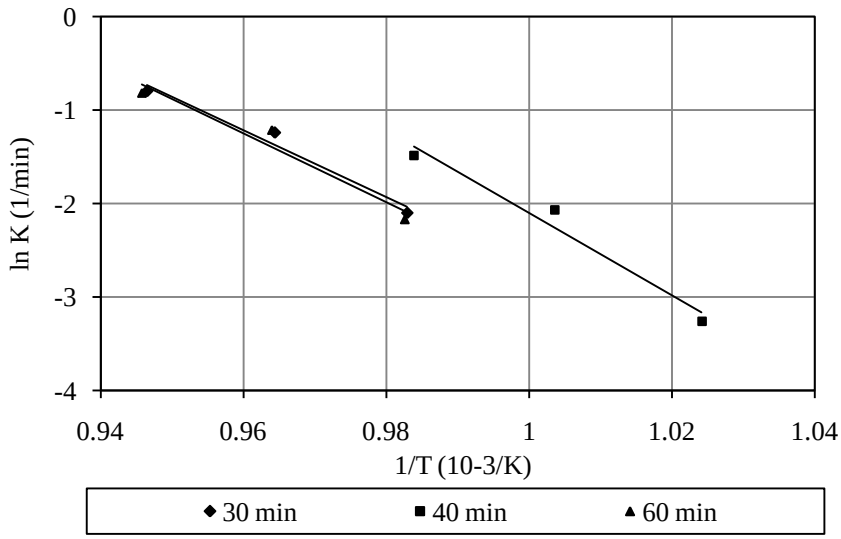

Figure 4-37: Plot of ln K against 1/T using reaction equation of zero order for different calcination time

Figure 4-37 illustrates plot of ln K against 1/T based on zero order reaction mechanism for three holding times during calcination. The plots are used to determine the activation energy of the reaction and kinetics constant involved. Three orders of reaction been tested and the best value of regression analysis simplify the best fit mechanism for the process. Table 4-14 summarizes the findings of kinetics analysis of the sample at different holding times.

Table 4-14: Kinetic analysis using each order of reaction for samples at different calcination time

Calcination time	Order	Kinetic parameters		
		E (kJ/mol)	ln A(1/min)	R^2
30 minute	Zero order	297.39	33.13	0.999
	First order	527.36	59.00	0.989
	Second order	757.32	87.44	0.977
40 minutes	Zero order	366.48	49.58	0.966
	First order	412.21	47.64	0.996
	Second order	526.36	61.62	0.991
60 minutes	Zero order	305.87	34.07	0.948
	First order	531.68	60.72	0.999
	Second order	757.49	87.37	0.994

Using regression analysis, the value of R^2 managed to fall in the range of 0.90-0.999 which indicates the experimental fits well with the reaction mechanism.

Calcination that been hold for 30 minutes is likely known to fit zero order reaction. However, first order reaction mechanism is likely suit the most once the holding time was extended to 40 and 60 minutes. In addition, activation energy was the highest when calcination was hold for 60 minutes compared to 30 minutes which is 297 and 51.68 kJ/mol respectively. Table 4-14 summarized the finding of the analysis. Holding time during calcination does not display direct relationship with activation energy for calcination process. Based on the same reaction order, Table 4-14 shows that activation energy is the lowest once calcination was hold for 40 minutes while it become highest once holding time is at 60 minutes. Therefore kinetic expression according to best suit reaction order at each calcination time is described as follows:

Calcination holding time = 30 min; $K = 2.44 \times 10^{14} \exp(-297.39/RT)$ mol/m^{2}min

Calcination holding time = 40 min; $K = 4.89 \times 10^{20} \exp(-412.21/RT)$ mol/m^{2}min

Calcination holding time = 60 min; $K = 2.35 \times 10^{26} \exp(-531.68/RT)$ mol/m^{2}min

4.6.4 Calcination at different heating rate

Change in heating rate is known to shift the ranges of reaction temperature and calcination duration. Therefore, the need to study its effect on kinetics is also important since it might be a factor for shifting the efficiency of synthesized CaO during carbonation. In addition, heating rate also may influence the kinetics of the synthesis process.

Figure 4-38 illustrates plot of ln K against 1/T using the zero order reaction mechanism. The plot is used to analyze activation energy and kinetic constant parameter of the calcination process. In addition, the analysis shows that the experimental data fits well with order of reaction where regression coefficient lies within 0.900-0.999.

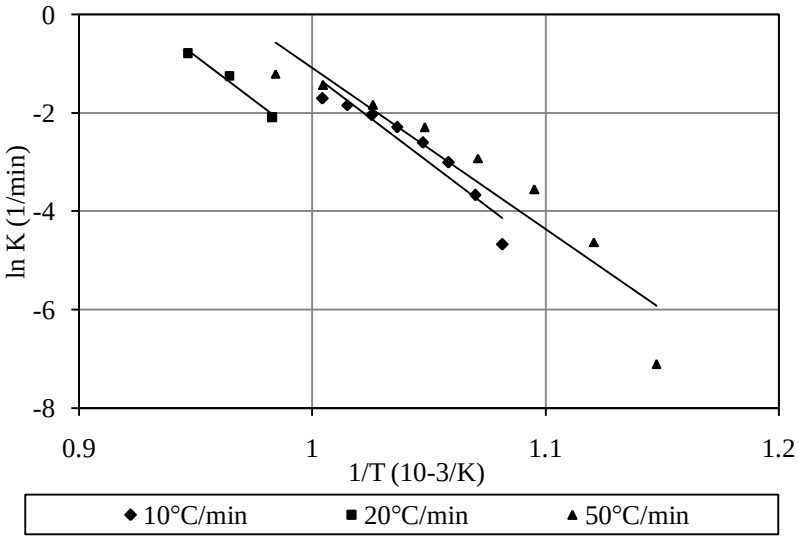

Figure 4-38: Plot of ln K against 1/T using reaction equation of zero order for different heating rate

Heating rate is observed to be independent towards activation energy and reaction constant. It shows that the reaction is better to be described by zero reaction order for heating rate of 10° C/min and 20°C/min but for faster heating rate (50°C/min), second reaction order fit the best with the experimental data. Activation energy at 50°C/min is highest among the three heating rate yet the activation energy at 10 and 20°C/min are almost the same which is around 297-299 kJ/mol. This behavior signifies that heating rate in this range (10-20°C/min) does not change much the kinetics and activation energy of the sample to initiate the reaction. Table 4-15 indicates the findings on kinetic analysis to synthesis CaO at different heating rate.

Table 4-15: Kinetic analysis using each order of reaction for samples at different heating rate

Heating rate	Order of reaction	Kinetics parameter		
		E (kJ/mol)	ln A(1/min)	R^2
10°C/min	Zero order	299.22	34.79	0.999
	First order	403.98	48.24	0.909
	Second order	508.65	61.69	0.979
20°C/min	Zero order	297.39	33.13	0.999
	First order	527.36	60.70	0.989
	Second order	757.24	87.86	0.977
50°C/min	Zero order	272.03	31.63	0.900
	First order	335.30	40.10	0.958
	Second order	398.49	48.58	0.968

Increase in heating rate will increase the activation energy of the process. Samtani et al. (2002) [7] also find the same trend in their study once heating rate is increased where the finding is described in Table 4-16. Therefore using the suitable reaction order, the equation for kinetic is different once calcination time is different. They are as follows:

Heating rate = 10°C/min; K= 1.29 x 10^{15} exp (-299.22/RT) mol/m^2min

Heating rate = 20°C/min; K= 2.44 x 10^{14} exp (-297.39/RT) mol/m^2min

Heating rate = 50°C/min; K= 1.25 x 10^{21} exp (-398.49/RT) mol/m^2min

Table 4-16: Findings on kinetic analysis done by Samtani et al. (2002) [7]

Heating rate (°C/min)	R^2	Activation energy (kJ/mol)	ln A (1/min)
5	0.9939	182.66	19.36
10	0.9959	173.21	18.45
20	0.9980	183.41	19.55
25	0.9980	185.42	19.77

4.6.5 Calcination using different carbonate sources

Three carbonate sources are used to synthesis CaO which are cockle shell, Aldrich $CaCO_3$ and mixed composition of cockle shell with Aldrich $CaCO_3$. The conditions applied are summarized in Table 4-10 which is based on the best calcination behavior of cockle shell. Figure 4-39 demonstrate a plot of ln K against 1/T which is used to estimate the reaction mechanism, activation energy and reaction constant of the sample.

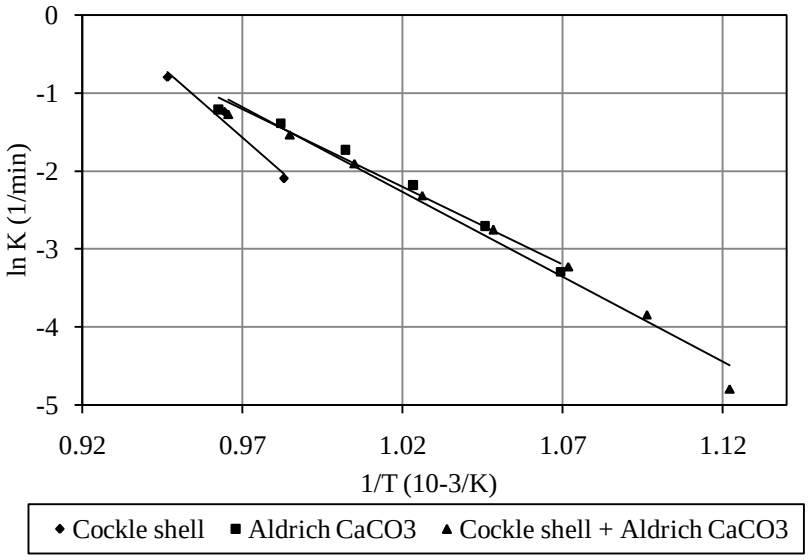

Figure 4-39: Plot of ln K against 1/T using reaction equation of zero order for different carbonate source

At stated calcination condition, the process for all of the carbonate sources in this study seems to suits first reaction order the best except for cockle shell. Based on the regression analysis done, the regression coefficient managed to obtain between the ranges of 0.900-0.999 which indicates the reaction mechanism fits with the experimental data. Table 4-17 summarizes the findings of kinetic analysis using different carbonate sources.

Taking the basis of first order reaction for all carbonate sources, the finding indicates that cockle shell record the highest activation energy which is 527.36 kJ/mol while Aldrich $CaCO_3$ is the lowest which is 238.69kJ/mol. However, once Aldrich $CaCO_3$ was mixed with cockle shell as the source to synthesis CaO, the recorded activation energy is reduced to 241.77kJ/mol. The finding illustrates that Aldrich $CaCO_3$ is able to minimize the kinetic energy of cockle shell to initiate decomposition process and synthesis CaO.

Table 4-17: Kinetic analysis using each order of reaction for samples with different carbonate source

Materials	Order of reaction	Kinetics parameter		
		E (kJ/mol)	ln A(1/min)	R^2
Cockle shell	Zero order	297.39	33.13	0.999
	First order	527.36	60.70	0.989
	Second order	757.24	87.86	0.977
Aldrich $CaCO_3$	Zero order	165.37	18.09	0.981
	First order	238.69	27.38	0.996
	Second order	312.02	36.63	0.974
Cockle shell + Aldrich $CaCO_3$	Zero order	180.75	19.91	0.981
	First order	241.77	27.90	0.988
	Second order	302.71	35.88	0.95

The difference in physical properties such as surface morphology and crystal structure and material source can be a likely factor of the observed behavior. As analyzed by SEM, Aldrich $CaCO_3$ which normally obtained from limestone is a calcite type of $CaCO_3$ polymorph where the crystal shape can be like cubic. On the other hand, cockle shell is obtained from mollusks marine living and aragonite type of $CaCO_3$ polymorph where the crystal shape is orthorhombic. Figure 4-8 illustrates the surface morphology of the sample once Aldrich $CaCO_3$ and cockle shell are mixed. In addition, the sample is a biomass type which can be a factor of impurities contained in the sample. The followings can be kinetic expression to synthesis CaO from each sample:

Source = Cockle shell; $K= 2.44 \times 10^{14} \exp(-297.39/RT)$ mol/m^{2}min

Source = Aldrich $CaCO_3$; $K= 7.78 \times 10^{11} \exp(-238.69/RT)$ mol/m^{2}min

Source = Cockle shell + Aldrich $CaCO_3$; $K= 1.31 \times 10^{12} \exp(-241.77/RT)$ mol/m^{2}min

4.6.6 Carbonation at different reaction temperature

The performance of synthesized CaO is tested at three reaction temperatures which are 500, 650 and 850°C. Hence, kinetic analysis which relies on temperature is conducted by implementing the model developed by Lee (2004) [48]. The method

which is discussed in Chapter 2.7 explained determination of activation energy and reaction constant of carbonation reaction within CaO and CO_2.

Based on the model developed by Lee (2004) [48], it can be observed that time, temperature and conversion parameter plays main role in the calculation step. Figure 4-40 illustrates carbonation conversion experienced by synthesized CaO at three reaction temperature. Using the conversion plot, the inverse value is constructed in Figure 4-41 where at each temperature can be described in two regions which are chemical reaction control and product layer diffusion control region.

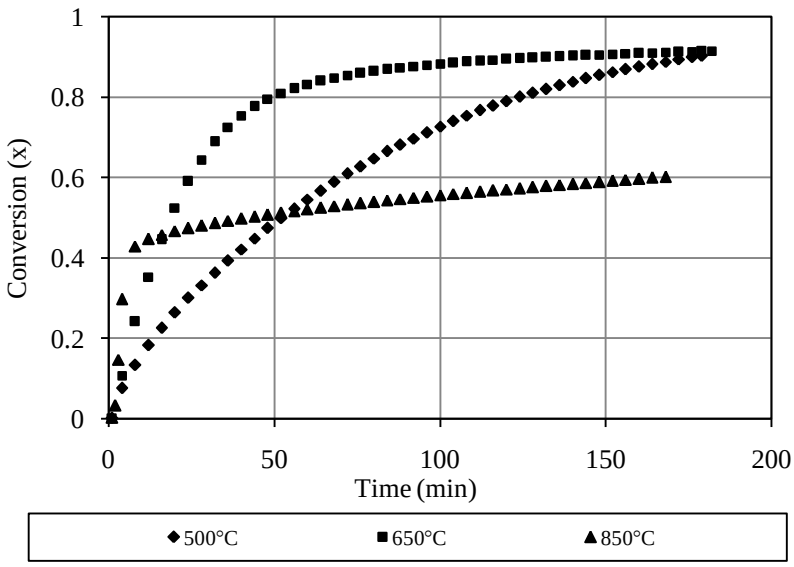

Figure 4-40: Plot of carbonation conversion against time in order to proceed with kinetic analysis developed by Lee (2004) [48]

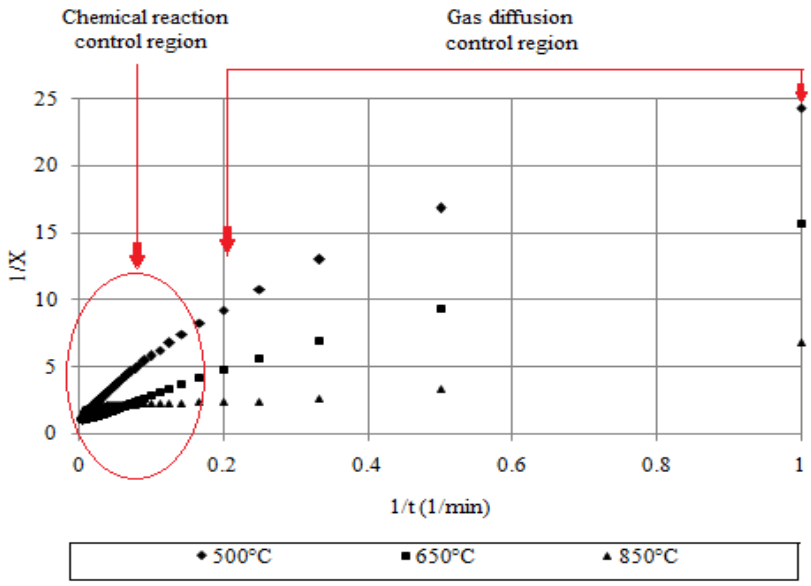

Figure 4-41: Plot of 1/X against 1/T in order to obtain regions of chemical reaction kinetic control and product layer diffusion control

Initial rapid increment in Figure 4-41 shows chemical control kinetic region while the second region is product layer diffusion region [48]. The recognition of each control region is important since kinetics analysis is determined based on region. Figure 4-42 (a) and (b) illustrates plot of 1/X against 1/t in separation control region factor to further conduct regression analysis. The figures indicate the best fit curve for each control region.

According to model developed by Lee (2004) [48], linear expression generates from each regime is used to construct plot of ln K with respect to inverse absolute temperature (1/T) in order to estimate the kinetics parameters. In this case, carbonation reaction was monitored at three reaction temperature. Figure 4-43 illustrates the linear plot of ln K against inverse absolute temperature at three reaction temperature for each regime. Regression analysis shows the value of R^2 lies in the range of 0.8-0.99. Therefore, this model is suitable with the reaction in this study.

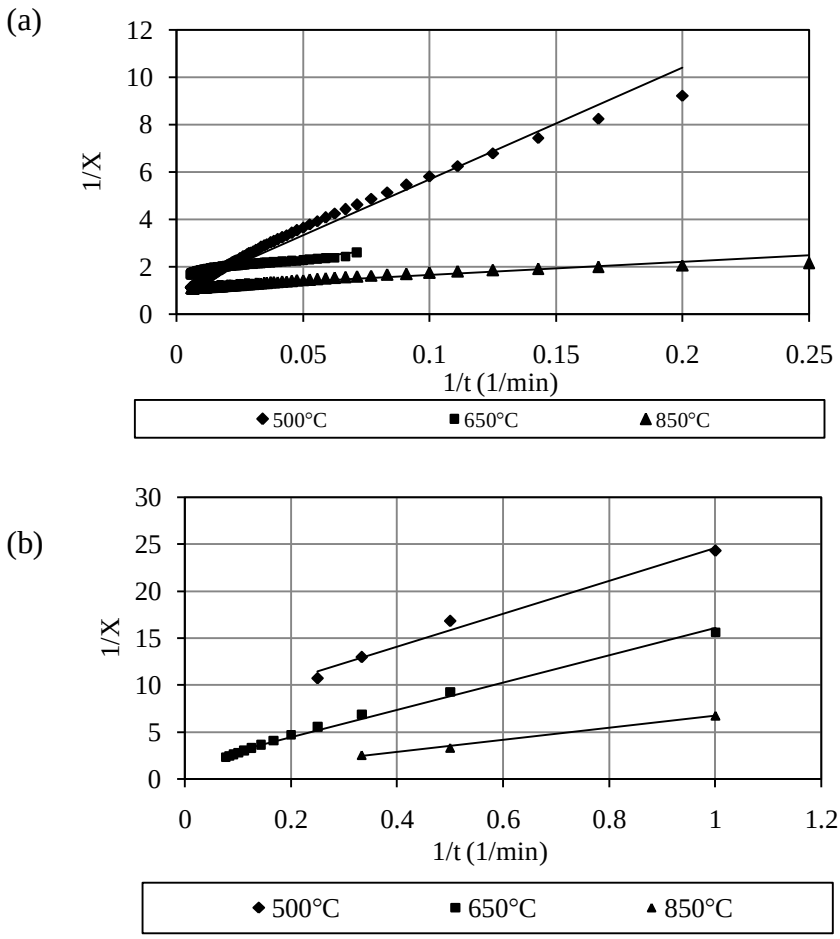

Figure 4-42: Plot of 1/X against 1/t for (a) chemical reaction kinetic control and (b) product layer diffusion control

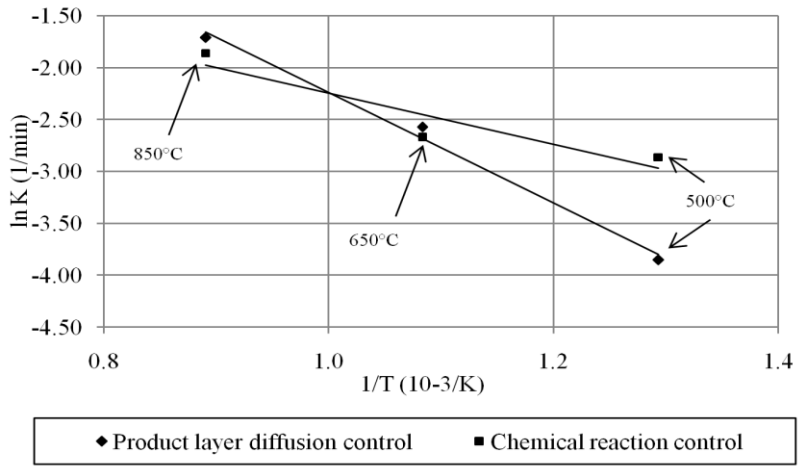

Figure 4-43: Plot of ln K against 1/T in order to obtain kinetics parameter in regions of chemical reaction control and product layer diffusion control regimes

Table 4-18 described the kinetics analysis of carbonation reaction for the synthesized CaO from cockle shell. The activation energy for product layer diffusion control region is greater than in chemical reaction control region. Lee (2004) [48] who conducts the analysis using Bhatia and Perlmutter (1983) [19] and Gupta and Fan (2002) [27] also formed the same trending. Table 4-19 described the findings obtained by Lee (2004) [48].

Table 4-18: Kinetics analysis for calcination and carbonation reaction using cockle shell

Region	Temperature (°C)	Kinetics parameter				
		ln K (1/min)	1/T (10^{-3}/K)	E (kJ/mol)	ln A	R^2
Product layer diffusion control	850	-1.713	0.890	40.863	1.16	0.918
	650	-2.573	1.083			
	500	-3.853	1.293			
Chemical reaction control	850	-1.860	0.890	31.778	4.44	0.884
	650	-2.673	1.083			
	500	-2.864	1.293			

Table 4-19: Kinetics analysis obtained by Lee (2004) [48] for CaO carbonation

Region	Bhatia and Perlmutter (1983)		Gupta and Fan (2002)	
	E (kJ/mol)	ln A (1/min)	E (kJ/mol)	ln A (1/min)
Product layer diffusion control	189.3	1.57×10^{10}	102.5	2.33×10^{5}
Chemical reaction control	72.2	1.03×10^{4}	72.7	1.16×10^{4}

According to Lee (2004) [48] activation energy for product layer diffusion control region is higher than chemical reaction control region since the resistance in product layer in greater. CO_2 gas needs to have higher kinetic energy to diffuse through solid state layer of $CaCO_3$ to initiate carbonation reaction. In contrast, chemical reaction control region refers to reaction at the surface of the adsorbent with lesser resistance from product layer. Therefore the reaction can be initiated using lesser kinetic energy.

4.7 Chapter Summary

Material characterization of cockle shell, commercial material (Aldrich $CaCO_3$ and CaO), synthesized CaO and carbonated sample are conducted using XRD, XRF, SEM, EDX and physisorption analyzer. The findings show that 95-99% of the samples are made up of $CaCO_3$ and after calcination at right condition, CaO is synthesized with purity of ~99%. Cockle shell is analyzed to be made up of Aragonite, a polymorph of $CaCO_3$ while commercial $CaCO_3$ type is mainly calcite. Through SEM, needle–like structure of Aragonite can be observed and the structure change into more spherical shapes after calcination similar to that of commercial CaO. Physisorption analysis shows that cockle shell and synthesized CaO are mesoporous material, similar to that of commercial $CaCO_3$ and CaO. In addition, surface area owned by cockle shell and synthesized CaO is observed to be higher.

The reactivity of synthesized CaO and evaluation of its efficiency during carbonation is able to be conducted by using TGA. TG curves recorded weight loss and weight gained by the samples which has undergone the calcination process and carbonation reaction respectively. dTG curve simplified the rate of weight change with respect to temperature or time. The study found that efficiency of synthesized CaO to capture CO_2 is mostly influenced by calcination temperature, holding time, heating rate and particle size of the sample.

In Nitrogen atmosphere, using particle size less than 0.125mm is the best option to synthesized CaO. The calcination temperature is best to be at 850°C at heating rate 20°C/min and being hold for 30-40 minutes. Within this condition, synthesized CaO is able to experience carbonation conversion of 0.9 and estimated to capture 0.72 kg of CO_2 for every kilogram of synthesized CaO used. Calcining the shell at very high temperature and longer holding time at high heating rates by using large particle size of the sample is an unfavorable condition to synthesis an efficient CO_2 adsorbent.

The behavior of calcining and carbonation for cockle shell, Aldrich $CaCO_3$ and mixed composition of cockle shell and Aldrich $CaCO_3$ at calcination temperature of 850°C for 40 minutes and carbonation temperature at 650°C, demonstrates that synthesized CaO from cockle shell experience highest carbonation conversion and

CO_2 capacity. However, during PKS gasification in absence of steam, GC analyzer records more CO_2 in the outlet flow rate once synthesized CaO is used as the CO_2 adsorbent where CO_2 composition is ~24 % higher than using Aldrich CaO. Utilization of synthesized CaO is favorable during gasification with steam. CO_2 released is ~16% lesser once it is applied in the reaction. The different performance of synthesized CaO might due to different reaction condition such as steam, temperature mixing of the sample and gas flow rate.

In addition, kinetics during calcination also demonstrates to greatly dependent on reaction temperature other than heating rate, particle size, and calcination holding time. Further increased in temperature, helps to reduce the activation energy of the reaction. At calcination temperature of 750°C, activation energy is 399.83kJ/mol but decrease to 222.40kJ/mol once calcination temperature is increased to 950°C. Mixing Aldrich $CaCO_3$ with cockle shell is able to reduce activation energy needed to synthesis CaO although it does not provide significant improvement for carbonation efficiency. Futhermore, kinetics analysis shows that calcination of cockle shell and Aldrich $CaCO_3$ mostly suit with zero and first order reaction mechanism according to the conditions applied.

Model developed by Lee (2004) [48] is successfully applied in this study to analyze kinetic of carbonation reaction. The model required to separate carbonation conversion into two control region where kinetics analysis is determined according to the region. In this study there are two control regions involved which are chemical reaction control region and product layer diffusion region. Activation energy for diffusion region is higher than that of chemical control region which are 40.863kJ/mol and 31.788kJ/mol respectively. The resistance from product layer towards CO_2 gas and reaction surface is a likely reason for higher activation energy.

Overall, this chapter managed to solve the objectives of the study by interpreting properties of cockle shell, determining ideal condition to synthesis CaO from cockle shell, demonstrating its ability to capture CO_2 at high temperature and analyzing the performance of synthesized CaO is comparable to the commercial adsorbent.

CHAPTER 5

CONCLUSIONS AND RECOMMENDATIONS

5.1 Conclusion

Overall, this study is able to achieve its ultimate aim to synthesis CaO from waste cockle shell as potential material for CO_2 adsorbent since the performance of this biomass is comparable to commercial CaO. The synthesis process and CO_2 adsorption reaction via calcination and carbonation also are able to be illustrated by using TGA. Yet, the efficiency of synthesized CaO during carbonation is dependent on the condition of calcination and reaction conditions.

Material characterization of XRF, EDX, and XRD show that cockle shell is rich with $CaCO_3$ (~97-99% purity) and it also indicates CaO as major compound in the sample after calcination is conducted. XRD estimates that cockle shell is made up of aragonite, a polymorph of $CaCO_3$ which is orthombic crystal structure and normally has needle-like structure. This structure is further visualized by SEM and it the surface morphology of cockle shell is confirmed. SEM also been conducted for the synthesized CaO and the surface structure obtained is almost spherical.

Isotherm plot from physisorption analysis indicates that synthesized CaO has similar isotherm profile commercial adsorbent which is Type 2. Hysteresis loop of the plot also shows that the sample is mesoporous material which can be an extra point for the synthesized adsorbent in capturing CO_2. In addition, surface area of synthesized CaO is found to be greater than commercial CaO. Therefore, based on these analyses, cockle shell can be a good source for $CaCO_3$ and the synthesized CaO also shown to have a good property as a good adsorbent for CO_2 capture.

TGA managed to demonstrate the reactivity of cockle shell calcination and carbonation reaction. Loss of ~44-45% from its initial weight indicates CO_2 is removed from the shells while the remaining 55% of calcined shell can be considered as the synthesized CaO. By referring to the analysis done by EDX, calcination is observed to be hold at more than 20 minutes to ensure enough time to remove carbon from the shell and convert it into CaO. However, various calcination conditions such as sample particle size, calcination temperature, calcination duration and heating rate are observed to have less influence on the stability of cockle shell calcination. Yet, it varies the ability of synthesized CaO to capture CO_2 during carbonation reaction.

The findings described that sample at smallest particle size (less 0.125mm) provides highest carbonation conversion and capacity compared to the sample with larger particle size. In addition, cockle shell that was calcined at 850°C demonstrates an ability to synthesize CaO with higher carbonation capacity compared to the one that been calcined at 950°C or 750°C. The duration of calcination is found to be ideal at 40 minutes and heating rate should be at 20 °C/minutes. The estimated amount of CO_2 captured per kilogram of synthesized CaO is found to be maximized at this conditions which is 0.72 kg CO_2 for every kg of synthesized CaO. Synthesis of CaO from Aldrich $CaCO_3$ based and mixed composition of cockle shell and Aldrich $CaCO_3$ is also conducted at stated condition but is unable to demonstrate higher CO_2 capacity than CaO synthesized from cockle shell.

However, once synthesized CaO is applied for gasification of PKS at reaction temperature of 900°C and holding time of 10 minutes, it is unable to capture more CO_2 compared to commercial CaO. GC reading shows CO_2 concentration in the outlet gas is increased by ~24% once synthesized CaO is applied. Inversely, synthesized CaO is able to capture more CO_2 than commercial CaO when steam is introduced to the reaction. CO_2 released is ~16% lesser once synthesized CaO is applied in the reaction. Although the gap difference is not huge, yet the synthesized CaO managed to capture a reasonable sum of CO_2. This behavior indicates that efficiency of synthesized CaO depending on the reaction conditions. Therefore, the conditions for

synthesis process and carbonation reaction need to be correct in order to obtain the best CO_2 capacity of the adsorbent.

Kinetics analysis describes that calcination process is greatly dependent on temperature and particle size other than heating rate, and calcination holding time. At calcination temperature of 750°C, activation energy is 399.83kJ/mol but decrease to 222.40kJ/mol once calcination temperature is increased to 950°C. Greater particle size also can increase activation energy of calcination. In this case, particle size less than 0.125mm required activation energy of 297kJ/mol while with particle size 2-4mm required 330.48kJ/mol. Heating rate and calcination holding time does not portray any basic or clear-cut relationship with activation energy. The value of activation energy does not observed to be very dependent on these conditions. Therefore, overall, smaller particle size sample and high calcination temperature are favorable conditions to initiate the reaction faster and easier since activation energy is minimized.

In addition, mixing Aldrich $CaCO_3$ with cockle shell at the same weight ratio does not able to reduce activation energy needed to synthesis CaO. Compared to cockle shell and mixed composition of Aldrich $CaCO_3$ and cockle shell, Aldrich $CaCO_3$ recorded to require lowest activation energy which is 238kJ/mol. Futhermore, kinetics analysis shows that calcination of cockle shell at different calcination conditions mostly suit with zero and first order reaction mechanism where regression analysis shows coefficient of determination, R^2, lies within 0.900-0.999.

Kinetic analysis using model developed by Lee (2004) [48] is successfully applied in this study to analyze kinetic of carbonation reaction. Carbonation of CaO is separated into two control regions which are chemical reaction control region and product layer diffusion region. Therefore, kinetic analysis is conducted for both regions. Activation energy for diffusion region is observed to be higher than control region which are 40.863kJ/mol and 31.788kJ/mol respectively. Resistance from product layer towards CO_2 gas and reaction surface is a likely reason for higher activation energy.

Generally, this study managed to achieve all of the objectives that been aimed before. Besides, value added of waste cockle shell as a potential alternative source for $CaCO_3$ other than limestone or magnesite also has been demonstrated. Since the performance of synthesized CaO from cockle shell can be comparable to the commercial adsorbent, therefore, it is possible for cockle shell to be implemented in the industries as the alternative CO_2 adsorbent during high temperature application.

5.2 Recommendations

As provided in Chapter 2, most of the studies run the CO_2 adsorbent through many cycles of calcination and carbonation. Therefore, in the future, synthesized CaO should be conducted in a number of cycles to determine its total capacity and endurance towards continuous adsorption activity. Besides, chemical treatment can be a good step towards novelty of synthesized CaO and improve its performance since the action of mixing commercial and synthesized CaO which is done in this study does not provide significant effect on its efficiency. Mixing cockle shell with chemical agent such as acetic acid, sulfuric acid, as been done by some researchers while doing modification to commercial CaO adsorbent, ionic liquid can be a good start to modify the structure and improves its capability. In addition, the performance of synthesized CaO should also be demonstrated in the reactor such as fixed bed or fluidized bed and pilot plant scale in order to better visualize its possibility to be adapted in the industries.

REFERENCES

[1] J. Butler, (2010, Aug. 10), “NOAA annual greenhouse gas index”, (accessed date: 2010, Aug. 20), http://www.esrl.noaa.gov/gmd/aggi.

[2] “Environment: Air Pollutant Index Report 1998-2008”, Department of Environment, Malaysia, (accessed date: 2010, Aug. 20), www.doe.gov.my.

[3] H. Lu, P. G. Smirniotis, F. O. Ernst, S. E. Pratsinis, "Nanostructured Ca-based sorbents with high CO_2 uptake efficiency", *Chemical Engineering Science*, vol. 64, no. 9, pp. 1936-1943, 2009.

[4] N. Nakatani, H. Takamori, K. Takeda, H. Sakugawa, "Transesterification of soybean oil using combusted oyster shell waste as a catalyst", *Journal Of Bioresource Technology*, vol. 100, no. 3, pp. 1510-1513, 2009.

[5] T. Weimer, R. Berger, C. Hawthorne, J. C. Abanades, "Lime enhanced gasification of solid fuels: Examination of a process for simultaneous hydrogen production and CO_2 capture", *Fuel*, vol. 87, no. 8-9, pp. 1678-1686, 2008.

[6] J. Rodriguez, M. Alonso, G. Grasa, J. C. Abanades, “Heat requirement in a calciner of $CaCO_3$ integrated in CO_2 capture system using CaO”, *Chemical Engineering Journal*, vol. 138, no. 1-3 , pp. 148-154, 2008.

[7] M. Samtani, D. Dollimore, K. S. Alexander, "Comparison of dolomite decomposition kinetics with related carbonates and the effect of procedural variables on its kinetic parameter", *Thermochimica Acta*, vol. 392-393, pp. 135-145, 2002.

[8] "Limestone forest and caves: WWF Malaysia 2006", (accessed date: 2009, June 18), www.wwf.org.my.

[9] M. C. Barros, P. M. Bello, M. Bao, J. J. Torrado, "From waste to commodity: transforming shells into high purity calcium carbonate", *Journal of Cleaner Production*, vol. 17, no. 3, pp. 400-407, 2009.

[10] Y. Li, C. Zhou, H. Chen, L. Duan, X. Chen, "CO_2 capture behavior of shell during calcination/ carbonation cycles", *Chemical Engineering Technology* vol. 32, no. 8, pp. 1176-1182, 2009.

[11] O. Levinspiel, “Fluid particle reaction kinetic” in *Chemical Reaction Engineering; 3rd Edition*, USA, Johns Wiley & Sons, 1999, ch. 25, pp. 566-586.

[12] F. Garcia-Labiano, J. Adanez, A. Abad, L. F. deDiego, P. Gayan, "Calcination of calcium-based sorbents at pressure in a broad range of CO_2 concentrations", *Chemical Engineering Science*, vol. 57, no. 13, pp. 2381-2393, 2002.

[13] V. Bouineau, M. Pijolat, M. Soustelle, "Characterization of chemical reactivity of a $CaCO_3$ powder for its decomposition", *Journal of European Ceramic Society*, vol. 18, no. 9, pp. 1319-1324, 1998.

[14] C. Cheng, E. Specht, "Reaction rate coefficients in decomposition of lumpy limestone of different origin", *Thermochimica Acta*, vol. 449, no. 1-2, pp. 8-15, 2006.

[15] B. R. Stanmore, P. Gilot P, "Review- calcination and carbonation of limestone during thermal cycling for CO_2 sequestration", *Fuel Processing Technology*, vol. 86, no. 16, pp. 1707-1743, 2005.

[16] J. Khinast, G. F. Krammer, C. Brunner, G. Staudinger, "Decomposition of limestone: the influence of CO_2 and particle size on the reaction rate", *Chemical Engineering Science*, vol. 51, no. 4, pp. 623-634, 1996.

[17] J. C. Abanades, D. Alvarez, "Conversion limits in the reaction of CO_2 with lime", *Energy and Fuels*, vol. 17, no. 2, pp. 308-315, 2003.

[18] E. Bonquet, G. Leyssens, C. Schonnenbeck, P. Gilot, "The decrease of carbonation efficiency of CaO along calcination-carbonation cycles: experiments and modelling", *Chemical Engineering Science*, vol. 64, no. 9. pp. 2136-2146, 2009.

[19] S. K. Bhatia, D. D. Perlmutter, "The effect of product layer on the kinetic of CO_2-lime reaction", *AlChE Journal*, vol 1, no. 1, pp.79-86, 1983.

[20] D. Alvarez, M. Pena, A. G. Borrego, "Behavior of different calcium-based sorbents in a calcination/carbonation cycle for CO_2 capture", *Energy & Fuels*, vol. 21, no. 3, pp. 1534-1542, 2007.

[21] S. N. Izura, T. K. Hooi, "Shaping the future of cockle industry in Malaysia", presented at National Fisheries Symposium (NAFIS), Kuala Terengganu, Terengganu, 14-16 July, 2008.

[22] I. Ar, G. Dogu, "Calcination kinetics of high purity limestones", *Chemical Engineering Journal*, vol. 83, no. 2, pp. 131-137, 2001.

[23] K. Sulaiman, "Ternakan kerang sumber ekonomi nelayan", *Agrobiz Utusan Malaysia*, 6 March 2007, pp 6-7.

[24] Z. A. B. Zakaria, N. Zakaria, Z. Kasim, "Mineral composition of the cockle (*Anadara granosa*) shells, hard clamp (*Meretrix meretrix*) shells and corals (*Porites* spp.): A comparative study", *Journal of Animal and Veterinary Advances*, vol. 3, no. 7, pp. 445-447, 2004.

[25] "Pelan induk pembangunan pertanian 2005", (accessed date: 2009, Feb. 14), www.bernama.com/selangor_maju/pembangunan_pertanian.htm.

[26] "Maps of Malaysia and Singapore", (accessed date: 2011, March 7), www.myMalaysiabooks.com.

[27] H. Gupta, L-S. Fan, "Carbonation-calcination cycle using high reactivity calcium oxide for carbon dioxide separation from flue gas", *Industrial Chemical Engineering Resources*, vol. 41, no. 16, pp. 4035-4042, 2002.

[28] C. S. Martavaltzi, A. A. Lemonidou, "Development of new CaO based sorbents material for CO_2 removal at high temperature", *Microporous and Mesoporous Materials*, vol. 110, no. 1, pp. 119-127, 2008.

[29] G. N. Karagiannis, T. C. Vaimakis, A. T. Sdoukos, "The effect of procedural variables and mechanical activation on the thermal decomposition of calcite. An approach by experimental design", *Thermochimica Acta*, vol. 262, pp. 129-144, 1995.

[30] J. P. Sanders, P. K. Gallagher, "Kinetic analyses using simultaneous TG/DSC measurements part I: decomposition of calcium carbonate in argon", *Thermochimica Acta*, vol. 388, no. 1-2, pp. 115-128, 2002.

[31] K. Thambimuthu, M. Soltanieh, J. C. Abanades, "IPCC special report on CO_2 capture and storage", Cambridge University Press, pp. 431, 2005.

[32] S. Satyapal, T. Filburn, J. Trela, S. Jeremy, "Novel solid amine sorbents and applications for carbon dioxide removal, novel approaches to carbon

management: separation, capture, sequestration, and conversion to useful products", The National Academic Press, Washington, 2003.

[33] E. S. Rubin, A. B. Rao, "A technical, economic, and environmental assessment of amine-based CO_2 capture technology for power plant greenhouse gas control", Carnegie Mellon University, Pittsburgh, 2002.

[34] B. B. Sakadjian, M. V. Iyer, H. Gupta, L-S Fan, "Kinetics and structural characterization of calcium-based sorbents calcined under sub atmospheric conditions for the high temperature CO_2 capture process", *Industrial Engineering Chemical Resource*, vol. 46, no. 1, pp. 35-42, 2007.

[35] N. H. Florin, A. T. Harris, "Enhanced hydrogen production from biomass with in situ carbon dioxide capture using calcium oxide sorbents", *Chemical Engineering Science*, vol. 63, no. 2, pp. 287-316, 2008.

[36] G. Grasa, J. C. Abanades, A. J. Anthony, "Effect of partial carbonation on the cyclic CaO carbonation reaction", *Industrial Engineering Chemical Resource*, vol. 48, no. 20, pp. 9090-9096, 2009.

[37] M. Ives, R. C. Mundy, P.S. Fennell, J. F. Davidson, J. S. Dennis, A. N. Hayhurst, "Comparison of different natural sorbents for removing CO_2 from combustion gasses, as studied in a bench scale fluidized", *Energy and Fuel*, vol. 22, no. 6, pp. 3852-3857, 2008.

[38] M. V. Iyer, L-S. Fan, "High temperature CO_2 capture using engineered eggshells: A route to carbon management", US Patent, US 7 678 351 B2, March 16, 2010.

[39] S. Gaur, T. Reed, “Overview of thermal analysis method”, in *Thermal data for natural and synthetic fuel*, Marcel Dekker, New York, 1998.

[40] Z. Ye, W. Wang, Q. Zhong, I. Bjerle, "High temperature desulfurisation using fine sorbent particles under boiler injection conditions", *Fuel*, vol. 74, no. 5, pp. 743-750, 1995.

[41] L. Cheng, B. Chen, N. Liu, Z. Luo, K. Cen, “Effect of characteristics of sorbent on their sulfur capture capability at a fluidized bed condition”, *Fuel*, vol. 83, no. 7-8, pp. 925-932, 2004.

[42] R. H. Borgwardt, "Calcium oxide sintering in atmosphere containing water and carbon dioxide", *Industrial Engineering Chemistry Research,* vol. 28, no. 4, pp. 493-500, 1989.

[43] N. Hu, A. W. Scaroni, "Calcination of pulverized limestone particles under furnace injection condition", *Fuel,* vol. 75, no.2, pp. 177-186, 1996.

[44] S. Senthoorselvan, S. Gleis, S. Hartmut, P. Yrjas, M. Hupa, "Cyclic carbonation calcination studies of limestone and dolomite for C_{O2} separation from combustion flue gases", *Journal of Engineering for Gas Turbines and Power,* vol. 131, no. 1, pp. 011801-1 – 011801-8, 2009.

[45] D. Y. Lu, R. W. Hughes, E. J. Anthony, "Ca-based sorbent looping combustion for CO_2 capture in pilot scale dual fluidize beds", *Fuel Processing Technology,* vol. 89, no. 12, pp. 1386-1395, 2008.

[46] T. Ozawa, "A new method of analyzing thermogravimetric data", vol. 38, no. 11, pp. 1881-1886, 1965.

[47] D. Dollimore, P. Tong, K. S. Alexander, "The kinetic interpretation of the decomposition of calcium carbonate by use of relationships other than the Arrhenius equation", *Thermochimica Acta,* vol. 282-283, pp. 13-27, 1996.

[48] D. K. Lee, "An apparent kinetic model for the carbonation of calcium oxide by carbon dioxide", *Chemical Engineering Journal*, vol. 100, no. 1-3 , pp. 71-77, 2004.

[49] P. Sun, J. R. Grace, C. J. Lim, E. J. Anthony, "Determination of intrinsic rate constant of the CaO-CO_2 reaction", *Chemical Engineering*, vol. 63, no.1, pp. 47-56, 2008.

[50] S. E. Dann, *Reactions and characterizations of solids*, Wiley InterScience, The Royal Society of Chemistry, Loughborough, Britain, 2002.

[51] T. Hatakeyama, Z. Liu, *Handbook of thermal analysis*, John Wiley and Sons, England, 1998.

[52] Y. Wang, W. J. Thomson, "The effect of sample preparation on the thermal decomposition of $CaCO_3$", *Thermochimica Acta*, vol. 255, pp. 383-390, 1995.

[53] K. Sasaki, T. Yamashita, M. Tsunekawa, "Synthesis of aragonite from calcined scallop shells at ambient temperatures and their morphological

characterization by FE-SEM", *Journal of the Mining and Materials Processing Institute of Japan*, vol. 118, no. 8, pp. 553-558, 2002.

[54] *Chapter 7: Basics of X-ray diffraction Manual*, Scintag Inc, Cupertino, USA, 1999.

[55] J. R. Connolly, "Introduction quantitative X-Ray Diffraction methods", EPS 400-001, 2010.

[56] Z. Hu, M. Shao, Q. Cai, S.Ding, C. Zhong, X. Wei, Y. Deng, "Synthesis of needle-like aragonite from limestone in the presence of magnesium chloride", *Journal of Material Processing Technology*, vol. 209, no. 3, pp. 1607-1611.

[57] *Micromeritics ASAP 2020*, User Familiarization Training, Universiti Teknologi PETRONAS, Malaysia, April 7-8, 2010.

[58] P.A. Webb, C. Orr, *Analytical method on fine particle technology*, Micromeritics Instrument Corp., USA, 1997.

[59] B. K. Singh, P. Kumara, D. Adhikari, "Thermal decomposition kinetics of peanut shell", *Nature and Science*", ISSN 1545-0740, 2009.

[60] D. J. Jeon, S. H. Yeom, "Recycling wasted biomaterial, crab shells, as an adsorbent for the removal of high concentration of phosphate", *Bioresource Technology*, vol. 100, no. 9, pp. 2646-2649, 2009.

[61] M. Hartman, O. Trnka, V. Vesely, K. Svoboda, "Predicting the rate of thermal decomposition of dolomite", *Chemical Engineering Science*, vol. 51, no. 23, pp. 5229 – 5232, 1996.

[62] Z. Li, N-S. Cai, Y-Y. Huang, "Effect of preparation temperature on cyclic CO_2 capture and multiple carbonation-calcination cycles for a new Ca-based CO_2 sorbent", *Industrial Engineering Chemical Resources*, vol. 45, no. 6, pp. 1911-1917, 2006.

[63] M. Hassibi, "An overview of lime slaking and factors that affect the process", Chemco Systems, L.P., Monongahela, P.A, February 2009.

[64] J. K. Muehling, H. R. Arnold, J. E. House, "Effects of particle size on the decomposition of ammonium carbonate", *Thermochimica Acta*, vol. 255, pp. 347-353, 1995.

Appendix A

TGA reading for cockle shell calcined at 850°C for 40 minutes using heating rate of 20°C/min and particle size of less 0.125mm

Time	Temp.	TG	DTG	Time	Temp.	TG	DTG	Time	Temp.	TG	DTG
min	°C	%	%/min	min	°C	%	%/min	min	°C	%	%/min
1	51.74	99.80	0.029	51	869.01	52.86	0.018	101	665.95	72.83	-1.298
2	59.82	99.76	0.057	52	869.11	52.84	0.018	102	665.73	74.09	-1.212
3	73.10	99.68	0.073	53	869.18	52.83	0.009	103	665.52	75.28	-1.133
4	89.63	99.61	0.064	54	869.28	52.81	0.017	104	665.34	76.40	-1.084
5	108.17	99.56	0.029	55	869.33	52.80	0.011	105	665.16	77.48	-0.987
6	127.84	99.50	0.088	56	869.38	52.79	0.028	106	664.95	78.45	-0.926
7	148.41	99.39	0.068	57	869.43	52.77	0.021	107	664.79	79.37	-0.888
8	169.48	99.35	0.054	58	869.47	52.76	0.012	108	664.61	80.24	-0.837
9	190.88	99.25	0.113	59	869.52	52.75	0.017	109	664.47	81.05	-0.788
10	212.52	99.11	0.178	60	869.52	52.73	0.018	110	664.29	81.80	-0.730
11	234.21	98.88	0.258	61	869.53	52.72	0.012	111	664.15	82.50	-0.710
12	256.06	98.58	0.318	62	869.55	52.71	0.009	112	664.03	83.11	-0.611
13	277.88	98.25	0.346	63	869.56	52.70	0.010	113	663.93	83.69	-0.573
14	299.84	97.86	0.427	64	869.60	52.69	0.004	114	663.82	84.22	-0.523
15	321.78	97.44	0.378	65	869.61	52.68	0.014	115	663.68	84.70	-0.485
16	343.72	97.09	0.354	66	869.64	52.68	0.011	116	663.61	85.14	-0.436
17	365.41	96.77	0.260	67	869.63	52.67	0.005	117	663.49	85.53	-0.376
18	386.65	96.58	0.155	68	869.66	52.66	0.013	118	663.41	85.87	-0.352
19	407.89	96.43	0.132	69	869.67	52.66	0.011	119	663.35	86.18	-0.307
20	429.24	96.32	0.120	70	869.70	52.65	0.006	120	663.30	86.46	-0.297
21	450.57	96.22	0.112	71	869.71	52.65	0.004	121	663.24	86.71	-0.270
22	471.87	96.15	0.073	72	869.68	52.64	0.008	122	663.21	86.96	-0.249
23	493.06	96.09	0.058	73	869.72	52.63	0.008	123	663.18	87.18	-0.232
24	514.11	95.96	0.163	74	869.75	52.63	-0.005	124	663.14	87.38	-0.202
25	535.13	95.83	0.055	75	869.71	52.63	0.006	125	663.15	87.57	-0.191
26	556.10	95.79	0.012	76	869.73	52.62	0.003	126	663.11	87.74	-0.170
27	577.15	95.76	0.020	77	869.77	52.62	0.001	127	663.12	87.90	-0.144
28	598.17	95.74	0.015	78	869.76	52.61	0.005	128	663.12	88.05	-0.145
29	619.13	95.71	0.032	79	869.77	52.60	0.005	129	663.09	88.19	-0.126
30	640.19	95.68	0.029	80	869.76	52.60	0.005	130	663.11	88.32	-0.113
31	661.27	95.65	0.049	81	861.15	52.59	0.033	131	663.13	88.44	-0.099
32	682.46	95.62	0.039	82	843.60	52.58	0.031	132	663.16	88.55	-0.083
33	703.27	95.15	1.632	83	824.24	52.56	0.013	133	663.17	88.66	-0.087
34	723.30	91.37	5.372	84	804.76	52.55	-0.008	134	663.16	88.76	-0.082
35	743.27	83.66	9.603	85	785.25	52.54	-0.002	135	663.20	88.85	-0.081
36	763.20	71.49	14.079	86	765.74	52.53	0.008	136	663.18	88.94	-0.080
37	784.22	56.45	13.723	87	746.18	52.52	0.001	137	663.20	89.03	-0.066
38	809.65	53.33	0.142	88	726.39	52.50	0.014	138	663.19	89.11	-0.054
39	830.74	53.25	0.079	89	706.68	52.48	0.013	139	663.19	89.19	-0.066
40	851.39	53.17	0.074	90	687.12	52.46	0.022	140	663.22	89.26	-0.058
41	862.99	53.11	0.045	91	675.82	55.13	-6.262	141	663.22	89.33	-0.051
42	865.63	53.06	0.041	92	670.78	57.70	-2.259	142	663.22	89.40	-0.052
43	866.49	53.03	0.034	93	669.35	59.80	-2.027	143	663.23	89.46	-0.051
44	867.01	53.00	0.031	94	668.55	61.74	-1.905	144	663.22	89.52	-0.043
45	867.45	52.97	0.021	95	667.95	63.59	-1.819	145	663.20	89.58	-0.051
46	867.79	52.95	0.012	96	667.46	65.34	-1.733	146	663.18	89.64	-0.063
47	868.12	52.94	0.012	97	667.06	67.01	-1.648	147	663.19	89.69	-0.047
48	868.35	52.91	0.016	98	666.71	68.59	-1.557	148	663.16	89.74	-0.062
49	868.64	52.89	0.023	99	666.41	70.08	-1.464	149	663.16	89.79	-0.050
50	868.83	52.88	0.018	100	666.17	71.49	-1.380	150	663.16	89.83	-0.057

Time	Temp.	TG	DTG	Time	Temp.	TG	DTG
min	°C	%	%/min	min	°C	%	%/min
151	663.17	89.88	-0.054	211	663.45	91.09	-0.026
152	663.16	89.92	-0.052	212	663.44	91.10	-0.033
153	663.17	89.96	-0.040	213	663.47	91.11	-0.028
154	663.15	90.00	-0.045	214	663.52	91.12	-0.029
155	663.16	90.04	-0.075	215	663.53	91.13	-0.027
156	663.13	90.08	-0.054	216	663.59	91.14	-0.025
157	663.13	90.11	-0.045	217	663.59	91.15	-0.019
158	663.11	90.14	-0.048	218	663.61	91.16	-0.023
159	663.12	90.18	-0.049	219	663.62	91.16	-0.012
160	663.11	90.21	-0.051	220	663.64	91.17	-0.003
161	663.12	90.24	-0.053	221	663.66	91.18	-0.005
162	663.12	90.27	-0.048	222	663.67	91.19	-0.012
163	663.16	90.30	-0.050	223	663.67	91.20	0.008
164	663.16	90.32	-0.038	224	663.66	91.21	0.001
165	663.12	90.35	-0.038	225	663.66	91.22	0.008
166	663.15	90.38	-0.041	226	663.66	91.22	0.009
167	663.15	90.40	-0.043	227	663.69	91.22	0.016
168	663.14	90.42	-0.039	228	663.69	91.23	0.020
169	663.16	90.45	-0.033	229	663.71	91.23	0.010
170	663.18	90.47	-0.032	230	663.69	91.24	0.006
171	663.18	90.49	-0.036	231	663.68	91.25	0.011
172	663.22	90.52	-0.038	232	663.70	91.26	0.017
173	663.21	90.54	-0.023	233	663.69	91.27	0.021
174	663.20	90.56	-0.023	234	663.69	91.27	0.010
175	663.21	90.58	-0.032	235	663.68	91.28	0.001
176	663.24	90.60	-0.028	236	663.69	91.29	0.000
177	663.25	90.62	-0.018	237	663.68	91.29	0.007
178	663.23	90.64	-0.026	238	663.69	91.30	0.001
179	663.25	90.65	-0.018	239	663.67	91.31	0.000
180	663.26	90.67	-0.030	240	663.64	91.32	-0.004
181	663.25	90.69	-0.025	241	663.61	91.32	-0.002
182	663.28	90.70	-0.024	242	663.61	91.33	-0.003
183	663.29	90.72	-0.022	243	663.60	91.34	-0.008
184	663.29	90.74	-0.017	244	663.59	91.34	-0.010
185	663.31	90.75	-0.020	245	663.56	91.35	-0.021
186	663.29	90.77	-0.013	246	663.55	91.36	-0.013
187	663.32	90.78	-0.019	247	663.55	91.37	-0.019
188	663.32	90.79	-0.012	248	663.58	91.37	-0.025
189	663.31	90.81	-0.032	249	663.60	91.38	-0.025
190	663.37	90.82	-0.012	250	663.58	91.39	-0.028
191	663.34	90.84	-0.020	251	663.59	91.40	-0.029
192	663.35	90.85	-0.023	252	663.59	91.40	-0.022
193	663.38	90.87	-0.020	253	663.61	91.41	-0.031
194	663.39	90.88	-0.018	254	663.62	91.42	-0.018
195	663.39	90.90	-0.025	255	663.60	91.43	-0.021
196	663.40	90.91	-0.018	256	663.64	91.44	-0.021
197	663.41	90.93	-0.027	257	663.66	91.45	-0.018
198	663.42	90.95	-0.028	258	663.68	91.46	-0.007
199	663.41	90.96	-0.016	259	663.70	91.46	-0.017
200	663.38	90.97	-0.017	260	663.72	91.47	-0.010
201	663.42	90.99	-0.030	261	663.74	91.48	-0.012
202	663.44	91.00	-0.012	262	663.76	91.49	-0.004
203	663.43	91.01	-0.025	263	663.81	91.50	0.002
204	663.39	91.02	-0.033	264	663.82	91.51	0.002
205	663.40	91.03	-0.027	265	663.83	91.52	0.008
206	663.42	91.04	-0.029	266	663.85	91.52	0.002
207	663.41	91.06	-0.024	267	663.83	91.53	0.012
208	663.41	91.07	-0.037	268	663.82	91.54	0.019
209	663.43	91.08	-0.028	269	663.81	91.55	0.012
210	663.46	91.09	-0.029	270	663.80	91.56	0.010

Appendix B

TGA reading for Aldrich $CaCO_3$ calcined at 850°C for 40 minutes using heating rate of 20°C/min and particle size of less 0.125mm

Time	Temp.	TG	DTG	Time	Temp.	TG	DTG	Time	Temp.	TG	DTG
min	°C	%	%/min	min	°C	%	%/min	min	°C	%	%/min
1	52.19	99.90	0.001	51	868.68	54.58	-0.002	101	665.43	82.14	-0.193
2	60.21	99.92	-0.034	52	868.74	54.57	0.018	102	665.22	82.33	-0.186
3	73.39	99.95	-0.031	53	868.79	54.57	0.009	103	665.09	82.52	-0.203
4	89.86	99.99	-0.064	54	868.81	54.56	0.003	104	664.96	82.70	-0.133
5	108.30	100.03	-0.031	55	868.83	54.56	-0.006	105	664.80	82.85	-0.127
6	127.84	100.08	-0.057	56	868.85	54.56	-0.008	106	664.65	82.99	-0.132
7	148.26	100.13	-0.077	57	868.92	54.55	0.018	107	664.54	83.14	-0.124
8	169.16	100.20	-0.058	58	868.93	54.55	0.012	108	664.43	83.29	-0.125
9	190.47	100.26	-0.060	59	868.95	54.54	-0.002	109	664.33	83.43	-0.130
10	211.99	100.33	-0.059	60	868.96	54.54	0.002	110	664.19	83.58	-0.111
11	233.67	100.38	-0.049	61	868.97	54.54	0.007	111	664.10	83.70	-0.109
12	255.49	100.42	-0.036	62	868.98	54.53	0.013	112	664.00	83.82	-0.102
13	277.30	100.48	-0.139	63	868.99	54.53	0.014	113	663.91	83.93	-0.088
14	299.08	100.55	-0.045	64	868.99	54.52	0.005	114	663.82	83.99	-0.098
15	320.88	100.61	-0.027	65	869.01	54.52	0.012	115	663.74	84.09	-0.113
16	342.60	100.64	-0.042	66	869.02	54.52	0.007	116	663.61	84.19	-0.104
17	364.21	100.68	-0.038	67	869.05	54.51	0.009	117	663.51	84.27	-0.093
18	385.80	100.73	-0.030	68	869.03	54.51	0.021	118	663.42	84.34	-0.110
19	407.26	100.76	-0.013	69	869.03	54.51	0.006	119	663.34	84.42	-0.097
20	428.61	100.77	-0.036	70	869.03	54.50	0.006	120	663.27	84.49	-0.058
21	449.86	100.78	-0.034	71	869.04	54.50	0.002	121	663.21	84.52	-0.059
22	471.20	100.80	-0.026	72	869.05	54.50	-0.005	122	663.17	84.58	-0.085
23	492.59	100.81	-0.022	73	869.05	54.50	-0.001	123	663.17	84.65	-0.082
24	513.90	100.80	0.036	74	869.05	54.50	0.000	124	663.12	84.71	-0.065
25	535.13	100.72	0.038	75	869.05	54.50	0.014	125	663.10	84.77	-0.073
26	556.29	100.73	-0.002	76	869.06	54.49	-0.001	126	663.10	84.84	-0.066
27	577.44	100.77	-0.049	77	869.05	54.49	-0.001	127	663.07	84.90	-0.069
28	598.62	100.80	0.006	78	869.06	54.49	-0.007	128	663.07	84.96	-0.038
29	619.72	100.80	0.054	79	869.06	54.49	0.005	129	663.09	85.02	-0.031
30	640.88	100.60	0.396	80	869.05	54.48	-0.001	130	663.07	85.08	-0.044
31	662.02	99.82	1.132	81	860.38	54.48	-0.009	131	663.08	85.14	-0.036
32	683.10	98.13	2.155	82	843.18	54.47	-0.001	132	663.09	85.19	-0.040
33	703.99	95.11	3.791	83	823.81	54.46	0.011	133	663.07	85.25	-0.034
34	724.69	90.01	6.216	84	804.10	54.45	-0.008	134	663.06	85.30	-0.031
35	745.29	82.01	9.403	85	784.45	54.44	-0.008	135	663.07	85.35	-0.025
36	765.70	70.66	12.769	86	764.93	54.42	0.002	136	663.02	85.40	-0.030
37	786.78	57.24	11.939	87	745.35	54.41	0.020	137	663.04	85.45	-0.036
38	810.80	54.63	0.176	88	725.66	54.39	-0.003	138	663.01	85.50	-0.034
39	831.99	54.60	-0.006	89	706.05	54.37	0.019	139	662.99	85.55	-0.039
40	852.78	54.60	0.001	90	686.48	54.36	0.031	140	662.96	85.59	-0.042
41	864.36	54.59	0.005	91	676.14	57.79	-16.338	141	662.96	85.65	-0.042
42	866.92	54.59	-0.001	92	672.07	79.15	-2.027	142	662.95	85.69	-0.049
43	867.47	54.59	0.001	93	668.59	79.97	-0.567	143	662.95	85.74	-0.047
44	867.72	54.59	-0.001	94	667.81	80.42	-0.389	144	662.92	85.79	-0.045
45	867.88	54.59	-0.005	95	667.29	80.77	-0.323	145	662.89	85.83	-0.057
46	868.05	54.59	0.011	96	666.85	81.06	-0.293	146	662.84	85.87	-0.051
47	868.23	54.59	-0.010	97	666.48	81.32	-0.265	147	662.81	85.91	-0.045
48	868.36	54.59	-0.004	98	666.15	81.55	-0.234	148	662.76	85.96	-0.055
49	868.49	54.59	0.012	99	665.87	81.75	-0.219	149	662.76	86.00	-0.064
50	868.60	54.58	0.016	100	665.64	81.95	-0.190	150	662.78	86.04	-0.068

Time	Temp.	TG	DTG	Time	Temp.	TG	DTG
min	°C	%	%/min	min	°C	%	%/min
151	662.76	86.09	-0.066	211	663.20	87.99	-0.038
152	662.75	86.12	-0.052	212	663.23	88.01	-0.028
153	662.74	86.17	-0.057	213	663.22	88.04	-0.029
154	662.69	86.21	-0.062	214	663.22	88.06	-0.029
155	662.69	86.25	-0.058	215	663.24	88.08	-0.015
156	662.70	86.29	-0.053	216	663.26	88.11	-0.014
157	662.72	86.33	-0.068	217	663.26	88.13	-0.009
158	662.72	86.39	-0.104	218	663.26	88.15	-0.017
159	662.72	86.43	-0.064	219	663.28	88.18	-0.010
160	662.72	86.46	-0.053	220	663.27	88.21	-0.005
161	662.72	86.50	-0.045	221	663.27	88.23	-0.016
162	662.73	86.54	-0.044	222	663.28	88.25	-0.016
163	662.72	86.57	-0.056	223	663.30	88.28	-0.008
164	662.73	86.61	-0.050	224	663.27	88.30	-0.006
165	662.72	86.65	-0.063	225	663.26	88.32	0.002
166	662.74	86.68	-0.052	226	663.28	88.34	-0.002
167	662.73	86.72	-0.047	227	663.29	88.37	-0.004
168	662.72	86.75	-0.046	228	663.29	88.39	-0.005
169	662.74	86.78	-0.035	229	663.28	88.41	-0.008
170	662.76	86.82	-0.053	230	663.27	88.44	-0.005
171	662.77	86.85	-0.028	231	663.25	88.46	-0.019
172	662.77	86.88	-0.041	232	663.21	88.48	-0.013
173	662.75	86.91	-0.052	233	663.23	88.50	-0.011
174	662.77	86.94	-0.036	234	663.18	88.52	-0.028
175	662.77	86.97	-0.040	235	663.16	88.54	-0.026
176	662.77	87.00	-0.029	236	663.15	88.57	-0.032
177	662.83	87.04	-0.044	237	663.13	88.59	-0.031
178	662.81	87.07	-0.036	238	663.14	88.61	-0.041
179	662.83	87.10	-0.048	239	663.14	88.63	-0.026
180	662.83	87.13	-0.044	240	663.14	88.66	-0.049
181	662.85	87.16	-0.041	241	663.14	88.68	-0.039
182	662.87	87.19	-0.043	242	663.15	88.70	-0.044
183	662.86	87.22	-0.040	243	663.16	88.72	-0.037
184	662.87	87.25	-0.048	244	663.18	88.74	-0.042
185	662.87	87.28	-0.051	245	663.19	88.77	-0.041
186	662.88	87.31	-0.046	246	663.22	88.79	-0.050
187	662.88	87.34	-0.042	247	663.24	88.81	-0.037
188	662.87	87.37	-0.042	248	663.26	88.83	-0.036
189	662.87	87.40	-0.040	249	663.27	88.85	-0.025
190	662.85	87.42	-0.040	250	663.29	88.87	-0.050
191	662.89	87.45	-0.050	251	663.33	88.89	-0.024
192	662.88	87.48	-0.033	252	663.37	88.92	-0.035
193	662.87	87.51	-0.052	253	663.40	88.94	-0.008
194	662.88	87.54	-0.047	254	663.40	88.96	-0.013
195	662.88	87.56	-0.046	255	663.39	88.98	-0.014
196	662.87	87.59	-0.051	256	663.41	89.00	0.012
197	662.90	87.67	-0.038	257	663.38	89.02	0.009
198	662.90	87.71	-0.038	258	663.38	89.04	-0.012
199	662.91	87.74	-0.037	259	663.38	89.06	-0.004
200	662.91	87.77	-0.037	260	663.36	89.08	0.008
201	662.92	87.81	-0.036	261	663.32	89.10	-0.016
202	662.92	87.84	-0.036	262	663.32	89.12	-0.011
203	662.93	87.87	-0.035	263	663.28	89.14	-0.009
204	662.93	87.91	-0.035	264	663.28	89.16	-0.019
205	662.94	87.94	-0.034	265	663.27	89.18	-0.025
206	662.94	87.97	-0.034	266	663.24	89.20	-0.013
207	662.95	88.00	-0.034	267	663.24	89.22	-0.036
208	662.95	88.04	-0.033	268	663.22	89.24	-0.039
209	662.96	88.07	-0.033	269	663.23	89.25	-0.023
210	662.96	88.10	-0.032	270	663.23	89.27	-0.051

Appendix C

TGA reading for Aldrich $CaCO_3$ mixed with cockle shell, calcined at 850°C for 40 minutes using heating rate of 20°C/min and particle size of less 0.125mm

Time	Temp.	TG	DTG	Time	Temp.	TG	DTG	Time	Temp.	TG	DTG
min	°C	%	%/min	min	°C	%	%/min	min	°C	%	%/min
1	52.16	100.00	0.010	51	867.94	54.43	-0.003	101	665.53	74.40	-0.899
2	60.24	100.00	0.005	52	868.07	54.43	-0.008	102	665.33	75.29	-0.849
3	73.37	100.00	0.003	53	868.17	54.43	-0.002	103	665.12	76.14	-0.824
4	89.82	100.01	-0.020	54	868.24	54.43	0.001	104	664.94	76.98	-0.811
5	108.25	100.02	-0.027	55	868.30	54.43	-0.008	105	664.78	77.74	-0.743
6	127.74	100.04	-0.021	56	868.34	54.44	-0.008	106	664.61	78.48	-0.721
7	148.18	100.06	-0.031	57	868.39	54.43	0.002	107	664.46	79.19	-0.694
8	169.10	100.08	-0.019	58	868.40	54.43	-0.005	108	664.26	79.86	-0.669
9	190.43	100.07	0.054	59	868.41	54.43	0.012	109	664.12	80.51	-0.666
10	212.00	100.02	0.051	60	868.44	54.42	0.009	110	663.93	81.13	-0.602
11	233.67	99.94	0.117	61	868.44	54.42	0.006	111	663.75	81.70	-0.578
12	255.45	99.81	0.145	62	868.48	54.41	-0.002	112	663.62	82.25	-0.555
13	277.24	99.67	0.163	63	868.51	54.42	-0.003	113	663.47	82.77	-0.512
14	299.06	99.50	0.169	64	868.55	54.42	0.012	114	663.39	83.22	-0.451
15	320.87	99.32	0.186	65	868.57	54.41	0.001	115	663.29	83.68	-0.453
16	342.81	99.16	0.162	66	868.62	54.42	-0.004	116	663.23	84.11	-0.424
17	364.33	99.02	0.118	67	868.67	54.42	0.002	117	663.17	84.51	-0.395
18	385.62	98.94	0.060	68	868.67	54.41	0.005	118	663.13	84.89	-0.368
19	406.99	98.90	0.030	69	868.64	54.41	-0.002	119	663.11	85.25	-0.339
20	428.39	98.88	0.020	70	868.67	54.41	0.007	120	663.09	85.59	-0.299
21	449.55	98.86	-0.004	71	868.64	54.41	0.010	121	663.07	85.88	-0.292
22	470.75	98.85	-0.004	72	868.67	54.41	0.005	122	663.05	86.17	-0.279
23	492.01	98.83	0.011	73	868.68	54.41	0.009	123	663.05	86.46	-0.259
24	513.23	98.82	0.055	74	868.70	54.41	-0.003	124	663.03	86.73	-0.255
25	534.29	98.74	0.079	75	868.69	54.41	-0.002	125	663.02	86.99	-0.249
26	555.20	98.75	-0.060	76	868.70	54.41	-0.003	126	662.94	87.23	-0.223
27	576.09	98.81	-0.042	77	868.70	54.40	0.003	127	662.92	87.46	-0.237
28	597.00	98.81	0.004	78	868.68	54.40	0.008	128	662.86	87.68	-0.210
29	617.95	98.62	0.368	79	868.70	54.40	0.007	129	662.85	87.89	-0.200
30	638.97	97.94	0.954	80	868.71	54.40	-0.008	130	662.85	88.09	-0.186
31	659.86	96.56	1.762	81	859.85	54.40	-0.007	131	662.80	88.29	-0.201
32	680.74	94.21	2.819	82	842.60	54.40	0.002	132	662.77	88.47	-0.188
33	701.41	90.56	4.378	83	823.43	54.39	0.001	133	662.76	88.64	-0.168
34	721.88	84.99	6.606	84	803.63	54.39	0.019	134	662.71	88.80	-0.168
35	742.20	76.77	9.557	85	783.88	54.38	-0.003	135	662.65	88.96	-0.169
36	762.45	65.51	12.390	86	764.31	54.38	-0.011	136	662.60	89.11	-0.159
37	785.01	55.21	4.752	87	744.75	54.36	0.015	137	662.55	89.26	-0.153
38	807.92	54.57	0.081	88	725.14	54.35	0.021	138	662.51	89.40	-0.155
39	828.80	54.52	0.039	89	705.69	54.34	0.031	139	662.47	89.53	-0.149
40	849.38	54.49	0.017	90	686.13	54.32	0.020	140	662.40	89.66	-0.135
41	861.14	54.48	0.013	91	675.10	56.40	-9.876	141	662.38	89.79	-0.144
42	864.13	54.46	0.003	92	670.41	62.98	-2.578	142	662.34	89.90	-0.131
43	865.24	54.46	0.012	93	668.68	65.03	-1.813	143	662.36	90.02	-0.117
44	865.89	54.45	-0.002	94	667.91	66.64	-1.508	144	662.38	90.13	-0.120
45	866.38	54.44	0.004	95	667.39	68.03	-1.324	145	662.39	90.24	-0.110
46	866.79	54.44	0.004	96	666.95	69.27	-1.199	146	662.42	90.34	-0.104
47	867.12	54.44	0.010	97	666.57	70.41	-1.107	147	662.45	90.44	-0.095
48	867.37	54.43	0.002	98	666.24	71.48	-1.046	148	662.48	90.54	-0.091
49	867.60	54.43	0.008	99	665.95	72.50	-0.987	149	662.45	90.64	-0.087
50	867.80	54.43	0.013	100	665.75	73.47	-0.937	150	662.48	90.73	-0.082

Time	Temp.	TG	DTG	Time	Temp.	TG	DTG
min	°C	%	%/min	min	°C	%	%/min
151	662.47	90.81	-0.080	211	662.54	93.54	-0.022
152	662.48	90.90	-0.077	212	662.55	93.57	-0.024
153	662.51	90.98	-0.081	213	662.56	93.59	-0.030
154	662.52	91.06	-0.057	214	662.53	93.62	-0.025
155	662.57	91.14	-0.055	215	662.54	93.64	-0.021
156	662.60	91.22	-0.051	216	662.54	93.67	-0.026
157	662.59	91.29	-0.044	217	662.54	93.69	-0.019
158	662.58	91.36	-0.062	218	662.55	93.71	-0.023
159	662.60	91.43	-0.056	219	662.56	93.74	-0.030
160	662.61	91.50	-0.060	220	662.57	93.76	-0.024
161	662.63	91.56	-0.055	221	662.58	93.78	-0.019
162	662.63	91.63	-0.049	222	662.59	93.81	-0.018
163	662.63	91.69	-0.061	223	662.59	93.83	-0.011
164	662.64	91.75	-0.038	224	662.60	93.85	-0.022
165	662.60	91.81	-0.054	225	662.61	93.87	-0.018
166	662.56	91.87	-0.056	226	662.63	93.89	-0.019
167	662.59	91.92	-0.058	227	662.61	93.91	-0.015
168	662.59	91.98	-0.055	228	662.58	93.93	-0.019
169	662.56	92.03	-0.056	229	662.59	93.95	-0.019
170	662.54	92.08	-0.049	230	662.57	93.97	-0.024
171	662.54	92.13	-0.053	231	662.60	93.99	-0.017
172	662.52	92.18	-0.056	232	662.56	94.01	-0.029
173	662.50	92.23	-0.056	233	662.58	94.03	-0.029
174	662.48	92.28	-0.060	234	662.59	94.05	-0.024
175	662.46	92.33	-0.062	235	662.57	94.07	-0.017
176	662.46	92.37	-0.072	236	662.59	94.09	-0.028
177	662.49	92.42	-0.061	237	662.60	94.11	-0.028
178	662.48	92.46	-0.046	238	662.57	94.13	-0.024
179	662.46	92.50	-0.066	239	662.56	94.15	-0.025
180	662.43	92.55	-0.055	240	662.60	94.17	-0.026
181	662.42	92.59	-0.051	241	662.58	94.19	-0.033
182	662.41	92.63	-0.056	242	662.60	94.21	-0.034
183	662.43	92.67	-0.059	243	662.64	94.22	-0.031
184	662.40	92.71	-0.060	244	662.63	94.24	-0.042
185	662.42	92.74	-0.051	245	662.66	94.26	-0.032
186	662.42	92.78	-0.051	246	662.66	94.28	-0.033
187	662.44	92.82	-0.045	247	662.67	94.29	-0.039
188	662.42	92.85	-0.056	248	662.67	94.31	-0.039
189	662.40	92.89	-0.045	249	662.72	94.33	-0.040
190	662.42	92.92	-0.050	250	662.71	94.34	-0.024
191	662.43	92.96	-0.052	251	662.71	94.36	-0.030
192	662.44	92.99	-0.043	252	662.74	94.38	-0.026
193	662.46	93.03	-0.045	253	662.79	94.40	-0.024
194	662.44	93.06	-0.047	254	662.81	94.41	-0.028
195	662.42	93.09	-0.043	255	662.86	94.43	-0.023
196	662.41	93.12	-0.040	256	662.91	94.45	-0.028
197	662.40	93.15	-0.050	257	662.96	94.46	-0.028
198	662.40	93.18	-0.040	258	662.99	94.48	-0.019
199	662.42	93.21	-0.043	259	663.00	94.49	-0.011
200	662.43	93.24	-0.042	260	663.02	94.51	-0.018
201	662.47	93.28	-0.043	261	663.01	94.53	-0.016
202	662.50	93.30	-0.036	262	663.05	94.54	-0.021
203	662.49	93.33	-0.034	263	663.06	94.55	-0.015
204	662.46	93.36	-0.036	264	663.05	94.57	-0.002
205	662.51	93.39	-0.044	265	663.05	94.59	-0.001
206	662.49	93.41	-0.027	266	663.06	94.60	0.000
207	662.48	93.44	-0.036	267	663.02	94.61	0.007
208	662.53	93.47	-0.024	268	663.03	94.63	0.001
209	662.51	93.49	-0.030	269	663.00	94.64	-0.001
210	662.54	93.52	-0.030	270	663.01	94.65	-0.007

Appendix D

GC reading for CO_2 concentration (ppm) in the outlet gas stream during PKS pyrolysis and steam gasification, using Aldrich CaO and Synthesized CaO as the adsorbents.

			Pyrolysis		Steam gasification	
Run	Time	Temp (°C)	Aldrich CaO	Synthesized CaO	Aldrich CaO	Synthesized CaO
1	0	50	0.00	0.00	0.00	0.00
2	4	50	0.00	0.00	0.00	0.00
3	8	50	0.00	0.00	0.00	0.00
4	12	50	0.00	0.00	0.00	0.00
5	16	50	0.00	0.00	0.00	0.00
6	20	50	0.00	0.00	0.00	1.17
7	24	130	0.00	11.37	0.00	8.77
8	28	210	1.87	11.26	3.45	13.59
9	32	290	3.89	11.76	7.53	22.93
10	36	370	2.33	13.31	7.01	28.28
11	40	450	6.61	39.89	16.95	71.39
12	44	530	5.46	70.52	15.52	13.52
13	48	610	27.72	19.16	62.47	9.60
14	52	690	4.90	13.01	15.46	13.76
15	56	770	5.31	11.66	15.76	13.59
16	60	850	4.74	10.46	16.94	11.10
17	64	900	4.61	8.72	14.09	1.04
18	68	900	3.04	6.25	7.26	0.88
19	72	900	1.61	4.10	4.36	0.73

LIST OF CONFERENCE AND PUBLICATION

M. Mohamed, S. Yusup, S. Maitra, "Decomposition Study of Calcium Carbonate in Cockle Shell", World Engineering Congress, 2010, August 1-5, Kuching, Sarawak, Malaysia.

M. Mohamed, S. Yusup, S. Maitra, "Decomposition Study of Calcium Carbonate in Cockle Shell", *Accepted with minor correction for Journal of Engineering Science and Technology,* 2011.

M. Mohamed, S. Yusup, U. Rashid, "Effects of Experimental Variables on Conversion of Cockle Shell to Calcium Oxide", *Under review for Indian Journal of Engineering and Material Science,* 2011.